12-2013

IDENTIFICATION OF NOVEL GENES REGULATING ELASTIC FIBER FORMATION THROUGH EXPRESSION PROFILING ANALYSIS OF ELASTOGENIC MODELS

Erin Sproul
Clemson University, erinpsproul@gmail.com

IDENTIFICATION OF NOVEL GENES REGULATING ELASTIC FIBER FORMATION THROUGH EXPRESSION PROFILING ANALYSIS OF ELASTOGENIC MODELS

A Dissertation
Presented to
the Graduate School of
Clemson University

In Partial Fulfillment
of the Requirements for the Degree
Doctor of Philosophy
Bioengineering

---

by
Erin Pardue Sproul
December 2013

Accepted by:
Martine LaBerge, PhD, Committee Chair
W. Scott Argraves, PhD, Advisor
Amanda LaRue, PhD
Dan Simionescu, PhD
Hai Yao, PhD

ABSTRACT

Background: Particularly important to the mechanical performance of native arterial blood vessels is elastin, an extracellular matrix (ECM) protein deposited by VSMCs in the form of elastic fibers, arranged in concentric lamellae in the media of the vessel wall. In addition to serving as major structural elements of arterial walls, providing extensibility and elastic recoil, elastic fibers also influence vascular cell behaviors. For these reasons tissue engineers are attempting to exploit elastic fiber biology to enhance vascular graft design and patency. Therefore, developing a greater understanding of the molecular mechanisms of elastogenesis may offer opportunities to control elastogenesis in tissue biofabrication.

Approach: To discover genes critical for elastogenesis we performed analysis of gene expression profiles associated with elastogenesis occurring *1)* during lung and aorta development, *2)* in the lung and skin in response to injury, and *3)* in vascular smooth muscle cells (VSMCs) stimulated to produce elastic fibers.

On the resulting convergent gene set we employed Promoter Analysis and Interaction Network Toolset (PAINT) to identify transcription factor binding regions. We also mapped binding sites for microRNA (miRNA) within the convergent gene set. Subsequent screening for potential regulators of elastogenesis were performed using pharmacological agonists and antagonists

along with plasmid vector transfection to augment expression. Differences in elastin transcription were measured by quantitative reverse transcriptase polymerase chain reaction (qRT-PCR) and by anti-elastin immunostaining in the development of a novel elastin ELISA. A 3D proof of concept tissue culture model containing fibroblasts and macroporous gelatin microcarrier beads was also established and immunostained for elastin.

Results: Our transcriptomic studies revealed a set of genes differentially regulated in all five models of elastogenesis tested. Aside from genes that have previously been established to act in the elastogenesis process there are >50 genes that have not been implicated in elastogenesis. Moreover, promoter analysis of clusters of genes from the 63-gene set having a similar pattern of regulation during developmental elastogenesis revealed two potential elastogenesis regulatory network of TFs. We hypothesize that these sets of genes contain novel positive and negative effectors of elastogenesis. Effects of agonists, antagonists, and expression vectors of these genes on elastin expression were quantified in cultured fibroblasts to identify agents that can be employed to accelerate elastogenesis during tissue biofabrication.

Conclusions: The findings highlight a group of genes whose expression is differentially expressed in multiple models of elastin formation and many not previously associated with elastogenesis and thus may represent novel

components of elastogenesis. Transcriptional regulatory network analysis revealed potential transcription factor regulators of elastogenesis. Candidate genes and transcription factors were regulated through agonist and antagonist treatment and transfection of plasmid expression vectors in order to augment elastogenesis in vascular tissue biofabrication.

TABLE OF CONTENTS

Table of Contents (Continued)

Table of Contents (Continued)

Table of Contents (Continued)

LIST OF ABBREVIATIONS

ASMC	Aortic smooth muscle cells
bFGF	basic fibroblast growth factor
CAT	Chloramphenicol acetyl-transferase
C/EBP	CCAAT/enhancer-binding protein.
ChIP	Chromatin Immunoprecipitation
EGFR	Epidermal growth factor receptor
EGR-1	Early growth response
FBS	Fetal bovine serum
HB-EGF	Heparin-binding epidermal growth factor-like growth factor
HDF	Human dermal fibroblasts
HFF	Human foreskin fibroblasts
IGF-1	Insulin-like growth factor-I
IL-1β	Interleukin-1β
MMP	matrix metalloproteinase
PPAR	Peroxisome proliferator-actived receptor
PKC	protein kinase C
qRT-PCR	Quantitative reverse transcription polymerase chain reaction
RASMC	rat aortic smooth muscle cells
Rb	retinoblastoma protein
RNA	Ribonucleic acid
siRNA	Small interfering RNA

TGFα	transforming growth factor-α
TNF-α	tumor necrosis factor-alpha
TGFβ1	transforming growth factor β-1
VSMC	vascular smooth muscle cells
WT1	Wilm's Tumor

LIST OF TABLES

Table Page

LIST OF FIGURES

List of Figures (Continued)

Figure Page

List of Figures (Continued)

Figure Page

List of Figures (Continued)

Figure Page

CHAPTER ONE

INTRODUCTION TO VASCULAR TISSUE ENGINEERING

1.1 Role of elastin fibers in tissue

Particularly important to the mechanical performance of tissues is elastin, an extracellular matrix (ECM) protein deposited by vascular smooth muscle cells (VSMCs) in the form of elastic fibers. Within blood vessels, especially large elastic vessels, elastic fibers constitute a major part of the ECM (30-57% w/w in the aorta) arranged in concentric lamellae in the media of the vessel wall (*3*). In addition to serving as major structural elements of arterial walls, providing extensibility and elastic recoil, elastic fibers also influence vascular cell behaviors such as biochemical signaling pathways. Disruption of elastic fibers can initiate and progressively lead to the pathology of life threatening complications such as atherosclerosis, aneurysm and vasospasms (*4, 5*).

The mechanism of elastogenesis encompasses the transcription of the elastin gene, the translation of the elastic fiber precursor monomer tropoelastin, migration to the plasma membrane, binding to the elastin receptor, self-assembly and cross-linking of tropoelastin by lysyl oxidase, deposition onto a microfibrillar scaffold, and finally, elongation into a mature elastic fiber (*6, 7*). A deficiency in any step may result in impaired, inhibited, or completely disrupted elastogenesis. Some (ECM) proteins are critical to the formation of functional elastic fibers as evidenced in genetically deficient mouse models. For example, fibulin-5 deficient mice are characterized by disorganized elastic fibers, a tortuous aorta with loss of compliance, severe emphysema, and loose skin (cutis laxa) (*8, 9*).

Tropoelastin in these mice is synthesized but not assembled properly as evidenced by accumulation of fragmented elastin without an increase of elastase activity (*8, 9*).

Because elastin is crucial to maintaining the native structural configuration (*10, 11*) and regulating signaling pathways (*12*), failure to regenerate a healthy elastin matrix in response to damage during disease (e.g., inflammation-mediated elastin degradation in atherosclerosis) can severely compromise elastic tissue homeostasis (*13, 14*). A major concern in the construction of tissue engineered elastin-rich tissue is the ability to regulate cell behavior and encourage the regeneration of elastin fibers.

Tissue engineers are attempting to exploit elastic fiber biology to enhance vascular graft design and patency, however overcoming the deficient quality of elastic fibers synthesized in vitro poses a challenge due to the ill-defined mechanism and insufficient knowledge of regulatory genes. Therefore, the goal of the study is to identify gene regulators of elastogenesis that may offer opportunities to control elastogenesis in tissue biofabrication.

1.2 Clinical problems related to elastin and significance

Human disease and elastin. DNA deletions and mutations in the elastin gene are associated with heritable diseases of the connective tissue (*14-20*). Supravalvular aortic stenosis (SVAS) and Williams-Beuren Syndrome are characterized by an elastin gene mutation and narrowing of the arterial tree and increased elastinolytic activity (*14-16*). Another mutation of the elastin gene

results in cutis laxa with clinical effects of inelastic skin associated with severe aortic disease and pulmonary emphysema(*17, 18*). Deletions in genes comprising the microfibrillar scaffold, such as fibrillin-1 result in Marfan's Syndrome with a phenotype of vascular disease, including aortic aneurysms and dissections (*19, 20*).

Biomechanical significance of defective elastin formation. The biological process of aging and certain diseases is characterized by a loss of tissue elasticity increasing the investigative efforts of biomaterials based on elastin for their application in tissue engineering. Challenges to elastin tissue engineering revolve around adequately controlling the process of elastin assembly into elastic fibers or organized layers of elastic lamellae. An organized ECM containing elastic fibers has superior mechanical structure and cellular signaling advantages over amorphous deposits of elastin typically synthesized *in vitro*. To address this impediment, we have employed DNA microarray transcriptomic profiling identify genes that are similarly regulated in a number of systems displaying increased expression of tropoelastin and increased formation of elastic fibers. The proposed research will contribute to a greater understanding of the molecular mechanisms of elastogenesis through identification and characterization of genes regulated in multiple experimental models of elastogenesis, which have not been previously identified. This understanding is expected to reveal new opportunities to induce cells to produce a functional elastin architecture in engineered vascular constructs. Ultimately, we expect this project to help

elucidate the mechanisms necessary for adequate control of elastogenesis in human vascular cells with clinical applications for repair and salvage of human vasculature.

1.3 Project rationale and objectives

The underlying mechanisms of elastogenesis remain largely ill-defined. Elastogenesis encompasses the biosynthesis of tropoelastin (TE), the elastic fiber precursor monomer, translocation of TE to the plasma membrane, TE binding to the elastin receptor, self-assembly and cross-linking of TE by lysyl oxidase, deposition of crosslinked TE onto a microfibrillar scaffold, and through iteration of this process, elongation into a mature elastic fiber (*6, 7*). A deficiency in any step may result in impaired or disorganized elastogenesis. Given that the mechanical structure and cellular signaling in elastin-containing tissues are dependent on elastic fibers, fabricated elastic constructs must be engineered to either have synthetic elastin-like components or elastin components produced by cellular constituents of the constructs.

1.4 Specific aims and hypotheses

Elastic fibers are critical for the function of multiple tissues including blood vessels, skin, lung, and auricular cartilage, periodontal ligaments and other connective tissue (*21-24*). An elastic fiber's structure is comprised of a core of amorphous tropoelastin surrounded by a microfibrillar scaffold, which contains numerous proteins such as fibrillin, microfibrillar-associated glycoproteins,

fibulins, and others (*25*). The elastic core imparts the ability for a tissue to expand in response to a force with minimal resistance and then recoil, or return to its original shape (*26, 27*). Many applications of tissue engineering require the property of elastic recoil to repair or replace damaged and diseased tissues (i.e., arterial grafts, skin grafts).

The overarching goal of this application was met by identifying regulators of elastogenesis, which will advance an approach to regenerative medicine involving accelerated production of elastic fibers. A number of studies point to the severe quantitative and qualitative deficiencies in the process of elastogenesis exhibited by cultured cells (*28, 29*). These deficiencies create an impediment to the engineering of tissues requiring functional elastin architecture. Through analysis of gene expression profiles associated with normal elastogenesis occurring during 1) mouse lung and aorta development, 2) elastogenesis in lung and skin in response to injury, and 3) in vascular smooth muscle cells (VSMCs) stimulated to produce elastin fibers, we will identify genes that appear to represent new players in the process of elastogenesis. We will also work toward development of a novel in vitro assay to quantify incorporation of elastin into the ECM of fibroblast monolayers, which we intend to use to further screen agents that modulate the activities of the putative elastogenic genes identified by our transcriptomic analysis. As a result of these studies, we expect that new elastogenesis related genes will be defined that offer new opportunities to regulate elastogenesis in elastic tissue biofabrication.

Based on these findings we hypothesize that expression profiling analysis can be used to identify modulatory genes of tropoelastin synthesis and elastic fiber assembly (elastogenesis) that have not been previously associated with the process. Experimentation outlined in this proposal will test this hypothesis by determining whether candidate genes regulate tropoelastin expression and elastic fiber assembly. These objectives will be reached through the following two interrelated specific aims:

Aim 1: Use DNA microarray based transcriptomic profiling to identify genes that are similarly regulated in processes in which elastogenesis is a key component.

Rationale and hypothesis:

A number of studies point to severe quantitative and qualitative deficiencies in the process of elastogenesis mediated by cultured cells(*28*). These deficiencies are an impediment to cell-based bioengineering of blood vessels requiring functional elastin architecture. DNA microarray expression data has been performed on in vivo developing elastin-rich tissues including the lung (W Scott Argraves, MUSC, Charleston, SC) and aorta (Robert Mecham, Washington University School of Medicine, St. Louis, MO) and additionally unpublished *in vitro* DNA microarray expression data of vascular smooth muscle cells (VSMCs) induced to synthesize elastin (WS Argraves and TN Wight, Benaroya Institute at Virginia Mason, Seattle, WA). Other expression profiling studies of *in vivo* wound healing occurring in elastin-rich tissues have already

been performed and the data uploaded to the NCBI Data GeoSets(*30, 31*). In light of the current caveats in synthesizing elastic fibers *in vitro*, a convergent analysis of DNA microarray expression profiling data in processes in which elastogenic is a key component (*in vivo* studies of nascent elastic fiber formation, *in vivo* regeneration of injured elastic fibers, and in vitro VSMCs induced to synthesize elastin) will elucidate genes regulated during elastogenesis that can be employed in elastic tissue engineering. The set of significantly regulated genes should include genes reported to be directly or indirectly involved with elastogenesis in addition to other genes not yet reported to be involved.

Approach: To discover genes critical for elastogenesis we will define a range of processes in which elastogenesis is a key component. We will conduct experiments to collect microarray data and gather publicly available microarray data to encompass multiple types of elastogenesis in different elastin-containing tissues: 1) development of native elastic fibers in lung and aorta, 2) regeneration of elastin in the wound healing response in the lung and skin, and 3) in cultured vascular smooth muscle cells stimulated to produce elastic fibers. We will analyze each data set individually to determine differentially expressed genes specific to each process and then converge individual datasets to discover regulated genes common to all elastogenic processes. From this study we will identify a set of consistently regulated genes common to five different microarray datasets in which elastogenesis is a key component which we will define as the "elastogenic gene set."

Aim 2: Determine if candidate genes are modulators of tropoelastin expression in an in vitro culture model.

***Rationale and hypothesis*:** Previous transcriptomic studies have revealed genes critical to elastic fiber formation that we anticipate to be consistently regulated in multiple elastogenic processes. Aside from genes previously established to act in elastogenesis, we expect to discover genes that have not been implicated in elastogenesis. We hypothesize that this convergent set of genes will contain positive and negative effectors of elastogenesis. Genes regulated during the formation of elastic fibers may play a critical role in elastogenesis, however it is possible that a regulated gene may not be essential to the process. It is also possible that even with a low false discovery rate of comparative transcriptomic analysis, a gene may be identified incorrectly as being regulated during elastogenesis. It is necessary to determine whether tropoelastin expression and elastic fiber assembly processes will be disrupted in the case a gene is not expressed. Through the use of transcription factor agonists/antagonists and plasmid expression vectors we will selectively augment/inhibit expression of upregulated genes and assess the resulting effects of elastin expression.

Approach: To discover genes critical for elastogenesis we will categorize genes into groups through coordinately regulated functional analysis and transcription

factor analysis as well as identify individual genes for experimental testing.

Characterization of elastic fibers from multiple processes reveals higher organization and mechanical strength in the developmental process compared to wound healing and in vitro formation of elastic fibers (*32*-*34*). We will refer to the native development of elastic fibers as the gold standard and place emphasis the expression patterns of the "elastogenic gene set." We will categorize genes into groups of potential enhancers and potential inhibitors of elastogenesis based on expression patterns similar or inverse to the expression pattern of the elastin gene in processes containing native development of elastic fibers. Enhancers of elastogenesis will be defined following the assumption of a similar expression pattern as elastin: at highest levels during periods of peak elastin expression (i.e., 4-21 days postnatal (d) in the developing aorta and 10-14 d in the developing lung) and expressed at lowest levels during minimum elastin expression. Conversely, it is reasonable to speculate that inhibitors of elastogenesis might display an inverse relationship to elastin: relatively low expression during peak periods of elastin expression (i.e., 4-21 d in the aorta and 10-14 d in the developing lung) and high levels of expression during the period in which elastogenesis subsides (i.e., >60 d postnatal in the aorta). Within the dataset there are 20 potential enhancers of elastogenesis and 39 potential inhibitors of elastogenesis.

Another consideration in the prioritization of genes for testing is the availability of agonists and antagonists for each gene. Cursory evaluations reveal that for most of the genes there are commercially available agonists and

antagonists and purified gene products. Furthermore, siRNAs can readily be employed to suppress the expression of candidate genes.

CHAPTER TWO

AN OVERVIEW OF ELASTOGENESIS

The term elastogenesis is first used in a 1964 study using electron light microscopy to compare the aortae from fetuses, newborns, and adult. Haust et al. clearly described a low density elastic matrix surrounded by a higher density elastic membrane, surrounded further by arranged filaments. These “elastic units” originated at the basement membrane of SMCs where they aggregate and fuse to form larger elements of elastic tissue, a process defined as elastogenesis.

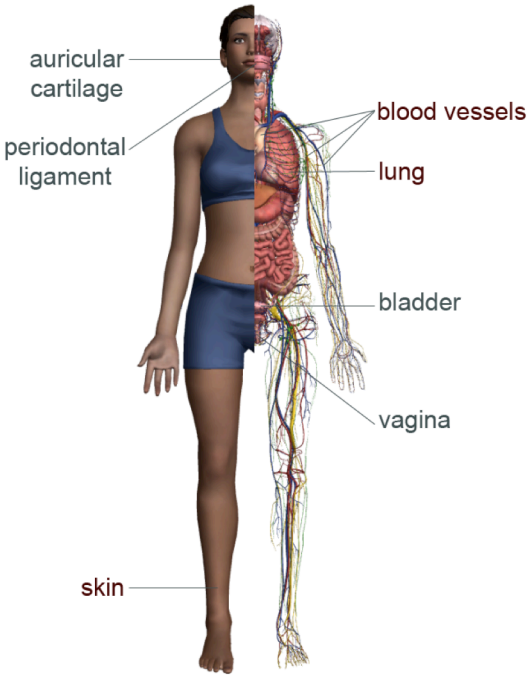

Figure 2.1. Elastin occurrence the body. Elastic fibers are found predominantly in connective tissues such as skin, lungs, and blood vessels (Kielty 2002).

It is now known that an elastic fiber is composed of a crosslinked tropoelastin core surrounded by a sheath of microfibrils that are based on the glycoprotein fibrillin. There are also a multitude of elastic fiber associated molecules shown to be essential to elastic fiber formation through knock-out animal studies such as lysyl oxidase (LOX) (*35, 36*) and fibulin-4 (*37*) and -5 (*8, 9*). This chapter will provide a background on the formation of elastic fibers, elastogenesis, and demonstrate the need to better understand elastogenesis for tissue engineering applications.

2.1 Elastin Fiber Structural Arrangement and Function

2.1.1 Chemical Composition of Elastic Fiber

Elastin is an extracellular matrix protein encoded by a single gene on the human chromosome 7q11.23 codes for elastin (*38*). Elastin contains a highly conserved amino acid sequence (VGVAPG), rich in a high concentration of non-polar amino acids proline (10%) and glycine (33%) resulting in a hydrophobic protein. Elastin contains additional amino acids such as OH-proline (1%), alanine, valine, and leucine (40-50%) (*39*) as shown in Table 2.1. The polypeptide chains in elastin are cross-linked by unique polyfunctional heterocyclic acids called desmosine and isodesmosine, as opposed to typical disulfide bridges. These distinctive internal linkages and inherent hydrophobicity make elastin a stable protein, resistant to the normal breakdown characteristic of most proteins.

Elastin is secreted as a soluble monomer, tropoelastin, which has a secondary structure characterized by alternating hydrophobic (β-sheet) and hydrophilic (α-chain) regions encoded by separate exons (*40*). The secondary structure of elastin consists of 10% α-helices, 40% β-sheets, and 50% undefined conformations (*41*). The hydrophilic regions are alanine- and lysine-rich, while the hydrophobic domains are rich in proline, valine, and glycine (*42*). Lysyl oxidase (LOX), a copper-dependent enzyme (*39*), crosslinks targeting domains (*43*) of

Table 2.1. **Amino acid composition of elastin derived from bovine aorta.** Values are expressed as a percentage of the total amino acid residues. Desmosine and Isodesmosine are expressed as lysine equivalents (Balazs 1970).

Amino Acid	Percent
Proline	11.27
Glycine	33.24
Alanine	22.39
Valine	13.13
Leucine	5.82
Phenylalanine	2.97
Desmosine	0.96
Isodesmosine	0.55

the α-helical regions, via desmosine and isodesmosine linkages (*41*), to yield a crosslinked insoluble, yet flexible matrix protein.

2.1.2 Elastin ultrastructure

Elastin may be ultrastructurally organized into individual and networked fibers (e.g., loose fibers and loose or compact meshes) or inter-woven, non-fibrillar matrix structures (e.g., continuous sheets, fenestrated sheets) (Scott 1996). The fibrillar structures contribute to the elasticity of the tissues that contain them, allowing them to characteristically recoil, when distending forces are removed.

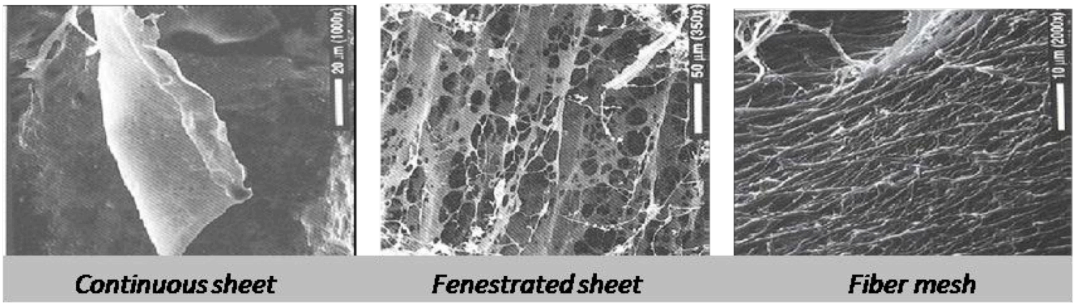

Figure.2.2 Elastin organization can vary depending upon its mechanical and functional role within different tissues. These differences in ultrastructure can be visualized with scanning electron microscopy (SEM) (Scott 1996).

Elastic fibers (~200-900 nm diameter) are major insoluble ECM assemblies deposited during early development in elastic connective tissues. They are composed of a central core of cross linked, amorphous elastin surrounded by microfibrils (Kielty 2002). The microfibrils are composed of a number of different glycoproteins, predominately fibrillin, which are essential both to maintain the integrity of the fibers and the ability of cells to interact and

respond to them. Microfibrils are typically 10 nm in diameter with an average periodicity of 57 nm (Lu 2006). They form linear bundles and are deposited as pre- scaffolds onto which soluble tropoelastin monomers then coalesce and are crosslinked. During the elastin deposition process, the microfibrils are displaced to the periphery of the growing elastin fibers, and typically appear electron-dense, as opposed to the electron lucent amorphous elastin.

2.1.3 Biochemical Roles of Elastin

In addition to rendering tissues elastic, vascular matrix elastin also regulates vascular cell behavior (*44, 45*). Correlative studies have demonstrated large changes in the composition and distribution of extracellular matrix (ECM) components during tissue development, cell differentiation, and in response to growth factor, hormone, and cytokines (*46*). Modulation of a variety of cellular functions, including secretory activities and gene transcription, occurs via interaction with the ECM. The ECM also serves as a reservoir for growth factors and cytokines (*44*). Therefore, ECM proteins, such as elastin, may influence cell development, survival (anchorage-dependent), proliferation, phenotype, migration, differentiation, and function (*47*).

Elastin affects cell-fate. Some cell types are dependent upon anchorage to the surrounding ECM for survival. Anchoring junctions, such as adherens junctions and hemidesmosomes formed by integrin transmembrane proteins, mechanically attach cells and their cytoskeletons to the ECM (*48*). Therefore, the presence or absence of elastin may influence cell viability. The phenotype (the

appearance and behavior of cells) also depends upon the ECM. For example, in pathologic conditions, elastin may be fragmented and the fragments may encourage SMCs to change from a contractile to a synthetic phenotype. Additionally, cell locomotion is affected by ECM components, including elastin, and requires an initial polarization of the cell to promote migration in a particular direction. Cell movement is in response to chemical and physical cues in the cell environment. Therefore, the physical properties of elastin influence cell movement, specifically inflammatory cells in scenarios of disease.

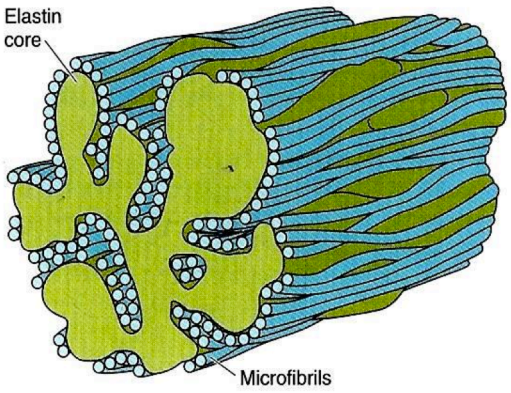

Figure 2.3. Elastin Fiber Structure. An individual elastic fiber is composed of a core of aggregated tropoelastin monomers surrounded by an outer sheath of microfibrils. The microfibrillar scaffold is primarily composed of the fibrillin proteins.

Tropoelastin, the soluble elastin precursor, influences chemotaxis (Indik 1990), stimulates vasodilation[53], regulates intracellular Ca^{2+} (Faury 1998), and promotes cell adhesion (Grosso 1991). Mature elastin also has numerous effects on vascular SMCs including inducing actin stress fiber orientation, inhibiting SMC proliferation, and regulating cell migration (Rodgers 2005).

2.2 Elastic Fiber Assembly

2.2.1. Formation of an Elastic Fiber

Mature elastic fibers are composed of a central core of elastin surrounded

by glycoprotein microfibrils (10-12 nm in diameter) (*49*). During the early stages of elastogenesis, these microfibrils are formed first in the extracellular matrix (ECM) space and play a major role in organizing elastin into elastic fibers. The major microfibrillar components are fibrillin -1 and -2 that polymerize in a head-to-tail manner to yield the microfibrils. Calcium binding stabilizes the linear and rigid structure of fibrillin monomers, their interactions, the lateral packing of microfibrils, and thus the three-dimensional organization of their macroaggregates. While the ECM is organizing the microfibrillar scaffold for elastin deposition, the elastin monomers are synthesized within the cell.

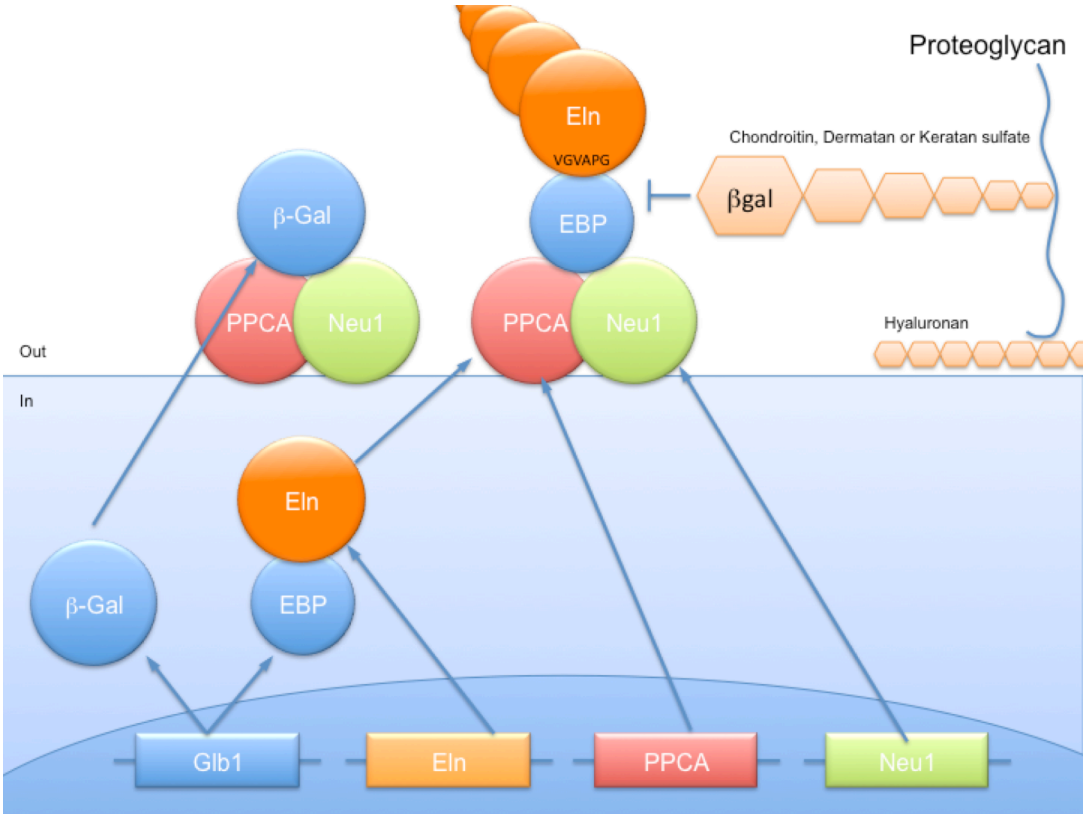

Figure 2.4 Elastogenesis involves the secretion of tropoelastin monomers to the extracellular space. Within the cell, the elastin binding protein (EBP), a splace variant of Beta galactosidase, binds to tropoelastin monomers to provide stability and prevent self-aggregation of elastin. EBP chaperones elastin where it is secreted through the plasma membrane and binds to transmembrane proteins cathepsin A (PPCA) and neuraminidase 1 (NEU1) forming the elastin receptor. Betagalactosidase sugars can bind to the EBP causing a conformational change and release of elastin into the extracellular matrix.

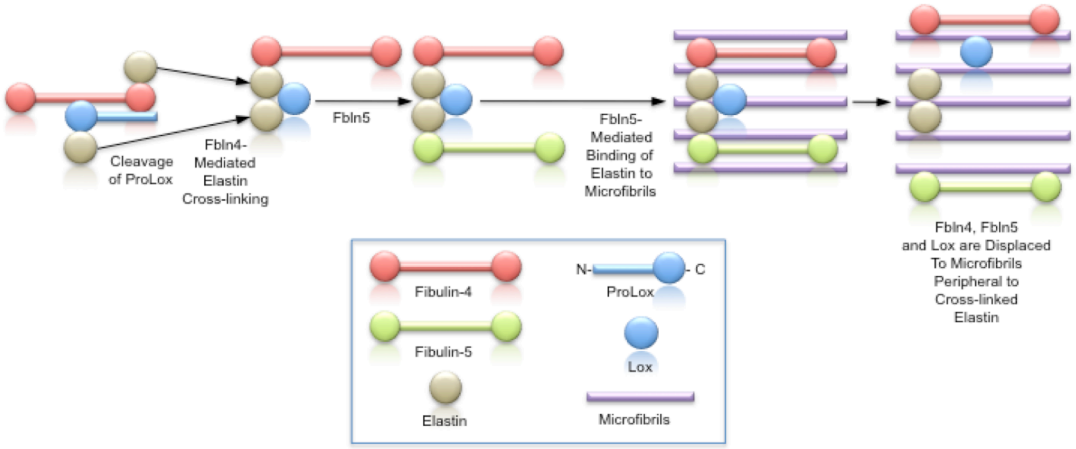

Figure 2.5 Fibulins facilitate the formation of elastic fibers through binding of elastin monomers and transportation to the microfibrillar scaffold. Tropoelastin monomers are crosslinked by lysyl oxidase (LOX) and aggregated forming the elastin-rich dense core of an elastic fiber. Fibulins assist the transportation of tropoelastin as it is assembled on the fibrillin rich scaffold that will form the outer sheath of the elastic fiber.

The soluble elastin precursor, tropoelastin, is first synthesized within the cell and is chaperoned to the plasma membrane for secretion by the elastin binding protein (EBP) which also prevents premature self-aggregating. EBP and tropoelastin are secreted and EBP binds to two integral membrane proteins, neuraminidase 1 and cathepsin A, on the cell surface that form a transmembrane link between the extracellular compartment and the cytoskeleton (*50*) (Figure 2.4). The complex of EBP, neuraminidase 1, and cathepsin A is known as the elastin receptor (*51, 52*) that tethers tropoelastin to the cell surface in the extracellular space where it interacts with the microfibrils and becomes oriented within a growing elastic fiber for eventual crosslinking (*53*) (Figure 2.5). EBP is bifunctional in that it also has galactolectin properties. It binds the hydrophobic VGVAPG sequence in elastin, the cell membrane, and galactosugars via three separate sites. The binding of galactosugars lowers its affinity for both tropoelastin and for the cell-binding site, resulting in the release of bound elastin

and the dissociation of the 67 kDa subunit from the cell membrane. Galactosugar-containing microfibrillar glycoproteins may therefore be involved in the coordinated release of tropoelastin by the cell (*54*) (Figure 2.4).

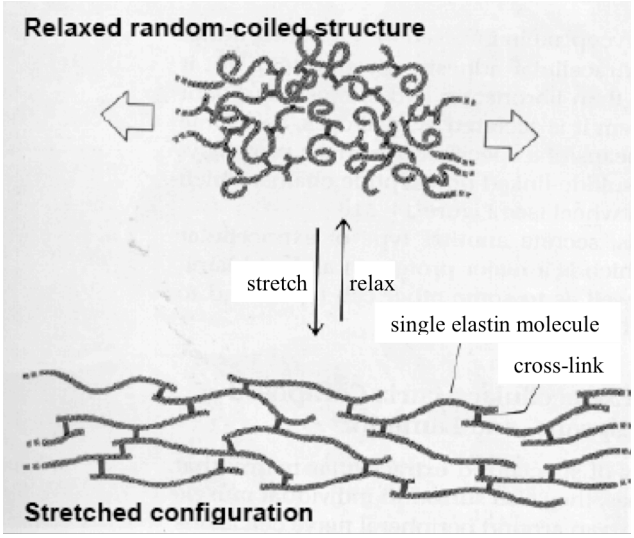

Figure 2.6. Elastin conformational shift from relaxation to stretch (*2*).

The tropoelastin deposited onto the microfibril matrix is then crosslinked into mature elastin. Crosslinking of elastin is initiated by the action of lysyl oxidase (LOX), a Cu^{2+} dependent endogenously produced enzyme that catalyzes the oxidative deamination of lysine residues into allysine (*55*). This is the only enzymatic step involved in elastin crosslinking. Subsequent formation of crosslinks between tropoelastin molecules by desmosine and isodesmosine occurs as a series of spontaneous condensation reactions, resulting in the production of a complete elastic fiber. The relative proportion of microfibrils to elastin declines with increasing age of the animal, adult elastic fibers having only a very sparse peripheral mantle of microfibrillar material (*56*).

Elastin fibers form random coiled structural networks that allow them to be stretched and then to recoil to their original state upon load-release (Figure 2.6). Elastic fibers formed by such aggregation vary in thickness, length and three-dimensional architecture depending on the direction and magnitude of the forces

exerted upon the tissue. This morphological diversification can be seen in different organ systems. In the aortic wall, elastic fibers form thick concentric lamellae in the tunica media with interlaminar connecting fibers scattered radially. Additionally, microfibrils are present as a complex meshwork throughout the aortic wall. It can be generalized that the elastic fibers are responsible for dilation and recoil, with the microfibrils acting as flexible links that make the aortic wall a working unit (*55*).

2.2.2 Dynamics and Mechanical Properties of Elastin

The mechanical properties of blood vessels influence a broad spectrum of physiologic phenomena, including blood pressure, flow rates, wall shear stress, biomolecules, and mass cell transport that, in turn, critically impact cardiovascular homeostasis. As mentioned previously, the mechanical properties of blood vessels stem from microstructural wall components, such as collagen

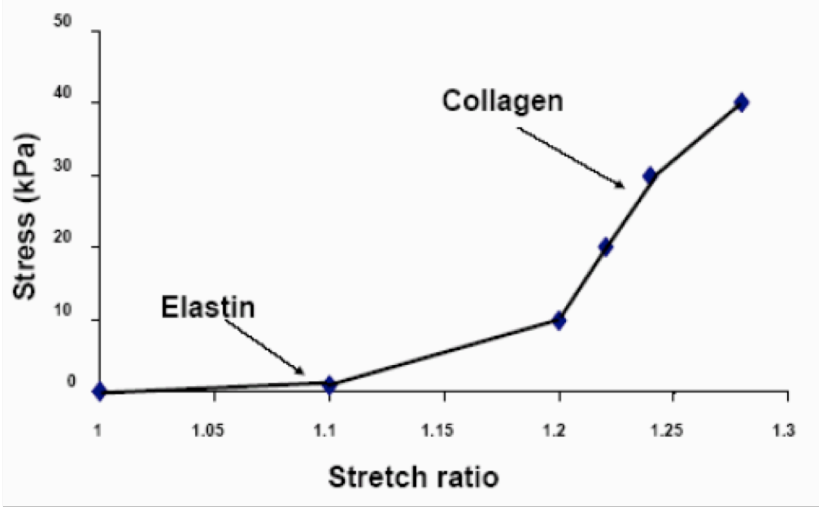

Figure 2.7. Stress-strain curve for a blood vessel demonstrates the mechanical role of elastin in response to initial strain. The blood vessel initially distends in response to strain as contributed by elastin. At a certain strain the mechanical stress load is distributed to the collagen fibers within the blood vessel and the blood vessel becomes stiffer as evidenced by the sharp slope increase of stress to strain (http://biochemistry.utoronto.ca/keeley/bch.html).

and elastin fibers, smooth muscle cells, and fibroblasts (*49*). Since these individual components take up loads at different stress levels, their source and location-specific differences, content and distribution within blood vessels, and their alteration in diseased states can render the mechanical properties of blood vessels complex and difficult to predict. Collagen and elastin affect the mechanical behavior of vessels in different ways (Figure 2.7). Strain is initially accommodated by elastin allowing the vessel to expand with minimal resistance, and, eventually strain is strongly resisted by collagen preventing overexpansion. While collagen provides rigidity, elastin allows the connective tissues in blood vessels to stretch and then recoil to their original positions. A study by Gundiah *et al.* (*57*) has shown that axial elastin fibers in intimal and adventitial layers, and circumferential medial fibers help distribute tensile stresses during vessel inflation and relaxation, conclusively providing evidence that emphasizes mechanical importance and indispensability of elastin fibers in the aortal anatomy.

2.3 Role of Extracellular Matrix Proteins in Elastogenesis

2.3.1 Fibulins as Regulators of Elastogenesis

Several members of the fibulin protein family also play important roles in elastogenesis. For example, fibulin-5 (Fbln5) is essential to the incorporation of elastin into the core of elastic fibers; Fbln5 knockout mice have been shown to produce abnormal elastic fibers with elastin situated in globules on the surface of the microfibril scaffold (*58*). Although fibulin-2 (Fbln2) knockout mice do not show an obvious phenotype, double knockouts of Fbln2 and Fbln5 exhibit a more

severe phenotype than Fbln5 knockouts; the aortas of double knockout mice have thin, disorganized internal elastic laminae and show abnormal repair after injury (*59*).

2.3.2 Proteoglycans as Regulators of Elastogenesis

A number of studies point to an inhibitory role for certain proteoglycans (PGs) in the assembly of elastic fibers (*60-62*). Mechanistically, this is thought to involve β-galactosugars PGs acting to displace tropoelastin from the elastin binding protein (EBP) (*63*). Indeed, addition of either chondroitin sulfate (CS) chains, or the CS PG, versican, decreases elastic fiber formation (*60*). Furthermore, impaired elastic fiber assembly is observed in Hurler disease and Costello syndrome in which there is an accumulation of glycosaminoglycans (GAGs) (*64*). Similarly, increased elastin accumulation has been achieved in the rat carotid artery by seeding of VSMCs transduced to express a GAG-deficient form of the PG, biglycan (*61*).

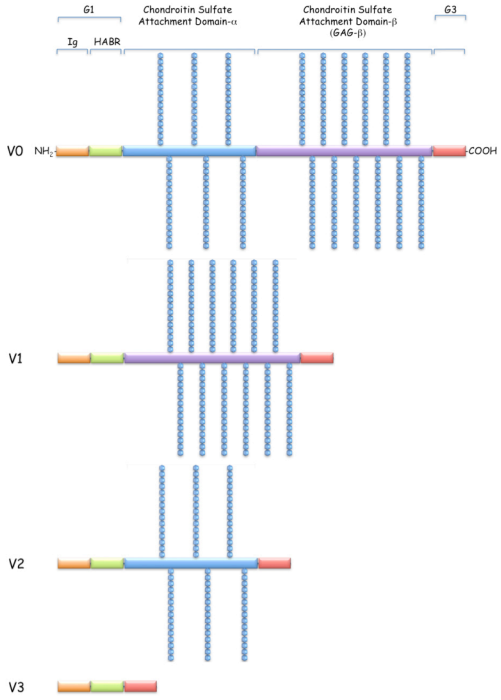

Figure 2.8. Alternate splicing of versican mRNA produces 4 distinct isoforms. Versican V3 is the smallest variant at 73 kDa and contains no GAG attachment sites.

2.3.3 Versican V3 as a Regulator of Elastogenesis

Other extracellular matrix proteins have also been found to associate with elastic fibers and affect the process of elastogenesis. One such molecule is versican, a large chondroitin sulfate proteoglycan found in a variety of soft tissues. Versican contains four main domains as shown in Figure 2.8. The N-terminal region binds to the glycosaminoglycan hyaluronan; aggregates of versican and hyaluronan associate with the cell surface and influence cell shape, cell division, and other processes. The C-terminal region serves a variety of regulatory functions and binds to integrins and extracellular matrix components. The remainder of the molecule is composed of two large regions containing binding sites for chondroitin sulfate (*65*).

Four versican splice variants of varying length have been identified. The full-length V0 isoform contains all four of the major domains, including both chondroitin sulfate-binding regions. The V1 and V2 variants are missing the β and α chondroitin sulfate-binding regions, respectively, and the V3 isoform consists of only the N-terminal and C-terminal regions with no chondroitin sulfate binding sites as shown in Figure 2.5.

Previous studies have shown that the chondroitin sulfate side chains of proteoglycans such as versican can disrupt the process of elastogenesis, leading to decreased elastin deposition in the extracellular matrix and abnormal elastic fiber assembly (*66*). The V3 form of versican, however, lacks these inhibitory side chains. In fact, the overexpression of V3 in arterial smooth muscle cells has been

shown to lead to increased elastic fiber formation in rat arterial smooth muscle cells both in vitro and in vivo (*67, 68*).

Furthermore, V3 has been shown to promote elastogenesis and improve the structural and functional properties of engineered vascular constructs (*69*). The positive effects of V3 on elastogenesis have been attributed to its ability to displace GAG containing variants of versican from binding sites in the vicinity of elastic fiber assembly complexes (i.e., EBP-tropoelastin complexes). Consequently, the suppressive effects of GAG moieties would be relieved and elastic fiber assembly would proceed.

2.4 Elastic Fibers in Vascular Disease

A common pathologic feature of vascular disease is the disruption of elastic fibers and the accumulation of SMCs within the intima between the endothelium and medial layer of the vessel wall resulting in the progressive occlusion of blood flow. Under normal conditions, vascular SMCs in the *tunica media* of blood vessels are quiescent and embedded in a network of elastin-rich ECM that acts as a barrier to SMC migration and proliferation (*70*). During atherosclerosis, different cell types, including ECs, platelets, and inflammatory cells release mediators, such as growth factors and cytokines that induce phenotype change of vascular SMC from the quiescent "contractile" phenotype state to the active "synthetic" state, causing them to release matrix proteases degrading the ECM (including elastin) allowing them to aggressively migrate into the subendothelial space and contribute to neointima formation (*71*). The

degradation of vascular elastin exposes other medial components (i.e. collagen, SMCs) to very high tensile stresses (*57*). The high plasticity of SMCs makes these cells susceptible to mechanically induced phenotypic changes that may result in continued aggravated protease secretion and ECM degradation.

Since vascular SMCs modulate their phenotype readily, external factors in the arterial wall must instruct them to maintain a quiescent, contractile state if homeostasis is to be achieved. This regulation of vascular SMC activity occurs through defined receptor interactions and signaling pathways. In contrast to other matrix proteins, both in vitro and in vivo studies implicate elastin matrix as a negative regulator of SMC activity within the arterial wall (*72*). Thus elastin regulates vascular homeostasis by signaling SMCs through defined pathways to localize around the elastic fibers in organized lamellar units and remain in a quiescent, contractile state. The disruption of elastin by vascular disease, or direct mechanical injury can interrupt cell-matrix signaling and directly up-regulate SMC hyper-proliferation (*70*). The disruption of elastin is not simply an end product of vascular disease, but an important contributor to the pathogenesis of occlusive vascular disease. Preventing elastin matrix degradation following vascular injury or restoring the lost/ degraded vascular elastin matrix is imperative for vascular homeostasis restoration (*72*).

In disease states, wherein elastin has been broken down, the binding of elastin peptides (the soluble products of elastin degradation) via the elastin receptor (EBP and two other integral membrane proteins), G protein-coupled receptors (GPCR), or other integrins results in activation of G proteins and

opening of calcium channels (*73*). The Rho signaling cascade can be stimulated by elastin and is mediated by GPCRs, the largest family of transmembrane receptors (*74, 75*). A study by Karnik proposed a molecular mechanism for vascular SMCs in which elastin activates a G-protein-coupled pathway (*75*), inhibits adenylate cyclase, reduces cAMP levels (*76*), and stimulates Rho induced actin polymerization (*75*).

Under pathologic conditions, such as in atherosclerosis and within abdominal aortic aneurysms (AAAs), elastin breaks down to generate elastin peptides at an accelerated rate. These elastin degradation products up-regulate SMC proliferation and activate phagocytic cells (*73*). Elastin peptides are released and through their interaction with receptors present on the surface of fibroblasts, phagocytes, lymphocytes, SMCs, and endothelial cells (ECs) elicit a variety of biologic effects such as matrix-metalloproteinase (MMP) over-expression, greater Ca^{2+} influx, enhanced vasorelaxation and chemotactic activity. In atherosclerotic and neointimal lesions, SMCs migrate from the tunica media through the internal elastin lamina to the intima. Protease release by these SMCs is responsible for further elastin destruction in the arterial wall. Elastin is similarly enzymatically degraded by MMPs in aneurismal vessels, specifically MMP-2 and MMP-9 released by activated SMCs and infiltrated leukocytes, which leads to formation of floppy, de-elastized vascular segments, susceptible to rupture (*77*). The degradation of elastin is the result of a proteolytic cascade that involves the cooperation of several degradative enzyme types such as serine proteases, matrix metalloproteinases, and cysteine proteases (*71*). These may be present in

latent forms under healthy physiologic conditions, yet become activated following vessel wall injury.

2.5 Engineering Strategies to Promote Elastin Regeneration

Elastin is crucial to maintaining the native structural configuration (*11, 78-80*) and regulating the cell-signaling pathways (*12, 81-83*) of blood vessels. Thus, the failure to reinstate a healthy elastin matrix, when damaged by disease (e.g., inflammation-mediated elastin degradation in atherosclerosis) can severely compromise vessel homeostasis (*13*). In addition to achieving functional and complete endothelialization, a major concern in the development of tissue-engineered vascular constructs is the ability of scaffolding materials to modulate SMC behavior and encourage the regeneration of elastin-rich matrix.

2.5.1 Synthetic Scaffolds

The most widely used synthetic scaffolds are poly-lactic (PLA), poly-glycolic acid (PGA), and poly-L-lactic acid (PLLA). Although these scaffolds are not ideal from the standpoint of eliciting poor cell attachment, PLLA has been shown to favor elastogenesis (*84*). SMCs seeded onto polyhydroxyalkanoates synthesize uniformly aligned elastin and collagen fibers in the direction of blood flow. Previous attempts by Stock *et al.* (*85*) to regenerate elastin on lamina-coated PGA scaffolds in vitro, did not replicate the amounts and ultrastructure of elastin, synthesized by the same scaffolds when implanted in vivo (*85*). This underlies the absence of cell signals controlling elastin mRNA expression in vitro and also leads to the conclusion that biosynthesis and crosslinking of elastin

appears to be one of the most complex and tightly regulated processes during blood vessel maturation. Application of mechanical stimuli (e.g., dynamic stimulation), growth factors (e.g., TGF-β), and of stem cells (e.g., endothelial progenitor cells) can upregulate amounts of elastin biosynthesis within synthetic scaffolds but not to the extent of mimicking native arterial elastin (*84*). Thus, biological scaffolds, and more importantly ECM scaffolds, which theoretically would be expected to elicit more closely native cell responses have gained much attention in the context of elastic tissue regeneration (*84*).

2.5.2 Biological Scaffolds

Biological scaffolds are normally fabricated from one or all the components such as elastin, collagen, glycosaminoglycans and more recently fibrin, which has been clinically approved for promotion of elastin biosynthesis when incorporated in a three dimensional (3D) arrangement within scaffolds. Each of these components differs in the levels of elastin biosynthesis they elicit. Previous studies have shown enhanced elastin biosynthesis by rat neonatal SMCs cultured onto hyaluronic acid gel scaffolds as compared to controls (plastic) (*84*). Collagen scaffolds fail to regenerate substantial elastin in vitro even in presence of seeded vascular SMCs. Long and Tranquillo showed higher levels of elastin biosynthesis by neonatal vascular SMCs seeded onto fibrin scaffolds and within fibrin-collagen constructs (*86*). Cells entrapped and cultured within 3D fibrin gels allowed formation of complex elastin geometries similar to that observed in native elastin. Although promising, above results were generated by

neonatal SMCs and dermal fibroblasts; both cell types that retain high elastogenic potential, unlike adult SMCs (*87*). Also, the organization of elastin fibers into structural networks, and their mechanical properties were not characterized. This study validates previous claims as to the overall superiority of 3D, ECM-based cell scaffolds over 3D synthetic scaffolds or two dimensional (2D) monolayer cell cultures to efforts to simulate the chemical and physical environment of tissues (*86, 88*). Cells within 3D scaffolds come into contact with other cells and ECM in three dimensions and are therefore expected to more closely evoke native cell responses than 2D substrates.

Lee et al. has demonstrated in a study involving SMCs seeded onto ECM scaffolds that the phenotype of SMCs in engineered tissues is strongly regulated by the chemistry of scaffold in vitro, as a result of which SMCs exhibited a differential cell growth and ECM production depending upon the scaffold to which they adhered (*89*). More specifically elastin production was stimulated on PGA scaffolds, used as controls in comparison to enhanced collagen production onto collagen I scaffolds (*89*). In this study 2D culture models still provide useful information since trends in scaffold chemistry-dependent variations of cell phenotype and matrix synthesis are maintained, but not necessarily to the same levels, when translated into a 3D culture system. The physical and mechanical characteristics of the scaffold are important only to exaggerate or dampen scaffold-chemistry-dependent cell responses or direct the structural organization of the synthesized matrix towards defined end goals (*89*). Since gene expression of cells cultured within 3D scaffolds, as within native tissues, can be regulated by

various scaffold-derived cues including cell adhesion molecules, growth factors, and mechanical stimuli, ECM-based scaffolds are more likely to evoke native integrin-ECM interactions and preserve the native cell phenotype; similar variations in the type and extent of cell receptor-ECM ligand interactions with different ECM molecules can profoundly influence cell phenotype and matrix (e.g., elastin) synthesis (*86, 88, 90*). Successful upregulation of elastin synthesis and organization into mature elastic tissue is contingent on the selection of an appropriate scaffold material from among a subset of ECM molecules shown to actively facilitate elastogenesis in vivo

CHAPTER THREE

A CYTOKINE AXIS REGULATES ELASTIN FORMATION AND DEGRADATION

Elastogenesis is the process by which elastin-containing fibers and lamellae are formed. The process is subject to dynamic regulation during the development of tissues such as the lung and aorta where elastin biosynthesis is active in late stages of development and in the early postnatal period but is subsequently attenuated (*91-93*). Steady state, basal levels of elastin expression and breakdown remain low in adult tissues as well as in cells isolated from adult tissues (*94, 95*). Elastin expression is reactivated in diseases such as pulmonary hypertension, dermal elastosis, pseudoxanthoma elasticum, Buschke–Ollendorff syndrome, Moyamoya disease, cigarette smoke- induced emphysema, severe chronic obstructive pulmonary disease (COPD) and forms of progeria (*34, 96-103*), although in many of these disorders the elastin produced is disorganized and dysfunctional (*32-34*).

Much is known about the molecular mechanisms underlying elastin formation in development and disease. This understanding has been advanced through studies of the many human genetic disorders and pathologies of elastin-rich tissues e.g., Costello syndrome (*104*), cutis laxa syndrome (*105*) and Ehlers–Danlos syndrome (*106*). Studies of mouse models have contributed greatly to our understanding of the genes involved in developmental elastin formation (*107-109*). In addition, numerous positive and negative effectors of tropoelastin expression and elastin formation have been identified through in vitro

experimentation (Tables 3.1 and 3.2). Emerging from studies of elastin biology/pathobiology is a cytokine regulatory axis comprised of pro- and anti-elastogenic cytokines. In the present review we focus on highlighting salient components of this regulatory axis and their mechanisms of action on elastin biosynthesis and degradation.

3.1 Cytokines that promote elastin formation

3.1.1 Transforming growth factor β-1 (TGFβ1)

TGFβ1 is a member of the TGFβ superfamily of cytokines. TGFβ activation is normally kept under tight negative control through the process of extracellular matrix sequestration/latency (*110*). Increased TGFβ1 signaling drives pathogenesis of multiple diseases (e.g., fibrotic diseases of the liver, kidney, lung and skin), most of which impact elastin formation and breakdown. For example, TGF-β1 overexpression results in severe interstitial and pleural fibrosis accompanied with increased deposition of elastin (*111*). Overexpression of active TGFβ1 in experimental abdominal aortic aneurysms is associated with preservation of medial elastin (*112*) Indeed, numerous studies have established that TGFβ1 augments both tropoelastin mRNA abundance (*113-116*) and elastin formation (*115, 117*). Mechanistically, TGFβ1 mediates these effects by modulating tropoelastin promoter activity, mRNA stability and elastin degradation.

A number of studies demonstrate that TGFβ1 exerts positive effects on tropoelastin transcription. In human embryonic lung fibroblasts, TGFβ1 activates tropoelastin transcription via the phosphatidylinositol 3-kinase/Akt/p38 signaling

pathway (*118*). In transgenic mice expressing a chloramphenicol acetyltransferase (CAT) reporter gene under control of the human elastin promoter, CAT activity is greatly elevated in the skin of TGFβ1 treated animals (*119*). Furthermore, in chick embryo aorta cells transfected with an elastin promoter-CAT construct, CAT activity is increased by addition of TGFβ1 (*120*). By contrast, elastin promoter/CAT reporter studies performed in skin fibroblasts showed that TGFβ1 did not change the promoter activity (*121*). These and other findings indicate that the effects of TGFβ1 on elastin transcription are cell-type specific. Consistent with this conclusion are findings of McGowan (*122*) showing that TGFβ1 stimulates elastin formation in neonatal lung fibroblasts but not in adult lung fibroblasts or adult lung smooth muscle cells. Furthermore, embryonic aorta cells and tendon fibroblasts also display differential responsiveness to TGFβ1 (*120*). These differential effects have been attributed to cell type-specific nuclear transcription factors that bind to a TGFβ1-responsive element located in the −196 to −12 region of the elastin promoter (*120, 123*).

TGFβ1 also acts post-transcriptionally to stabilize tropoelastin mRNA transcripts (*121, 124*). Indeed, TGFβ1 can relieve tropoelastin mRNA instability in cutis laxa fibroblasts in which tropoelastin mRNA is highly unstable (*116*). Mechanistically, this involves a regulatory GA-rich sequence located in the 3′ UTR of the tropoelastin transcript referred to as the G3A site (*125, 126*). Individuals of several families with inherited cutis laxa have mutations in the tropoelastin gene located in the vicinity of the coding sequencing for this regulatory element (i.e., located near the 5′ end of exon 30) (*125*). Elements

related to the elastin GA-rich sequence are enriched in stable RNAs of other genes and mediate binding of mRNA stability factors, including CUGBP1 (*127*). Whether CUGBP1 or another such protein binds to the G3A site and influences decay of the tropoelastin mRNA and whether TGFβ1 influences binding to the site remain to be established.

The tropoelastin mRNA stabilization effects of TGFβ1 are mediated through several TGFβ signaling pathways including the Smad signaling pathway, the phosphatidylcholine (PC)-specific phospholipase C (PLC)-protein kinase C (PKC)-delta pathway and the TGFβ-activated kinase (TAK1)-stress-activated protein kinase p38 pathway (*124, 128*). This is supported by evidence showing that TGFβ-stimulated tropoelastin mRNA accumulation can be blocked by inhibitors of PLC, PKC and p38 as well as by transgenic expression of the inhibitory Smad, Smad7 (*128*).

TGFβ1 may also stabilize elastin mRNA by reducing the expression of microRNAs. Recent studies show that expression of the microRNA, miR-29, is reduced by TGFβ1 (*129*) and that the 3′UTR of elastin mRNA is a target of miR-29 (*130, 131*). Furthermore, miR-29 mimics decrease elastin mRNA levels in dermal fibroblasts and vascular smooth muscle cells (*132*). Moreover, in the developing mouse aorta, an upregulation in the expression of miR-29 as well as several other microRNAs that have targets in the elastin mRNA (i.e., the miR-15 family members miR-195 and miR-497) accompanies the downregulation of elastin mRNA in the period between the newborn and adult (*130, 131*).

The ability of TGFβ to augment elastin expression also relates to

hyaluronan signaling. Studies have shown that TGFβ1 and hyaluronan oligomers (consisting of 3 to 9 glucuronate and N-acetylglucosamine disaccharides) act synergistically to enhance elastin levels in the extracellular matrix of cultured vascular smooth muscle cells (*133*). Intriguingly, TGFβ treatment of vascular smooth muscle cells from experimentally induced aortic aneurysms does not elicit a change in elastin synthesis, but treatment with a combination of TGFβ and hyaluronan oligomers enhances elastin protein levels in the extracellular matrix (*134*). Hyaluronan oligomers interact with the major receptor for hyaluronan, CD44, and it is thought that hyaluronan oligomers disrupt endogenous hyaluronan interactions with CD44 (*135*). Since CD44 has direct and indirect interactions with other signaling receptors, including TGFβ receptor type I and epidermal growth factor receptor (EGFR), disruption of hyaluronan-CD44 binding can influence the activity of a variety of downstream signaling pathways. The CD44-EGFR interaction may be of particular relevance to the pro-elastin effects of hyaluronan oligomers since EGFR signaling appears to be anti-elastogenic (*136*). Thus, hyaluronan oligomers may interfere with suppressive effects of EGFR signaling on elastin expression. Studies describing EGFR signaling effects on elastin are discussed below.

TGFβ1 also limits elastin degradation by decreasing levels and activity of elastolytic proteases including matrix metalloproteinase (MMP)-2 and -9 (*112*). Indeed, TGFβ blockade exacerbates elastin degradation and decreases levels of elastin in medial layers of blood vessels (*137*). By contrast, overexpression of a mutated, active form of TGFβ1 in animals having experimentally induced aortic

aneurysms leads to reduction in the expression of elastolytic MMPs and preservation of elastic fibers in the medial layers of injured aortas (*112*). TGFβ1 also elicits effects on MMP activity by augmenting expression of tissue inhibitors of MMPs (TIMPs) (*138*). Similarly, TGFβ1 sustains levels of the plasmin inhibitor, PAI-1, which prevents activation of the elastolytic protease MMP-9 (*137, 139*).

3.1.2 Insulin-like growth factor-I (IGF-I)

IGF-1 has been implicated as a positive regulator of elastogenesis occurring in the developing aorta (*140, 141*) and in pathologies including atherosclerosis (*142*). Like TGFβ, IGF-I elicits positive effects on elastin expression (*143-145*). Also similar to TGFβ, the effects of IGF-I on elastogenesis appear to be cell type specific. For example, IGF-I increases steady state levels of tropoelastin mRNA and soluble elastin production in neonatal aortic smooth muscle cells, but it elicits no change in tropoelastin expression in pulmonary fibroblasts, which also express the type I IGF-I receptor (*144*).

IGF-I regulation of elastin expression involves the interaction of two members of the Sp-family of transcription factors, Sp1 and Sp3, with elements of the elastin promoter (*142, 145-147*). These transcription factors have opposing effects on elastin transcription such that Sp1 promotes elastin transcription whereas Sp3 represses Sp1-mediated enhancement of elastin transcription. IGF-I acts to both promote Sp1 binding to the elastin promoter and abrogate Sp3 interaction with the elastin promoter (*142*).

Key to the process by which IGF-I mediates Sp1 interaction with the

elastin promoter is the formation of a complex between Sp1 and phosphorylated retinoblastoma protein (Rb) (*142, 145-147*). IGF-I acts to promote the formation of a cyclinE–cyclin-dependent kinase 2 (cdk2) complex, which mediates cdk2-dependent phosphorylation of Rb on threonine-821 (Thr821) (*147*). Phosphorylation of Rb(Thr821) recruits Sp1 to Rb. The resulting complex binds to a retinoblastoma control element within the elastin gene promoter and stimulates tropoelastin transcription (*147*).

Intriguingly, the IGF-I-induced effects on Rb phosphorylation and elastin expression are counter balanced by pro-proliferative stimuli transmitted through the mitogenic Ras/MEK/ERK pathway. For example, dermal fibroblasts treated with the mitogen, PDGF-BB, display decreased levels of phosphorylated Rb(Thr821) and reduced elastin deposition (*147*). PDGF-BB also increases

Table 3.1: Effectors that augment elastin biosynthesis in cultured cells.

Effector	Cell type	Method of elastin measurement								Publications
		TE mRNA	TE ELISA	Desm ELISA	[^{3}H]-Val/ Leu	Elastin RIA	EM	Elastin ICC	Elastin IP/IB	
Aldosterone	Fibroblast (cardiac, fetal, H)	X			X			X		(Bunda et al., 2007)
Bleomycin	Fibroblast (ligament, fetal, B)				X	X				(Mecham et al., 1981)
Coenzyme Q(10)	Fibroblast (dermis, H)	X								(Zhang et al., 2012a)
Cyclic GMP	Fibroblast (ligament, fetal, B)				X	X				(Mecham et al., 1985)
Cdk4 inhibitor (PD0332991)	Fibroblast (dermis, H)	X			X			X	X	(Sen et al., 2011)
	Fibroblast (dermis, CS subjects, H)							X	X	(Sen et al., 2011)
Dexamethasone	Fibroblast (dermis, TGFβ-R1 mutant, H)	X			X		X	X		(Barnett et al., 2011)
	Fibroblast (ligament, fetal, B)				X	X				(Mecham et al., 1981)
Fibulin-5	Fibroblast (dermis, neonatal, H)	X						X	X	(Katsuta et al., 2008)
Hyaluronan oligomers	VSMC (aorta, R)			X					X	(Joddar and Ramamurthi, 2006)
Heparin sulfate	Fibroblast (dermis, H)	X						X	X	(Annovi et al., 2012)
HGF	Fibroblast (vocal fold, H)		X							(Luo et al., 2006)
IGF-I	VSMC (aorta, neonatal, R)	X			X					(Rich et al., 1992; Wolfe et al., 1993)
	Fibroblast (dermis, H)	X			X			X	X	(Sen et al., 2011)
Insulin	VSMC (aorta, H)				X			X	X	(Shi et al., 2012)
IL-1β	Fibroblast (dermis, adult, H)	X								(Mauviel et al., 1993)
Mek inhibitor (PD98059)	Fibroblast (dermis, H)							X	X	(Sen et al., 2011)
Neuraminidase	VSMC (aorta, H)							X		(Hinek et al., 2008)
Ras inhibitor (radicicol)	Fibroblast (dermis, CS subjects, H)							X	X	(Sen et al., 2011)
Retinoic acid	Fibroblast (dermis, embryo, C)	X			X				X	(Tajima et al., 1997; McGowan et al., 2000)
Stretch	Stem cell (adipose, H)			X						(Colazzo et al., 2011)
	Stem cell (bone) & Fibroblast (ligament, R)	X							X	(Bing et al., 2012)
TGF-β1	Fibroblast (dermis, neonatal, H)	X						X		(Westermarck et al., 1995; Katsuta et al., 2008)
	Fibroblast (dermis, H)	X	X							(Zhang et al., 1995)
	Fibroblast (lung, neonatal, R)	X			X					(McGowan and McNamer, 1990)
	Fibroblast (dermis, H)	X								(Kahari et al., 1992b; Zhang et al., 1995)
	VSMC (aorta, P)		X							(Liu and Davidson, 1988)
TGF-β2	Fibroblast (dermis, H)	X								(Kahari et al., 1992b)

TE, tropoelastin; Desm; desmosine; EM, electron microscopy; AA, amino acid; ICC, immunocytochemistry; RIA, radioimmunoassay; IP, immunoprecipitation; IB, immunoblot; VSMC, vascular smooth muscle cells; H, human; C, chicken; B, bovine; R, rat; CS, Costello syndrome.

levels of phosphorylated Rb(Ser780), which is elevated in Costello syndrome fibroblasts that display H-Ras driven proliferation and decreased elastogenesis. Quenching of the increased proliferation of Costello syndrome fibroblasts by treatment with inhibitors of Ras, MEK or cdk4 induced up-regulation of Rb(Thr821) phosphorylation, decreased Rb(Ser780) phosphorylation and recovery of their elastogenesis deficiency (*147*). These findings fit with observations indicating that an inverse relationship exists between elastin deposition and cell proliferation (*14*).

3.2 Cytokines that inhibit elastin formation

3.2.1 Basic fibroblast growth factor (bFGF)

Basic fibroblast growth factor (bFGF, also known as FGF2) is a major negative regulator of elastogenesis. bFGF decreases elastin gene transcription in aortic smooth muscle cells (*148*) and pulmonary fibroblasts (*149*). Furthermore, in mice bearing compound deficiency of the FGF receptors, 3 and 4, elastin deposition is not downregulated postnatally in the lungs (*150*). While these findings highlight that FGF signaling plays a role in attenuating developmental elastogenesis in the lung, it is unclear whether this involves bFGF or other FGFs. bFGF is the candidate elastin suppressor in the periodontal ligament (PDL), in which elastin expression is normally negligible. bFGF is expressed in the PDL (*151*) and has been shown to suppress transcription of tropoelastin in cultured PDL cells (*152*). Interestingly, PDL cells grown in culture express tropoelastin mRNA (*152*), suggesting that the suppressive mechanism operative in the PDL in

vivo is released when the cells are placed in culture.

bFGF represses elastin gene transcription by augmenting expression of the transcription factor Fra-1 (also known as fos-like antigen 1), that subsequently binds to a sequence located at −564 to −558-bp in the elastin promoter, heterodimerizing with c-Jun to form an inhibitory complex (*153*). bFGF-dependent repression of tropoelastin mRNA expression can be blocked by inhibition of MEK1, indicating that the MEK/ERK pathway mediates the response of the growth factor (*154*).

The potent suppressive effects of bFGF may underlie attenuated/ defective elastogenesis observed in wound healing processes in which bFGF levels are increased, such as in dermal, cerebral, hepatic, renal and tendon wound healing (*155*). bFGF expressed in these in vivo settings or even in cultured cells may oppose the action of positive effectors of elastogenesis. Indeed, bFGF has been shown to inhibit the ability of TGFβ1 to induce elastin expression by vascular smooth muscle cells (*156*). The suppressive effects of bFGF on elastogenesis would appear to be an unfavorable consequence to therapeutic use of bFGF in wound healing, if elastin synthesis is a desired endpoint.

bFGF has also been shown to decrease the expression of mRNA encoding lysyl oxidase (*157*), the enzyme that catalyzes tropoelastin crosslinking. Interestingly, lysyl oxidase inactivates bFGF through promoting covalent crosslinking of bFGF monomers to form multimers (*158*). It is not known whether lysyl oxidase might cross link bFGF to elastin, but bFGF is released by elastase

treatment of cultures of pulmonary fibroblasts and pulmonary artery smooth muscle cell (*149, 159*), suggesting that the growth factor may be bound to elastin. Release of extracellular matrix-bound bFGF has also been reported to occur in response to burn injury of skin, another tissue rich in elastin (*160*). Elastase release of bFGF could contribute to impaired elastin synthesis in pulmonary obstructive diseases in which elastase degradation of elastin is operative.

3.2.2 Heparin-binding epidermal growth factor (HB-EGF)

HB-EGF is an EGF receptor (EGFR/ErbB1) ligand that reduces tropoelastin mRNA expression and matrix accumulation of elastin protein (*161, 162*). HB-EGF mediates these effects through a mechanism that, like bFGF, involves stimulation of ERK1/2 phosphorylation and nuclear accumulation of Fra-1 (*162*). This is supported by findings showing that siRNA suppression of HB-EGF expression leads to increased levels of elastin protein and decreased levels of Fra-1 protein (*161*). In addition, other findings show that inhibition of ERK1/2 activation using MEK1/2 inhibitors reduces both HB-EGF-induced Fra-1 accumulation and HB-EGF-downregulation of tropoelastin mRNA expression (*162*). HB-EGF also induces the expression of bFGF, which could amplify the suppressive effects of HB-EGF on elastin expression (*162*).

3.2.3. Epidermal growth factor-like growth factor (EGF)

EGF is a cytokine produced in response to injury (*163, 164*). EGF and TGFα-like cytokines are released by neo- natal rat lung fibroblasts treated with

neutrophil elastase, a protease associated with excessive elastolysis in emphysema (*165*). Similar to the action of HB-EGF, EGF causes decreases in tropoelastin mRNA stability and insoluble elastin deposition (*136, 166*). Tropoelastin mRNA destabilization by EGF can be blocked by the EGFR inhibitor, AG1478, and the MEK/ERK inhibitor, U0126 (*136*). Dicamillo et al. (2006) concluded that the EGFR/MEK/ERK signaling cascade acts in opposition to TGFβ1 signaling to override the positive effects of TGFβ1 on tropoelastin mRNA stability.

3.2.4 Transforming growth factor-α (TGFα)

TGFα is an EGFR ligand that is expressed by airway epithelial and interstitial cells following lung injury (*164, 167, 168*), including the pathogenesis of cystic fibrosis lung disease (*169*). TGFα is thus implicated in the elastolysis and defective elastin repair associated with pathological remodeling of the lung. Indeed, overexpression of TGFα in the neonatal lung leads to disorganized and fragmented elastin fibers in the alveolar septae (*170*). Like EGF, TGFα is released by lung fibroblasts in response to neutrophil elastase treatment, causing tropoelastin mRNA destabilization via activation of the EGFR/MEK/ERK signaling cascade (*136, 171*).

3.2.5 Tumor necrosis factor-alpha (TNF-α)

TNF-α, a proinflammatory cytokine, suppresses tropoelastin mRNA levels in skin fibroblasts, aortic smooth muscle cells and lung fibroblasts (*121, 165*).

Conversely, TNF-α knock- out mice display increased vascular elastin expression (*172*), which may account for findings that TNF-α-deficient mice are resistant to aneurysm formation (*173*).

In cultured aortic smooth muscle cells, the inhibitory effects of TNF-α on elastin gene expression involve the transcription factor AP-1 binding to a region in the elastin promoter located between −290 and −198 bases pairs (*113*). AP-1 complexes are heterodimers of Jun and Fos family members, each activated via the MAP kinase signaling pathway. As mentioned above, bFGF exerts its repressive effects on elastin transcription via the Fos family member Fra-1 (*153*), downstream of MEK1/ERK1/2 pathway signaling (*154*). It is therefore possible that TNF-α also downregulates tropoelastin transcription via MAP kinase pathway effects on AP-1.

Another dimension to the relationship between TNF-α and elastin is that TNF-α promotes elastin breakdown through enhanced release of elastolytic enzymes (*174-176*). For example, TNF-α induces production of the elastolytic MMPs, MMP-2 and MMP-9, by vascular smooth muscle cells (*177*).

Like EGF, TNF-α is released by lung fibroblasts in response to neutrophil elastase treatment and has been shown to abrogate TGFβ-induced enhancement of tropoelastin mRNA expression (*121, 165*). Enhanced TNF-α expression also occurs in response to cigarette smoke exposure and its increase correlates with pulmonary elastin breakdown, a precursor to emphysema (*178*). TNF-α induced elastin degradation is also linked to vasculitis stemming from Kawasaki disease as well as vascular aneurysms (*179*). In fact, in Lactobacillus

casei cell wall extract-induced coronary arteritis, abrogation of TNF-α activity by TNF-α-blocking agents or deletion of the TNF receptor-1 protects against elastin degradation and aneurysm formation (*179*). Furthermore, doxycycline, which inhibits MMP-9 enzymatic activity, can mitigate TNF-α-induced coronary elastin breakdown (*180*).

3.2.6 Interleukin (IL)-1β

IL-1β is a pro-inflammatory cytokine released in pathologies involving elastin-rich tissues (e.g., COPD and asthma) (*181*). Similar to TNF-α, IL-1β enhances the release of elastases in skin and uterine fibroblasts (*182, 183*). Induction of elastase expression may underlie the disruption of elastin fibers observed in alveolar septa of mouse lungs induced to express IL-1β (*184, 185*). Moreover, mice deficient in a negative regulator of IL-1β signaling, interleukin-1 receptor antagonist, develop femoral artery aneurysms displaying degradation of both the internal and external elastic lamina (*186*).

In addition to its effects on elastase expression, IL-1β causes changes in elastin transcription. In neonatal lung fibroblasts IL-1β reduces elastin gene transcription (*187, 188*). The mechanism by which elastin transcription is negatively regulated in response to IL-1β is most thoroughly defined in neonatal lung fibroblasts. In these cells, IL-1β promotes nuclear localization of the p65 subunit of NF-κβ that subsequently interacts with Sp1 to downregulate elastin transcription (*188*). This is supported by findings showing that: 1) overexpression of p65 downregulates tropoelastin mRNA levels (*188*), and 2) that inhibition of

NF-κβ blocks the effects of IL-1β on elastin transcription in neonatal rat lung fibroblasts (*189*). Similarly, other studies show that p65 binds Sp1 proteins and interferes with transcription of at least one other extra- cellular matrix protein, type α1(I) collagen (*190*).

The effect of IL-1β on NF-κβ also increases the expression of the transcriptional repressor CCAAT/enhancer-binding protein (C/EBP)-β (LIP), which binds to a GCAAT-containing sequence located at −56 to −62 bp in the elastin promoter (*189*). Like IL-1β, C/EBPβ protein levels are increased in lung

Table 3.2: Effectors that inhibit elastin biosynthesis in cultured cells.

Effector	Cell type	Method of elastin measurement										Publications
		TE mRNA	TE ELISA	Desm ELISA	[^{3}H]-Val/ Leu	Elastin RIA	AA analysis	EM	Elastin ICC	Elastin IP/IB	Fastin elastin	
Ascorbic acid	VSMC (aorta & lung, P)	X	X									(Davidson et al., 1997)
	Fibroblast (dermis, P)	X	X									(Davidson et al., 1997)
bFGF (FGF-2)	VSMC (aorta, R)	X							X	X		(Wachi et al., 2005)
	VSMC (aorta, P)		X									(Davidson et al., 1993)
	Fibroblast (dermis, H)	X	X									(Davidson et al., 1993; Zhang et al., 1995)
	Fibroblast (vocal fold, H)	X										(Luo et al., 2006)
Cdk2 inhibitor (CVT313; Purv)	Fibroblast (dermis, H)	X							X			(Sen et al., 2011)
	Fibroblast (dermis, CS subjects, H)								X	X		(Sen et al., 2011)
Chondroitin sulfate	VSMC (aorta & ductus, fetal, S)		X	X					X			(Hinek et al., 1991)
Cycloheximide	Fibroblast (ligament, fetal, B)				X	X						(Mecham et al., 1981)
Dermatan sulfate	VSMC (aorta & ductus, fetal, S)		X	X					X			(Hinek et al., 1991)
Elastin mimetic peptides	VSMC (aorta, H)										X	(Patel et al., 2011)
EGF	Fibroblast (lung, fetal, RFL-6, R)		X				X			X		(DiCamillo et al., 2006)
Estradiol	SMC (vaginal, H)										X	(Chakhtoura et al., 2012)
HB-EGF	Fibroblast (lung, neonatal, R)	X										(Liu et al., 2003)
	Epithelial cells (mammary gland, H)								X	X		(Bertram and Hass, 2009)
IFN-γ	Fibroblast (dermis, H)	X										(Kahari et al., 1992a)
IL-1β	Fibroblast (lung, neonatal, R)				X		X	X				(Berk et al., 1991)
miR-29 mimics	Fibroblast (dermis, H)	X										(Zhang et al., 2012b)
	VSMC (aorta, H)	X										(Zhang et al., 2012b)
Okadaic acid	Fibroblast (dermis, H)	X										(Westermarck et al., 1995)
PDGF-BB	Fibroblast (dermis, H)				X				X			(Sen et al., 2011)
PMA	Chondrocyte (auricle, fetal, B)	X	X									(Parks et al., 1992)
Proteasome inhibitor (MG132)	Fibroblast (lung, neonatal, R)	X										(Kuang and Goldstein, 2005)
Theophylline	Fibroblast (ligament, fetal, B)				X	X						(Mecham et al., 1981)
TGFBRI inhibitor (anisomycin)	Fibroblast (lung, fetal, RFL-6, R)	X										(DiCamillo et al., 2006)
TGF-β neutralizing antibody	Fibroblast (lung, fetal, RFL-6, R)	X										(DiCamillo et al., 2006)
TNF-α	Fibroblast (vocal cord, H)		X									(Luo et al., 2006)
	Fibroblast (dermis, H)	X										(Kahari et al., 1992a)
	VSMC (aorta, R)	X										(Kahari et al., 1992a)
TPA	Fibroblast (dermis, H)	X										(Kahari et al., 1992a)
	VSMC (aorta, R)	X										(Kahari et al., 1992a)
Vitamin D_3	Chondrocyte (auricle, fetal, B)	X	X									(Pierce et al., 19

TE, tropoelastin; Desm; desmosine; EM, electron microscopy; AA, amino acid; ICC, immunocytochemistry; RIA, radioimmunoassay; IP, immunoprecipitation; IB, imm
vascular smooth muscle cells; H, human; B, bovine; P, pig; R, rat; S, sheep; Purv; purvalanol; PMA, phorbol myristate acetate; TPA, 12-O-tetradecanoylphorbol-13-acetate; CS, Costello syndrome.

fibroblasts exposed to cigarette smoke (*191*). Importantly, levels of C/EBPβ proteins are regulated in lung fibroblasts by the ubiquitin-proteasome path- way, and proteasome inhibitor treatments downregulate tropoelastin mRNA expression (*192*). C/EBP family members also bind to Rb, and the complexes bind to C-EBP binding sites on DNA (*193*). Whether Rb-C/EBP proteins interfere with the pro-elastin transcriptional activity of Rb-Sp1 remains to be determined.

3.3 Cytokines that have dual effects on elastin formation

3.3.1 IL-1β

By contrast to the anti-elastogenic effects exerted by IL-1β on neonatal lung fibroblasts, several studies show that IL-1β promotes tropoelastin mRNA expression in adult dermal fibroblasts (*194, 195*). For example, in dermal fibroblasts isolated from transgenic mice expressing the human elastin promoter linked to a CAT reporter, IL-1β increases CAT activity (*194*). Furthermore, subcutaneous IL-1β injection into these transgenic mice increases CAT activity in the skin, indicative of a robust positive effect on elastin transcription (*196*). The molecular basis for the effects of IL-1β on elastin expression in skin fibroblasts is not clear.

3.3.2 TGFβ

Despite the preponderance of evidence indicating that TGFβ is a pro-elastogenic factor, increased TGFβ activity as seen in Marfan syndrome (MFS) (*197*) is associated with elastic fiber degeneration and decreased tropoelastin

mRNA levels (*198*). This, together with the fact that noncanonical, Smad-independent, TGFβ-mediated Erk1/2 activation drives aortic aneurysm progression in MFS (*199*), appears to indicate that TGFβ signaling through the noncanonical, Smad-independent, MAP kinase pathway has suppressive effects on elastin RNA levels.

3.4 Conclusions

The cytokine-governed elastin regulatory axis is comprised of pro- and anti-elastogenic cytokines that control the biosynthesis and break- down of elastin through transcriptional and post-transcriptional mechanisms. How cytokines exert opposing effects on elastin transcription (Fig. 1) hinges on the

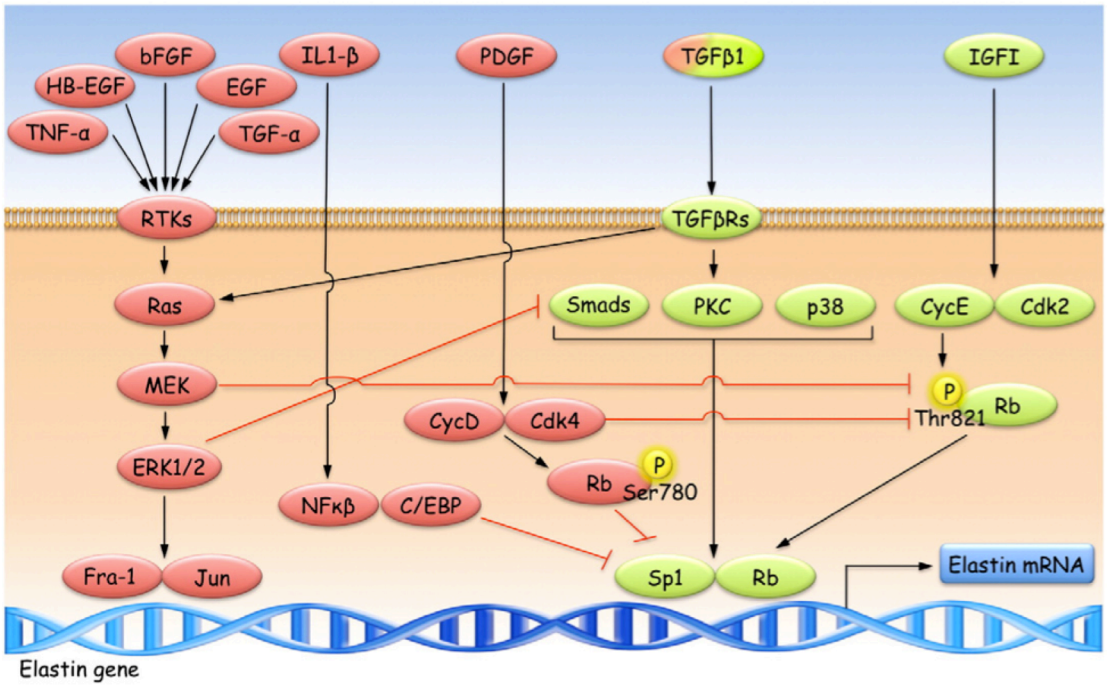

Figure 3.1. Cytokine signaling cascades that influence tropoelastin transcription. Cytokines and signaling pathway intermediates highlighted in *red* act to suppress tropoelastin transcription. Cytokines and signaling pathway intermediates highlighted in *green* act to promote tropoelastin transcription. RTK, receptor tyrosine kinases.

way in which they influence cell cycle regulatory constituents, particularly cyclin-cyclin dependent kinase complexes and their substrates. For example, cytokines such as IGF-I induce tropoelastin transcription by promoting cyclin E/cdk2-dependent phosphorylation of Rb(Thr821) which recruits Sp1 to bind the elastin gene promoter and stimulate transcription (*147*). Counterbalancing this process is mitogenic cytokine signaling via the Ras/MEK/ERK cascade. Cytokines such as EGF, HB-EGF and TGFα, which stimulate this cascade through activation of EGFR, exert suppressive effects on elastin biosynthesis and/ or catabolism. Likewise, Ras/MEK/ERK pathway signaling mediated by bFGF, PDGF-BB and TNF-α also elicit suppressive effects on elastin expression, as does noncanonical, Smad-independent Ras/MEK/ERK signaling stimulated by TGFβ1. Importantly, cytokine stimulated Ras/MEK/ERK signaling acts in opposition to the pro-elastin effects of canonical TGFβ1 signaling, possibly through attenuation of nuclear accumulation of activated SMADs (*200*). Similarly, Ras/MEK/ERK-mediated initiation of the cell-cycle progression acts to attenuate the elastin transcription-promoting effects of IGF-I.

CHAPTER FOUR

DNA MICROARRAY BASED TRANSCRIPTOMIC PROFILING TO IDENTIFY GENES THAT ARE SIMILARLY REGULATED IN PROCESSES IN WHICH ELASTOGENESIS IS A KEY COMPONENT

4.1 Introduction

DNA microarray technology is a high-throughput quantification of the expression of thousands of genes at the same time within a sample. The technology is based on a DNA chip containing thousands of DNA probes (oligos), each containing on the order of picomoles of a section of DNA sequence localized to a specific location on the chip. The chip comes into contact with copy DNA (cDNA) created from an experimental sample and cDNAs hybridized to the probes. Probe-target hybridization can then be detected and quantified by fluorophore-labeled targets. DNA microarray analyses generate vast amounts of data on expression intensities within the sample for each DNA probe present on the chip. The advent of this massive data-generating assay results in endless approaches to data analysis.

This technology is novel in that it enabled quantification of the co-expression of sets of genes in a given tissue in given conditions that can be analyzed to predict gene regulatory networks. DNA Microarray studies suggest a correlated action of different elements of the gene regulation machinery and their potential interaction. The information gained offers an unprecedented opportunity to fully characterize biological processes.

4.2 Materials and Methods

4.2.1 Identification of Processes in which Elastogenesis as a Key Component.

The formation of elastic fibers, elastogenesis, is prominent in fetal and postnatal development but adult fibroblasts do not assemble elastic fibers under normal conditions (*201, 202*). During elastogenesis the elastin gene is upregulated from a quiescent state and then returns to a baseline level. We identifie processes where the elastin gene is upregulated as in the window of development.

Elastic fibers synthesized during development are considered the gold standard by which wound injury elastic fibers and in vitro elastic fibers are compared and of the quality that tissue engineers aspire to synthesize. However, considering other processes in which elastin is a key component is essential in order to further refine the “elastogenic developmental set” and to eliminate genes that are specific to development and inessential to elastogenesis. In vivo processes for consideration occurred in tissues in which mature elastic fibers are a primary component. Microarray data from in vitro cell culture was selected in cells that synthesize elastic fibers in their derived tissue *in vivo* (i.e., vascular smooth muscles cells (VSMCs), fibroblasts, etc.) (*21-24*).

Criteria for determining processes in which elastogenesis is a key component relied upon 1) the process occurs in a recognized elastic fiber containing tissue or elastin producing cell as determined by histological literature and 2) the elastin gene is significantly upregulated over a time course.

It is a recognized risk that comparison of commonly regulated genes from

lower quality or defective elastic fibers may exclude certain critical genes. It is also a possibility that identification of significantly regulated genes in an opposing direction to development may elucidate genes responsible for elastic fiber defects in wound repair and *in vitro*.

4.2.2 Transcriptomic Profiling During Developmental Models

The formation of elastic fibers, elastogenesis, is prominent in fetal and postnatal development and developmental elastin fibers are the gold standard by which tissue engineered elastin fibers are compared. It is therefore essential to understand the biological processes occurring during elastogenesis through DNA microarray analysis of simultaneous gene expression during development of elastin-containing tissues of animal models.

4.2.2.1 Transcriptomic Profiling of the Developing Lung

Elastogenesis primarily occurs during development with elastin produced in the lung during late fetal, neonatal, and early postnatal growth coinciding with alveolarization (*91*). Tropoelastin mRNA is barely detectable in the adult lung. We isolatee RNA from C57BL/6 mouse lung tissue from postnatal day (d) 5 to adult (8 months) at 5 developmental stages (4 samples/stage) before, during and after elastogenesis.

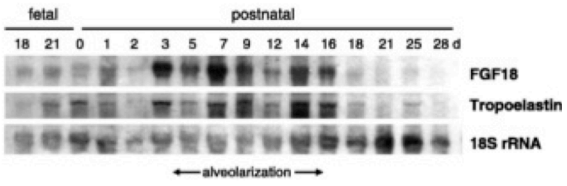

Figure 4.1. Elastin expression profile in developing rodent lung. A study by Chailley-Heu illustrates a developmental peak in elastin expression profile in postnatal rat lung by Northern blot showing an increase in elastin expression corresponding to alveolar septation in the rat (*1*)

4.2.2.1.1 RNA Preparation from Developing Lung Tissue

Lungs from wild type C57BL/6 mice were extracted for RNA preparation at 5, 7, 10, 14, and 225 days postnatal (n = 3 for each time point, n = 4 for 225 days). Mice aged 5, 7, and 10 days postnatal were sacrificed by decapitation, mice aged 14 days were sacrificed by CO_2 inhalation followed by cervical dislocation, and adult mice aged 225 days postnatal were sacrificed by isoflurane inhalation followed by cervical dislocation according to standard laboratory protocols approved by the Animal Research Committee at the Medical University of South Carolina and at Clemson University. For each mouse, the left lung was removed and stored in RNALater® solution pending RNA extraction. Due to protocol concerning differences in lung function at various time points, It was not possible to control the euthanation procedure variations prior to lung tissue extraction. Neonatal animals have underdeveloped lungs that would not respond to CO_2 inhalation while it would be inhumane not to treat adult animals otherwise. It is possible that the inhalation procedure variations could contribute to differences in gene expression but efforts were taken to act fast minimizing the effects of chemicals on lung tissue.

For each mouse, a maximum of 30 mg lung tissue was homogenized in Trizol® reagent and extracted with 0.2 mL chloroform per mL Trizol. Total RNA was extracted from the aqueous phase of each sample with a Qiagen RNeasy® Plus Mini Kit according to the manufacturer's instructions. The RNeasy technology combines the selective binding properties of a silica-based

membrane with the speed of microspin technology. Genomic DNA was removed in a single, rapid centrifugation step by passing each sample over a gDNA eliminator column. RNA longer than 200 bases within the sample is then bound to the RNeasy silica membrane with a specialized high-salt buffer system while contaminants are efficiently washed away. High-quality RNA was eluted in 30 µl water of which 1 uL was used to measure concentration and quality with a Bioanalyzer 2100 (Agilent Technologies, Palo Alto, CA).

4.2.2.1.2 Synthesis of Biotin-Labeled cRNA Targets and Hybridization to Affymetrix Gene Chips

Synthesis of double-stranded cDNA from RNA, in vitro transcription of biotin-labeled cRNA targets, and fragmentation of target cRNA were performed as outlined by Affymetrix protocols (Affymetrix, Santa Clara, CA). Fragmented cRNA samples were hybridized overnight at 45°C to Affymetrix Mouse GeneChip MG_U74Bv2. Posthybridization washing and phycoerythrin-streptavidin staining and fluorescence scanning were performed using Affymetrix instrumentation in accordance with manufacturer protocols.

4.2.2.1.3 Analysis of DNA Microarray Data

The resulting scans (CEL files) containing gene hybridization intensities were normalized using Robust Multichip Average (*203*) implemented with the ArrayQuest web-based analysis system. Normalized hybridization values were imported into the analysis tool dChip 2005 (*204*) for subsequent analysis. Gene

probe IDs differentially expressed during lung development were identified using both statistical analysis and presence thresholds. Statistical analysis was performed with Significance Analysis of Microarrays (SAM, www-stat.stanford.edu). In this analysis, a gene was determined to be differentially regulated if the false discovery rate (FDR) < 5%. A gene was considered "present" if at least two of three samples per timepoint had non-absent calls (P or M) in at least one timepoint.

4.2.2.2 Transcriptomic Profiling of Developing Aortic Tissue

Tropoelastin expression in the aorta occurs at the end of embryonic development through one month postnatal development in mice (*205, 206*). Dr. Robert Mecham (Washington University School of Medicine, St. Louis, MO) contributed raw DNA microarray data on Affymetrix MG_U74Bv2 chips (unpublished) from an analysis of mouse aortae ranging from embryonic day 14 to postnatal day 180. There was 1 sample (each a pool of 3 aortas) for each developmental stage. Statistical analysis was performed by standard deviation across a gene probe > 0.5 and having a gene presence call > 20% for developmental stages of a particular gene probe.

4.2.3 Transcriptomic Profiling During Injury Models

One challenge to microarray analysis of developmental models is to distinguish which processes are important for specific elastic fiber formation and which represent general changes that occur during development. This issue was

addressed with incorporation of additional animal models in which elastic fiber formation occurs such as during wound healing processes. The goal was how to distinguish the elastic fiber formation-specific pathways from developmental regulatory pathways.

4.2.3.1 Transcriptomic Profiling of a Lung Injury

Transcriptome data was analyzed from a time course of mouse lung injury induced by intraperitoneal injection of naphthalene (*31*). Naphthalene injection had been shown to selectively kill Clara cells in the lung while leaving bronchiolar stem cells intact, allowing these cells to repair the damaged tissue and fully restore the epithelial layer (*207*). Due to the high levels of elastic fibers present in the lung, a model of lung repair that fully restores a normal epithelium should show significant expression changes in genes related to elastic fiber formation

Mouse lungs were injected with naphthalene and lungs collected in at 1 d, 2 d, 3 d, and 6 d post-injection and compared to saline-injected control mice (n=4 samples/timepoint) and microarray analysis was performed at the University of Pittsburgh Cance Center Clinical Microarray core using Codelink 20K Mouse Bioarrays (Applied Microarrays, Tempe, AZ). Microarray data files (CEL files) were obtained from the National Center for Biotechnology Information Gene Expression Omnibus (NCBI GEO) Datasets website. The processed data had been log2 transformed and normalized to the geometric mean across all samples. The online CNIO IDconverter tool was then used to obtain gene symbols and EntrezGene IDs from the provided GenBank Accessions for all

transcripts (*208*). Analysis of variance (ANOVA) was used to statistically compare each post-injury time point (n = 4 for each time point) and control lung samples (n = 4) with alpha set at 0.05. This means that if a p-value for a gene probe is < 0.05 then the null hypothesis that there is no difference between timepoints is rejected. A gene probe was determined to be “present” if at least two of four samples per timepoint had non-absent calls (P or M) in at least one timepoint.

4.2.3.2 Transcriptomic Profiling of a Skin Injury

In order to eliminate organ specific gene expression in an injury model, we identified another injury model in an elastin-rich organ, the skin. Gene expression during wound healing by punch biopsy in the mouse skin was observed in various stages of healing from 1 to 6 days post-injury (*209*). The wound healing of the skin after an injury involves the formation of elastic fibers, however the quality of the fibers is less than optimal with disorganization and an increase in fibrosis resulting in some scar tissue. For our studies, we obtained the raw microarray data from the National Center for Biotechnology Information Gene Expression Omnibus (NCBI GEO) Datasets website.

CEL files for the microarray analysis were downloaded from the NCBI GEO Datasets website and normalized by the Robust Multichip Average (RMA) method using Affymetrix Expression Console software. To be considered present, a gene must be called present in at least two of the three control samples and in at least two out of three samples in one of the post-injury time

points. Analysis of variance (ANOVA) was used to statistically compare each post-injury time point (n = 3 for each time point) and control lung samples (n = 3) with alpha set at 0.05. This means that if a p-value for a gene probe is < 0.05 then the null hypothesis that there is no difference between timepoints is rejected. A gene probe was determined to be “present” if at least two of three samples per timepoint had non-absent calls (P or M) in at least one timepoint.

4.2.4 Transcriptomic Profiling During In Vitro Elastic Fiber Formation

One challenge to microarray analysis of animal models is to distinguish which processes are important for specific elastic fiber formation and which represent general changes that occur in a complex living organism. This issue was addressed with incorporation of the following in vitro culture model in which versican variant V3 stimulates elastic fiber formation in vascular smooth muscle cells (VSMCs). The goal was how to identify the elastic fiber formation-specific pathways from the total changes in gene expression.

4.2.4.1 Versican V3-transduction of Vascular Smooth Muscle Cells (VSMCs)

Versican, a large (>1000kDa) chondroitin sulfate proteoglycan is found in the extracellular matrix (ECM) of a variety of soft tissues. The smallest (73kDa) of the 4 identified splice variants has been reported to augment tropoelastin expression and elastic fiber formation in rat VSMCs(*210*), however the mechanism by which V3 overexperession upregulates elastogenesis is unclear. To identify changes in gene expression that may underlie V3 induced

elastogenesis, we employed DNA microarray expression analysis to quantify shifts in mRNA levels in V3 transduced and control ASMCs.

Primary rat vascular smooth muscle cells (VSMCs), passage 8-12, were transduced with lentiviral vector containing versican (V3) variant or control (empty vector) in the laboratory of Dr. Thomas Wight (Benaroya Research Institute at Virginia Mason, Seattle, WA). Of the six sets or pair of transductions, four pairs were cultured and harvested at the same time. One pair was from the same transduction but cultured at an earlier date. Another sample pair was from a different harvest of primary rat VSMCs and from a different transduction. All six sample pairs were grown for 15-21 days and the process of RNA extraction begun by the SolutionD method at the laboratory of Dr. Thomas Wight. The samples were then sent to Dr. Argraves lab for further RNA processing using RNeasy Plus Mini Kit (Qiagen) and integrity and concentration determined with a Bioanalyzer 2100 (Agilent Technologies, Palo Alto, CA).

4.2.4.2 DNA Microarray of V3-transduced VSMCs

Messenger RNA (mRNA) for all sets of V3-transduced VSMCs and empty vector-transduced VSMCs were reverse transcribed at the same time, to control for RT variations. Synthesis of biotin-labeled cRNA targets were made from the mRNA and hybridized onto Affymetrix rat GeneChips, RAE230A. Data was normalized by the Robust Multichip Average (RMA) method using Affymetrix Expression Console software. A gene was considered “present” if at least three of six controls or three of six V3-transduced samples had non-absent calls (P or

M). Statistical analysis using a paired Student's T test was performed for each gene probe to comparing the samples pairs each containing a control and experimental sample. A gene was considered statistically significant if it was "present" and $p < 0.05$. Additional analysis of the effects of V3 expression on VSMCs included a parameter to measure the ratio of average V3-transduced VSMCs gene expression vs. average empty vector-transduced VSMCs gene expression. Significance was set at a fold change of at least ±1.5 (at least 50% difference in expression levels).

An alternate approach to data analysis opted to average the normalized intensities from the 4 sample pairs cultured and harvested at the same time so as to treat the 4 samples as 1 sample pair. Subsequent statistical analysis was performed on the 3 sample pairs with a paired Students T-test across a gene probe and deemed significant if $p<0.05$ for a gene.

4.2.5 Convergent Analysis of Microarray Datasets

Information from the five DNA microarrays studies in which elastogenesis is a key component are summarized below including the most appropriate statistical analysis method for the given data to identify genes significantly regulated in each process (**Table 4.1**). Because the individual analyses were performed on various DNA microarray chips and identified by Probe Set IDs specific to their respective chip, a common ID for genes was needed to compare data from different microarrays. All Probe Set IDs from various chips were converted to gene symbols and re-identified as Mouse Genome 430 2.0 Probe

Table 4.1. Microarray datasets in which elastogenesis is a key component used in the convergent analysis.

Sample	Description	Source of Transcriptomic Data	Number of Genechips/ Sample	Statistical Criteria
Lung Development	Mouse lungs from P5 – 8 months (5 developmental stages; 3 samples/stage)[1]	Dr. Argraves (MUSC)	3-4/stage	FDR <5% (using SAM)
Aorta Development	Mouse aorta from E14 - P6 months[1]	Dr. Mecham (Wash Univ.)	1/stage (each a pool of 3 aortas)	StDev >0.5; Presence call >20%
V3-Transduced ASMCs	Rat aortic smooth muscle cells transduced with retrovirus expressing versican V3 or empty vector control[2]	Dr. Argraves (MUSC) and Dr. Wight (Benaroya Inst.)	6/ experimental group	p <0.05 (using Student's T-test)
Lung Injury	Mouse lung from 1-6 days following naphthalene injury and unwounded controls[3]	Snyder JC et al., 2009 (Data available through NCBI GEO DataSets)	4/stage	p <0.05 (using ANOVA)
Skin Injury	Mouse skin from 6h-10 days following skin punch biopsy and unwounded controls[4]	Chen L et al., 2010 (Data available through NCBI GEO DataSets)	3/stage	p <0.05 (using ANOVA)

[1], Affymetrix MG_U74Bv2 chips
[2], Affymetrix RAE230A chips
[3], Applied Microarrays Codelink 20K Mouse Bioarrays
[4], Affymetrix MG430v2.0 chips
E, embryonic day; P, postnatal; MUSC, Medical University of South Carolina; FDR, false discovery rate; StDev, standard deviation; NCBI GEO, National Center for Biotechnology Information Gene Expression Omnibus; ANOVA, analysis of variance

Set IDs using the Affymetrix NetAffx conversion tool. Using DChip microarray analysis software, the five gene sets were converged to determine the differentially regulated genes common to the 5 datasets. Heat maps for this set were created using GeneMesh to graphically represent expression patterns.

4.2.6 Microarray Validation of Gene Expression with Quantitative RT-PCR

Quantitative real-time polymerase chain reaction (qRT-PCR) was used to confirm expression changes observed in the microarray analysis. First-strand cDNA was prepared from total RNA (1 µg) using the iScript cDNA synthesis kit (Bio-Rad, Hercules, CA) according to the manufacturer's specifications. cDNA preparations were diluted 1:10, and 3 µL was used in 10-µl reactions.

The elastin gene was targeted with the TaqMan Gene Expression Assays (Applied Biosystems/Life Technologies, Grand Island, NY) containing primers for mouse/rat tropoelastin and a probe spanning the tropoelastin exon boundary 36-37. Other primers designed by Primer3 and NCBI Blast for genes identified by DNA microarray expression profiling to be regulated by microarray analysis were used in 10 μL reactions with the iQ SYBR green Supermix reagent (Bio-Rad, Hercules, CA).

Reactions were amplified in an iCycler real-time PCR detection system (Bio-Rad, Hercules, CA). The resulting data were analyzed with the PCR Miner software, which calculates individual threshold cycle values and gene efficiency for a set of primers. All gene expression levels were normalized to a housekeeping gene that is constitutively expressed at a relatively constant level across many or all known conditions. (e.g., βactin, GAPDH, and TATA-box binding protein) expression levels.

4.2.7 DNA-Chip Analyzer (dChip)

DNA-Chip Analyzer (dChip) (www.dchip.org) is a Windows software package for probe-level (e.g. Affymetrix platform) and high-level analysis of gene expression microarrays and SNP microarrays (*211, 212*). Gene expression or SNP data from various microarray platforms can also be analyzed by importing as an external dataset. dChip displays normalized probes from CEL files and can pool information across multiple arrays and automatic probe selection to handle cross-hybridization and image. Many high-level analyses are available in dChip,

but for our studies we utilized sample comparison, hierarchical clustering, SNP data visualization along the chromosome, and linkage analysis. In these functions the gene and sample information are correlated with the analysis results.

4.2.8 GeneMeSH

Another microarray analysis tool integrates categories available in the Medical Subject Headings (MeSH) hierarchical index with a given query set of genes. Additional tools are embedded as links to Entrez Gene information, Gene Ontology information, KEGG metabolic pathway diagrams, and intermolecular interaction information. An important visualization tool generates heat maps of Z-score normalized expression intensity values organized into MeSH clusters

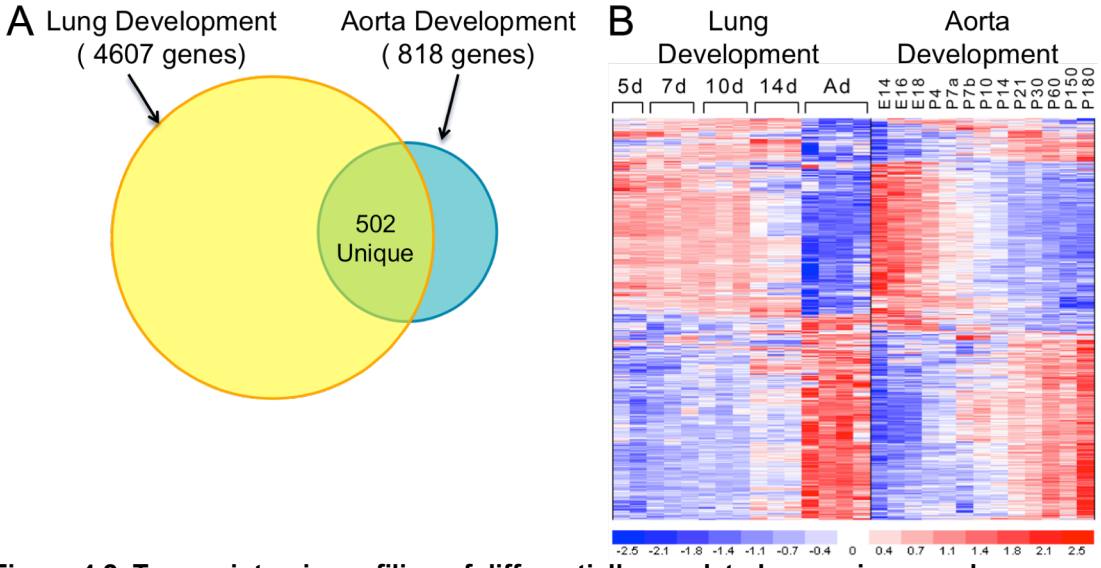

Figure 4.2. Transcriptomic profiling of differentially regulated genes in normal development reveals 502 unique genes. This group of genes known to regulate elastogenesis (i.e., elastin). There are likely genes not yet identified as regulating elastogenesis as well as genes incidental to elastic fiber assembly and common to development. ***A*** represents a schematic of convergent analysis to identify 502 genes common to the "developmental set" and ***B*** graphically depicts the heatmap of differential gene expression. There are many similar expression patters in the set.

(*213*). GeneMesh makes use of the heatmap.2 function in the R gplots package and probe pair annotations available through Bioconductor (*214*). GeneMeSH operates on gene expression data derived from microarray platforms Affymetrix, Agilent, and Illumina

4.3 Results

4.3.1 Transcriptomic Profiling of Developing Elastic Tissues

Convergent analysis of the developing mouse lung and developing mouse aorta revealed a common “developmental set” of 502 unique genes significantly regulated (**Figure 1**). Many of the genes have previously been associated with elastogenesis, while many may represent regulatory genes yet to be implicated in elastogenesis. It is unlikely that all 502 are involved in elastogenesis and may be an artifact of genes commonly regulated in development.

4.3.2 Transcriptomic Profiling of V3-transduced VSMCs Analysis of DNA microarray expression profiling data revealed that V3 significantly regulated expression of 783 genes (1090 probes) (**Figure 1**).

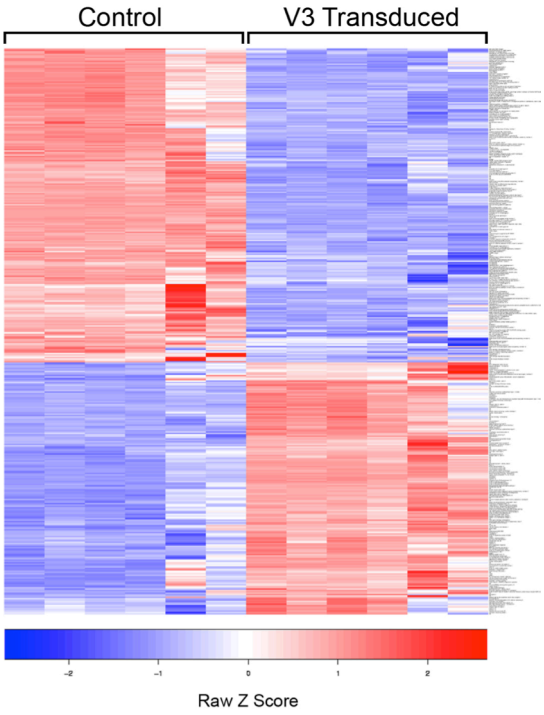

Figure 4.3. Heatmap displaying significantly regulated genes in response to Versican V3 expression in vascular smooth muscle cells (VSMCs). 1090 differentially expressed probes (783 individual genes) in aortic smooth muscle cells transduced to express versican V3 variant or with empty viral vector (Control). Fold change ≥1.5, p-value<0.05.

V3 up-regulated the expression of elastin (Eln) (3.3 fold) as well as a number of genes previously shown to be critical for elastogenesis including fibulin-5 (Fbln5) (7 fold), fibulin-2 (Fbln2) (2 fold), and neuraminidase (Neu1) (8.7 fold). Several other genes known to promote elastogenesis were down-regulated in V3 transduced ASMCs including transforming growth factor beta 1 (Tgfb1) (-1.5 fold) and microfibrillar associated protein 5 (Mfap5/Magp-2) (-2.4 fold). No change was detected in the expression of transcripts encoding a number elastin-related genes including lysyl oxidase (Lox), Lox-like protein (Loxl), Loxl2, fibulin-3, fibulin-4, fibrillin-1, fibrillin-2, Magp1, Mfap1, Ltpb4, emilin-1 and Igf-1. Together, these data demonstrate that versican V3 induces significant changes in mRNA expression of genes associated with elastogenesis.

4.3.3 Determination of the Elastogenic Gene Set

The process used to analyze the data from each microarray study and to combine the data from the five studies is summarized in Figure 4.5. Individual gene probes were determined to be significantly regulated within individual DNA microarray datasets as described previously in Table 4.1. Each of the five lists of gene probe ids were converted first to gene symbols and then converted into lists of all possible Mouse Genome 430 2.0 Probe Set IDs for those genes using the Affymetrix NetAffx conversion tool. Using DChip microarray analysis software, the intersections of the five gene sets were found as depicted in the Venn Diagram (Figure 4.5). Heat maps were created using DChip to examine their expression patterns over time.

4.3.4 Subsets of Elastogenic Gene Set

The convergent set of commonly regulated genes in the elastogenic gene set showed some similarities in the hierarchical

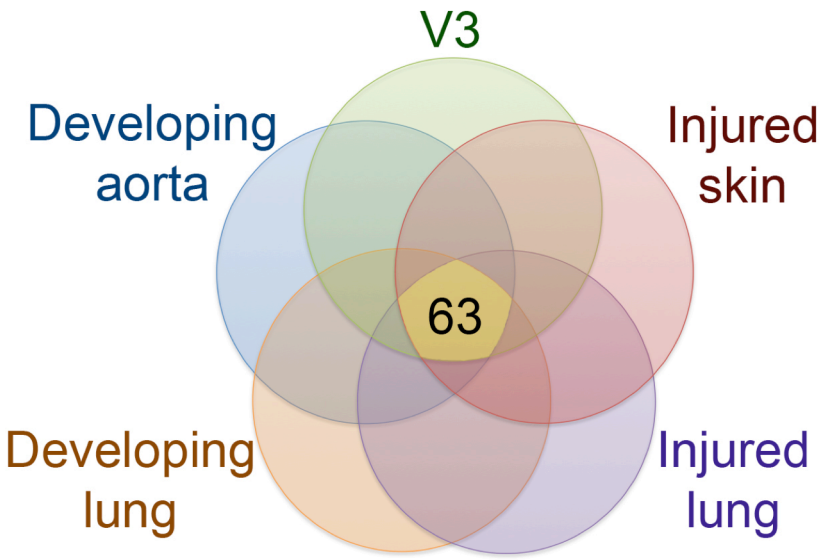

Figure 4.5. Convergent Venn diagram of differentially expressed gene sets in five processes containing elastogenesis to yield a 63-gene elastogenic gene set. The Venn diagram illustrates the intersection of five individual microarray analyses in which elastogenesis is a key component to yield 63 unique candidate elastogenic genes. The 63 genes within the "elastogenic gene set" are differentially regulated in all five processes as determined by statistical analysis specific to each

Figure 4.6. Expression patterns of the 63 candidate elastogenic genes. Convergent analysis revealed 63 genes commonly regulated genes in five processes in which elastogenesis is a key component.

clustering, however consistent expression patterns were not maintained throughout the injury models and the in vitro model. Because elastogenesis is prominent in fetal and postnatal development, developmental elastin fibers are the gold standard by which tissue engineered elastin fibers are compared. The expression patterns of the 63 elastogenic gene set in developing elastic tissues was used as the basis for subsequent categorization of the 63 candidate elastogenic genes into subsets for further analysis.

4.3.4.1 Heatmap of Developing Elastic Tissues

The expression patterns of the 63 elastogenic gene set in developing elastic tissues was used to create a subset of potential enhancers and potential inhibitors of elastogenesis. The heatmap was generated using dChip that

organized genes into a specific order by a hierarchical clustering algorithm (*215*) by using an average linkage method (*216*). The resultant heatmap depicted a clear distinction of two groups of similarly regulated genes as indicated at the horizontal green line (Figure 4.7).

The elastin gene was found in the top group along with other genes expressed at high levels in adult tissue. In the early lung and aortic development elastin is expressed at undetectable to low levels. As development progresses, elastin expression increases to a peak during the height of elastic fiber formation (10-14 days), and then returns to baseline levels in the adult tissue. Genes that followed a similar pattern of low to undetectable expression in both the early embryo and late adult with a peak of increased expression around day 10-14 were considered to behave in a similar expression pattern as elastin. Other genes known to enhance elastogenesis (Neu1, Fbln5) also follow this pattern. The group of 29 genes of the 63 "elastogenic gene set" were categorized into a subset of "potential enhancers" of elastogenesis. The bottom group of 34

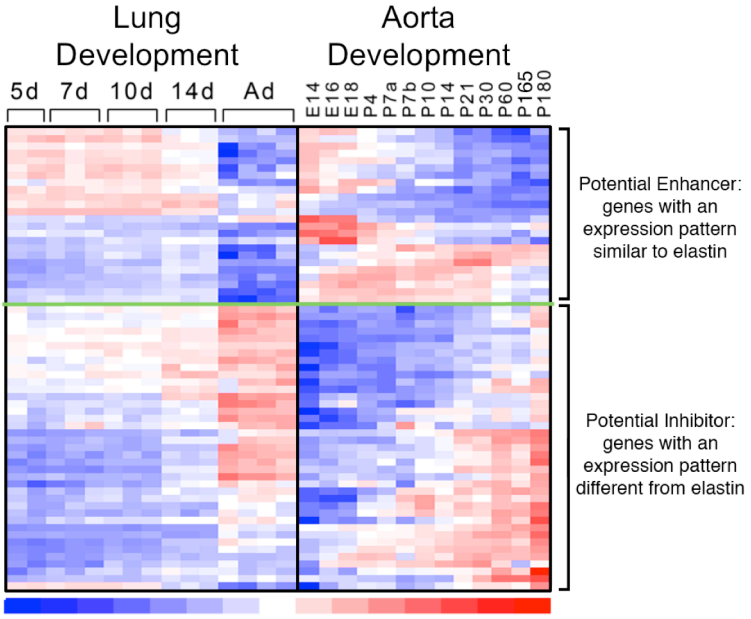

Figure 4.7. Heat map of potential enhancers and inhibitors of elastogenesis in the "elastogenic gene set." The graphical representation of the expression intensity values of the "elastogenic gene set" in the developing processes shows two distinct groups of similarly regulated genes

genes follows an expression pattern different from elastin with lower expression levels during development and higher expression levels during adult. These genes were categorized into a subset of "potential inhibitors" of elastogenesis.

Table 4.2. Criteria to Determine Subsets of the Elastogenic Gene Set

			Average Intensity Values Equation	
			Similar to Elastin	Different from Elastin
Processes in which elastogenesis is a Processes	Develop-ment:	Lung Development	Day 10 & 14 > Adult	Day 10 & 14 < Adult
		Aorta Development	Day 7-14 > Day 30-6 mo	Day 7-14 < Day 30-6 mo
	Injury:	Lung Injury	Day 2-3 > Unwounded	Day 2-3 < Unwounded
		Skin Injury	Day 5-10 > Unwounded	Day 5-10 < Unwounded
	V3-Transduced VSMCs		V3-transduced > Control vector transduced	V3-transduced < Control vector transduced

4.3.4.2 Subsets of Elastogenic Gene Set from Computational Analysis

The criteria employed on intensity values from microarray datasets in which elastogenesis is a key component to determine whether the gene probe of interest behaves in a similar or different manner as elastin is presented in Table 4.2. The raw intensity values from each gene probe of the 63 candidate elastin regulatory genes was subjected to the criteria above. If a gene probe does not meet the criteria for behaving similar to elastin then it is determined to behave different from elastin. In order for a gene probe to be categorized as having an expression pattern similar to elastin during the process of Development, it must meet the criteria for a similar expression pattern as elastin for both Lung Development and Aortic Development. Conversely, a gene probe must not meet

the criteria in both Lung Injury and Skin Injury to be categorized as having a different expression pattern as elastin during the Injury Process. These criteria provided the basis for hierarchal classification of genes as depicted in **Appendix A**.

The hierarchical analysis of the 63 genes identified in the convergent microarray analysis classified genes into groups based upon how similar or different its expression pattern was to the elastin gene's expression pattern in all five processes in which elastogenesis is a key component (**Appendix A**). The list of 63 genes was further subdivided based on expression patterns during development, the period at which native elastic fiber formation occurs. Table 4.3

Table 4.3. Similar/Different Subset of Candidate Elastogenic Genes

A

Gene Symbol	Gene Name
Eln	elastin
Cdc20	cell division cycle 20 homolog (S. cerevisiae)
Gap43	growth associated protein 43
Maged2	melanoma antigen, family D, 2
Mfap2	microfibrillar-associated protein 2
Ndn	necdin
Col5a1	procollagen, type V, alpha 1
Igf2r	insulin-like growth factor 2 receptor
Lox	lysyl oxidase
Col5a2	procollagen, type V, alpha 2
Col14a1	procollagen, type XIV, alpha 1
Sox11	SRY-box containing gene 11
Cdh11	cadherin 11
Hn1	hematological and neurological expressed sequence 1
Hnrnpa2b1	heterogeneous nuclear ribonucleoprotein A2/B1
Hmgb3	high mobility group box 3
Marcks	myristoylated alanine rich protein kinase C substrate
Myo1b	myosin Ib
Nnat	neuronatin
Npm1	nucleophosmin 1

B

Gene Symbol	Gene Name
Hexa	hexosaminidase A
S100a13	S100 calcium binding protein A13
Aebp1	AE binding protein 1
Cebpa	CCAAT/enhancer binding protein (C/EBP), alpha
Cebpb	CCAAT/enhancer binding protein (C/EBP), beta
Hk2	hexokinase 2
Por	P450 (cytochrome) oxidoreductase
Ptgis	prostaglandin I2 (prostacyclin) synthase
Ephx1	epoxide hydrolase 1, microsomal
Fasn	fatty acid synthase
Fxyd1	FXYD domain-containing ion transport regulator 1
Gas6	growth arrest specific 6
Timp3	tissue inhibitor of metalloproteinase 3
Aldoa	aldolase 1, A isoform
Apoe	apolipoprotein E
Cebpd	CCAAT/enhancer binding protein (C/EBP), delta
Cd9	CD9 antigen
Cdo1	cysteine dioxygenase 1, cytosolic
Ddt	D-dopachrome tautomerase
Dpep1	dipeptidase 1 (renal)
Dnajb2	DnaJ (Hsp40) homolog, subfamily B, member 10
Ech1	enoyl coenzyme A hydratase 1, peroxisomal
Gpx3	glutathione peroxidase 3
Gpx4	glutathione peroxidase 4
Gstm1	glutathione S-transferase, mu 1
Hp	haptoglobin
Ier3	immediate early response 3
Igfbp6	insulin-like growth factor binding protein 6
Nr1h3	nuclear receptor subfamily 1, group H, member 3
Phyh	phytanoyl-CoA hydroxylase
Timp2	tissue inhibitor of metalloproteinase 2
Cp	ceruloplasmin

identifies the genes that behave similar to elastin expression in the process of Development (both Lung Development and Aorta Development) as determined by the equations in Table 4.2. The genes that behave different from elastin expression during Development are listed in Table 4.2B. Subsequent promoter analysis was performed based upon these subsets.

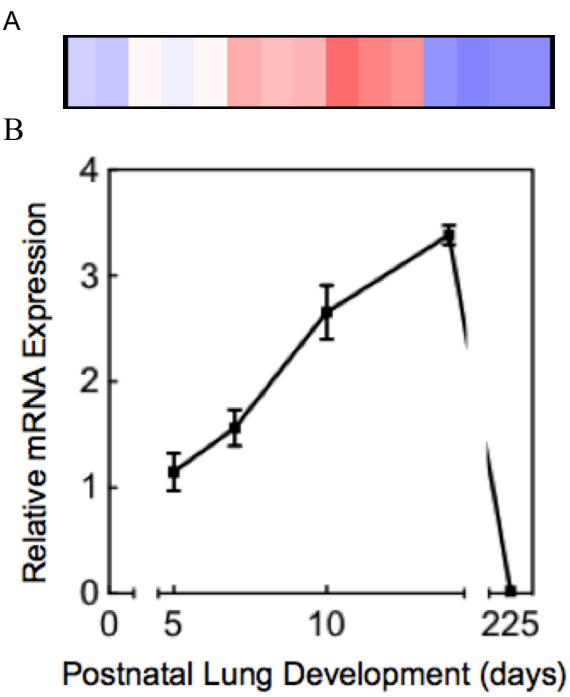

Figure 4.8. Validation of microarray elastin expression in developing mouse lung. **A**, The DNA microarray expression profile of relative elastin in mouse lung development correlates with qRT-PCR validation of developing mouse lung cDNA in **B**. The expression profile demonstrates a rise in elastin expression up to its peak around day 14 and no measurable expression in the adult lung.

4.3.5 Validation of Genes Identified in Microarray Analysis

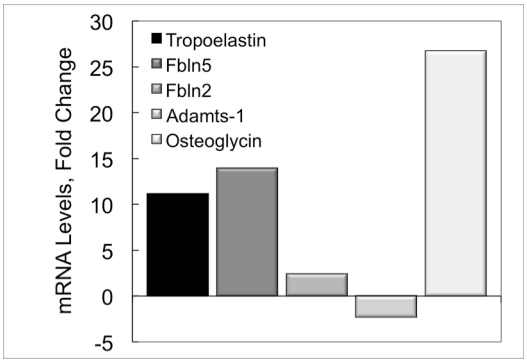

Figure 4.9. qRT-PCR validation of genes significantly regulated in V3-transduced VSMCs. Bars represent the ratio of gene expression in Versican V3-transduced vascular smooth muscle cells (VSMCs) compared to empty vector-transduced VSMCs (control).

Validation of elastin expression in microarray analysis was performed with cDNA from developing mouse lung. Figure 4.8 illustrates the expression profile depicting a peak elastin expression at day 14 and no measurable expression in the adult lung.

Table 4.4. qRT-PCR Validation of Genes Expressed in V3-Induced VSMCs

Gene	Forward Primer/Reverse Primer (5'-3')	Microarray FC[1]	QRT-PCR FC[1]
Tropoelastin	GGGCCTGGCCAAATCTATTC/GAGGACCCTGATGTGACGTTG	3.4	10.9
Fibulin-5	CGCCCCATCAAAGGGCCTCG/CCGCAGTCGGATCACGGAGC	9.4	13.8
Fibulin-2	GCGGTCAGGTGGGCTGTGTC/AGGCCCGGCAGGATGAGAGG	2.6	2.4
ADAMTS-1	GTAGATCCGTACACTATCCT/TATGTATGGTCTTTCAGATG	-2.3	-2.5
Osteoglycin	GTGCACAGCCAAGTGCTCCCA/TGCCTACATGTGGCTCCCCT	33, 21, 19[2]	27
	QRT-PCR control primers		
Beta actin	CTTGCAGCTCCTCCGTCGCC/ACATGCCGGAGCCGTTGTCG		

[1]Fold change (FC) values determined by DNA microarray analysis (Microarray) or quantitative RT-PCR (QRT-PCR) are shown for V3 transduced versus control virus transduced ASMCs.
[2]Multple FC values are reflective of changes observed for multple probe pairs corresponding to the Ogn transcript

Additional qRT-PCR was performed on cDNA from V3-transduced VSMCs and empty vector-transduced VSMCs using primers generated by Primer3 for genes identified as significantly regulated in the microarray dataset of V3-transduced VSMCs. The fold change of V3-transduce VSMCs vs. empty vector-transduced VSMCs calculated from qRT-PCR validation can be can be seen in Figure 4.9. Table 4.4 compares of the fold change of expression from qRT-PCR to the fold change calculated from DNA microarray expression intensities.

Table 4.5. 63 genes can be placed into statistically significant functional categories. Highlighted genes are known to e involved with elastic fiber formation.

A Functional analysis

Functional Term	P-value
Extracellular matrix	1.20E-05
Secreted	6.60E-05
Collagen	1.20E-03
Basement membrane	3.70E-03
CCAAT/enhancer-binding	8.10E-03
Signal	1.20E-02
Oxidoreductase	3.20E-02
Regeneration	4.40E-02
Hydroxylation	5.00E-02

B Secreted Subset

Gene Name
AE binding protein 1
S100 calcium binding protein A13
Apolipoprotein E
Ceruloplasmin
Collagen, type V, alpha 1
Collagen, type V, alpha 2
Collagen, type XIV, alpha 1
Ectonucleotide pyrophosphatase/ phosphodiesterase 2
Elastin
Glutathione peroxidase 3
Growth arrest specific 6
Haptoglobin
Insulin-like growth factor binding protein
Laminin, beta 2
Lysyl oxidase
Microfibrillar-associated protein 5
Microfibrillar-associated protein 2
Tissue inhibitor of metalloproteinase 2
Tissue inhibitor of metalloproteinase 3

4.3.6 Functional Analysis of Convergent Genes using Gene Ontology.

Convergent analysis produced 63 genes that represent "candidate elastogenic genes." Among these 63 were genes well established to effect elastogenesis, including tropoelastin, Lox, Mfap2 and Mfap5. Ontological analysis of the 63 genes revealed that the functional categories with highest significance were the "extracellular matrix" category (*p*=1.20E-05) and the "secreted protein" category (*p*=6.60E-05) (Table 4.5A). In addition to the elastin-related genes mentioned above, the ECM gene set included genes encoding Timp2, Timp3, laminin β2, ColVα1, ColVα2 and ColXIVα1 (Table 4.5B). The mechanism of elastic fiber formation may involve multiple signaling pathways that may not be normally activated due to the particular injury. It is also possible that not all genes involved in elastogenesis may be regulated on a transcriptional level.

4.4 Discussion

Microarray analysis was performed on five different processes in which elastogenesis was a key component. Two processes occur in elastin-rich tissues during the period of development, the gold standard of elastic fiber quality that tissue engineering applications strive to replicate. In order to distinguish commonly regulated genes involved in elastogenesis from genes specific to tissue development the DNA microarray analysis was expanded to include models of adult elastogenesis in response to an injury of an elastin-rich tissue. And finally, an in vitro model of a specific cell type was incorporated to

distinguish genes regulating elastogenesis from genes that are regulated in coordination of complex biological processes in an animal model. Five microarray sets were selected in which active elastin transcription had occurred over a length of time: 1) Developing lung, 2) Developing aorta, 3) Lung wound healing, 4) Skin wound healing, and 5) Versican V3-transduced vascular smooth muscle cells (VSMCs). Each dataset was analyzed for significantly regulated genes and through the used of dChip, convergent analysis of the five microarray datasets in which elastogenesis is a key component yielded a common set of 63 candidate elastogenic genes.

The list of 63 genes was further classified using gene ontology to be significantly enriched in extracellular matrix (ECM) genes. Elastic fiber assembly occurs at the cell surface within the ECM and mature elastic fibers reside within the ECM to play a role in mechanical motion and cellular signaling so it would follow that potential gene regulators in the 63-gene candidate gene set would be enriched in the ECM ontology. Coordinately the gene ontological function of secretion would match potential gene regulators of elastic fiber assembly and ECM signaling.

Further investigation into significant ontological processes indicates enrichment for oxidoreductase. This group comprises a set of enzymes that catalyze oxidation-reduction reactions that may prove to be a hindrance to elastogenesis. It is possible that oxidative and nitrosative modification of tropoelastin within the in vitro model are preventing elastic fiber assembly (*28*). In a study by Akhtar et al. oxidation reduced crosslinking and interactions with other

proteins required for elastic fiber assembly, including fibulin-4, fibulin-5, and fibrillin-2. Measurement of exogenously added oxidized tropoelastin showed less incorporation into the preexisting microfibrils of human retinal pigmented epithelial ARPE-19 cells compared to unoxidized tropoelastin as detected by immunofluorescence microscopy (*28*). Nitration of TE was confirmed using the rabbit anti-N-Tyr antibody, followed by a FITC-conjugated anti-rabbit secondary antibody (*28*). If the in vitro culture model for the elastin ELISA is undergoing any oxidative stress, it would follow that elastic fiber assembly may be impaired.

4.5 Conclusion

DNA microarray technology allowed for the use of high-throughput quantification of the concurrent expression of thousands of genes. Analysis of DNA microarray processes in which elastogenesis is a key component combined five processes to determine commonly regulated genes for elastic fiber formation and to distinguish those genes from coordinately regulated gene networks specific to a biological process or tissue. All five processes occurred in elastin rich tissues or cells and displayed an upregulation of the elastin gene. A convergent list of 63 differentially expressed genes was gleamed from the five processes: 1) Developing lung, 2) Developing aorta, 3) Lung wound healing, 4) Skin wound healing, and 5) Versican V3-transduced vascular smooth muscle cells (VSMCs).

Gene ontological analysis highlighted functional categories of extracellular matrix (ECM) and secretion, which follow the elastin gene beginning with

secretion of a tropoelastin monomer and subsequent assimilation into mature elastic fibers comprising the ECM. The enrichment for the ontological group of oxidoreductase enzymes may prove to be a hindrance to elastogenesis as oxidation of tropoelastin prevents proper elastic fiber assembly. This may pertain primarily to the elastogenic processes of wound healing that are undergoing oxidative stress and ultimate assembly of inferior elastic fibers compared to developmental elastic fibers.

The process of combining similar DNA microarray processes containing a shared element of elastic fiber assembly provides insight into novel gene regulatory networks involved in elastogenesis. Comparison within sets may also elucidate differences in elastic fiber quality among different processes. The information gained offers an unprecedented opportunity to fully characterize elastogenesis.

CHAPTER FIVE

TRANSCRIPTIONAL REGULATORY NETWORK ANALYSIS TO DETERMINE CANDIDATE GENE REGULATORY NETWORKS

5.1 Introduction

DNA microarray technology allows the simultaneous measurement of the expression of many thousands of genes. The challenge to analyzing vast datasets to characterize biological processes relies on tools for the efficient integration and interpretation of large datasets. Analysis of gene regulation can be expanded to include computational tools to combine other databases with known information on gene regulation.

One such computational tool, pathway analysis, involves looking for consistent but subtle changes in gene expression by incorporating either pathway or functional annotations. Pathway analysis is a promising tool to identify the mechanisms that underlie diseases, adaptive physiological compensatory responses and new avenues for investigation (*217*).

Other computational tools integrate functional genomics data, for example, from microarray-based gene-expression analysis with genomic sequence data to carry out transcriptional regulatory network analysis (TRNA) (*218*). TRNA combines bioinformatics to identify and analyze regulatory regions of genes with statistical significance testing to determine the likelihood of the binding of transcription factors (TF). We further refined our set of candidate elastogenic genes with TRNA to identify potential regulatory pathways for elastogenesis.

5.1.1 Gene Regulation

An organism is comprised of many different tissues that perform a wide range of functions yet the entire genome encoding these functions is found in every cell within the organism. This phenomenon is due to a process known as gene regulation, whereby only a fraction of genes in the genome are expressed in a given cell. Gene regulation occurs throughout the entirety of gene expression from chromatin organization, transcription, pre-mRNA processing, translation, and post-translational modifications but chiefly at the transcriptional level (*219*).

Transcription involves the conversion of the genetic code comprised of deoxyribonucleic acid (DNA) into messenger RNA (mRNA), which can then serve as a template for protein synthesis. The biological mechanism of transcription is regulated by an extensive network of proteins known as transcription factors (TFs) that bind to a complementary DNA sequence binding sites or transcriptional regulatory elements (TREs). The TREs are primarily located in the cis-regulatory region (promoter) of a gene approximately 100-1000 base pairs upstream (towards the 3' region of the anti-sense strand, or non-coding strand) (*220*), however some TREs have been found from 200bp downstream of the origin of replication (ORI), up to tens of thousands of bp upstream (*219*). When a TF binds to a corresponding TRE the level of transcription of the downstream gene can be initiated, stopped, up or down-regulated. Figure 5.2 shows the interaction of TFs/TREs with the promoter of a gene to regulate transcription.

5.1.2 Gene Regulatory Network

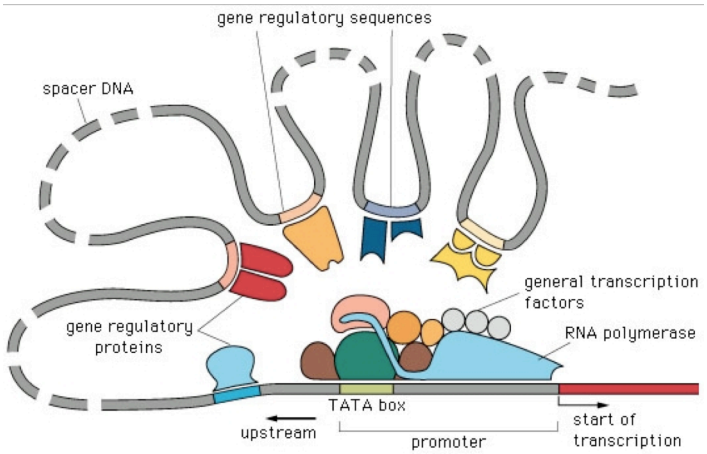

Figure 5.1. Gene Regulation. Transcription factors (TFs) bind to corresponding transcriptional regulatory elements (TREs) .The TFs/TREs interact with the promoter region upstream to the start of transcription to initiate, stop, up or down-regulate the level of transcription of the downstream

A multitude of genes interact in a systematic and interconnected network to regulate complex cellular processes such as development, differentiation, proliferation, cell cycle, and extracellular matrix organization. Transcription factors (TFs) serve as an important component of this network, responding to changes in the cellular environment by altering the gene expression of relevant genes (*221*). TFs specifically bind to a corresponding sequence of a TRE however TREs are not specific to a single gene. Multiple genes have the same TREs present resulting in an interconnected transcriptional regulatory network where TFs bind and regulate many different genes.

Understanding the complexity of these gene regulatory networks relies on the compilation of technological developments such as gene expression changes from microarrays, protein–DNA interaction and transcription factor activity data from protein binding assays, chromatin immunoprecipitation (ChIP) experiments (*222*), and DNA footprinting (*223, 224*), protein–protein interactions from two hybrid experiments and coimmunoprecipitation, and genomic sequence and ontology information in public databases (www.geneontology.org) (*220*). By

analyzing data from multiple sources of regulatory assays, we may achieve a better understanding of the dynamic systems of the gene regulatory network.

5.2 Materials and Methods

5.2.1 Promoter Analysis Technology

The binding of TFs to TREs is the crux of the biological mechanism of transcriptional regulation. Because these reactions are sequence specific, bioinformatics tools are able to access available databases containing annotated sequences for gene sequences and cross-compare databases of annotated TREs. By scanning the genome for sequence recognition, new technology is able to identify the presence of a TRE in the promoter region of a gene thus predicting the possibility of TF-TRE binding.

Many studies have taken this direct approach to promoter analysis to identify a good candidate set of network interactions (*225-227*). Promoter analysis has been utilized most successfully in yeast to develop sets of coregulated genes (67) and detailed gene regulatory networks for the galactose-utilization pathway (68). Promoter analysis can also be used to identify genomic regions containing unusually high concentrations of predicted TREs. One study in the developing Drosophila embryos identified enriched genomic regions for five active TFs of interest (*228*). Gene regulatory networks are also at play during development in to regulate cell fate in the embryo of sea urchins to control the specification of endoderm and mesoderm (*229*). The first study to employ promoter analysis to identify regulatory gene networks in higher order species

focused on transcriptional mechanisms that control cell cycle progression in humans (*230*). By analyzing the promoters in a set of genes whose expression is cell-cycle-dependent, Bury identified a set of 8 transcriptional factors whose binding sites were overrepresented.

Promoter analysis is able to identify transcription factor (TF) binding regions within the genetic code and thus predict binding of TFs that regulate gene expression. Through analysis of the promoter regions of the candidate elastogenic gene set, we analyzed the TF-binding site occurrences for over/under representation within our 63 candidate elastogenic genes. Transcriptional regulatory network analysis (TRNA) combines pathway analysis and statistical significance testing to identify potential transcription factor regulators of elastogenesis.

5.2.2 PAINT: Promoter Analysis and Interaction Network Generation Tool

The Daniel Baugh Institute for Functional Genomics/Computational Biology at Thomas Jefferson University developed a bioinformatics tool PAINT: Promoter Analysis and Interaction Network Generation Tool to automate the analysis of a given set of genes to produce an interaction matrix that represents a candidate set of interactions between the transcription factors and the genes.

PAINT is able to identify potential regulatory networks given an input set of genes of interest. PAINT processes a list of unique identifiers representing the genes of interest by referencing the database UpstreamDB to identify 5000 bp upstream and 100 bp downstream of a gene. This process is not organism-

specific as the key requirements are the availability of an annotated genome sequence. UpstreamDB was constructed for all the known and putative annotated genes in the Ensembl genome database for *Mus musculus*. This promoter sequence database is periodically updated by PromoterID/DBSync, which also serves to identify the transcription start site. The TFRetriever module makes use various transcription factor inspection/discover programs that can retrieve and process the sequences for TREs of known TFs. The unique gene sequences are processed by the FeasNet Builder component that produces a Candidate Interaction Matrix (CIM) for the genes of interest. Statistics are also generated within this module to compare the over-representation of the TREs in the set of given promoters with respect to a background set of promoters. The p-values are calculated using hypergeometric distribution (*230-232*) to give the probability that the observed counts for the TREs in the set of promoters could be explained by random occurrence in the reference set of promoters. The final PAINT component FeasNetBuilder constructs an interaction matrix representing a candidate set of connections in the regulatory network with the input genes of interest organized into rows and the columns corresponding to the TREs. The regulation of a gene is represented by the color of the box at the intersection of a row and column: red if a TRE was identified as over-represented in that gene's promoter, blue for under-representation, and black otherwise. The lower p-value ($0 < p < 0.01$) indicating a higher degree of significance for a particular TRE in a CIM are indicated in a brighter/lighter shade of red for over-representation or cyan for under-representation (*220*). The organization of the PAINT modules

from the input gene list to the visualization of a candidate regulatory network can be seen in Figure 5.1. In summary, the bioinformatics tool PAINT is able to process a given set of genes to generate a pruned list of transcription factors that are ranked on the likelihood of the involvement. The resultant data can be examined in detail in further experimental studies on gene regulation (*220*).

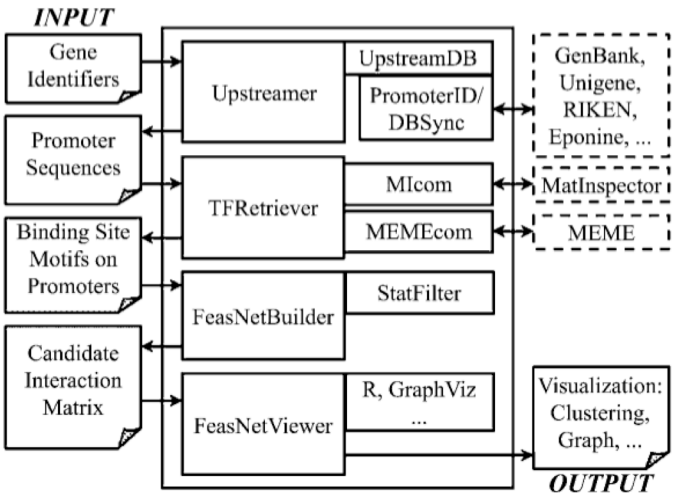

Figure 5.1. Flow of Data through the Bioinformatics Tool PAINT. The input and intermediate outputs are organized on the left. The five core components of PAINT are boxed in: UpstreamDB, PromoterID/DBsync, TFRetriever, FeasNetBuilder, FeasNet Viewer. Dash-outlined boxes represent external databases and programs utilized by PAINT.

In order to identify potential transcriptional regulators of elastogenesis in the 63 gene "elastogenic gene set" the bioinformatics tool PAINT (*218, 220*) was used to analyze the promoter sequences. Optimal parameters and input gene sets were determined with the assistance of Dr. Jeremy Barth in the COBRE Proteogenomics Facility at the Medical University of South Carolina. Because developmental elastogenesis is considered the gold standard for elastic fiber quality, PAINT analysis was performed on the "elastogenic gene set" subsets of "potential enhancers" and "potential inhibitors" derived from the microarray datasets from developing lung and developing aorta described in 4.3.1. Transcriptional regulatory elements (TREs) were identified as being significantly

overrepresented in the promoters of the enhancer or inhibitor subset with respect to a background set of promoters ($p<0.05$). Dr. Barth was able to access the TRANSFAC Pro licensed database to find TREs and he suggested analyzing a promoter region limited to 2000 bp upstream of the transcription start site and a False Discovery Rate (FDR) < 0.10.

5.2.3. UCSC Genome Browser

Transcription factor analysis using PAINT indicates the presence of a transcription factor (TF) binding sites (TREs) within the given parameter of base pairs designated during the search described previously. Resultant displays indicate the presence of a TRE but not the specific location. The University of California at Santa Cruz (UCSC) Genome Browser provides a way to examine genomic data and map specific TF binding sites. UCSC Genome browser can also include extensive annotation tracks for various data types including known chromatin immunoprecipitation (ChIP) datasets. The ENCODE function links to downloadable tracks and files corresponding to searchable terms. We downloaded BroadPeak ENCODE files for transcription factors regulated in PAINT analysis.

5.2.4 MicroRNA Analysis of Elastogenic Gene Set

MicroRNAs (miRNAs) are short, single-stranded RNAs that bind to messenger RNA (mRNA) to regulate gene expression, usually by blocking translation. A wide range of biological processes involve miRNA-mediated

regulation as a key component such as developmental timing, metabolism, apoptosis, cardiac and skeletal muscle proliferation (*233*) and neuronal gene expression (*234*). Changes in expression, copy number or mutations of miRNA can lead to diseases in humans including cancer. MicroRNA expression is prevalent in almost all cell types and conserved among most species suggesting miRNAs are vital to biological processes.

Recent studies show that expression of the microRNA, miR-29, is reduced by TGFβ1 (*129*) and that the 3′UTR of elastin mRNA is a target of miR-29 (*130, 131*). Furthermore, miR-29 mimics decrease elastin mRNA levels in dermal fibroblasts and vascular smooth muscle cells (*132*). Moreover, in the developing mouse aorta, an up regulation in the expression of miR-29 as well as several other microRNAs that have targets in the elastin mRNA (i.e., the miR-15 family members miR-195 and miR-497) accompanies the down regulation of elastin mRNA in the period between the newborn and adult (*130, 131*).

Numerous resources exist predicting miRNA binding based on sequence complementarity. One such tool is microRNA.org, a resource for microRNA target predictions and microRNA expression that uses the miRanda algorithm that computes optimal sequence complementarity between a set of mature microRNAs and a given mRNA using a weighted dynamic programming algorithm (*235*). The microRNA expression profiles were taken from a recent profiling study across ~250 small RNA libraries collected from human, mouse and rat tissues and cell lines (*236*).

Target mRNA searches were performed on each of the 63 genes in the candidate elastogenic gene set. All isoforms of miRNAs were collected for the mouse genome and organized based on number of occurrences. Additionally, genes were sorted based upon number of miRNA.

5.3 Results

5.3.1 Defining Candidate Regulatory Interactions

Transcriptional regulatory network analysis revealed potential transcription factor (TF) regulators of the subsets of the candidate elastogenic genes as

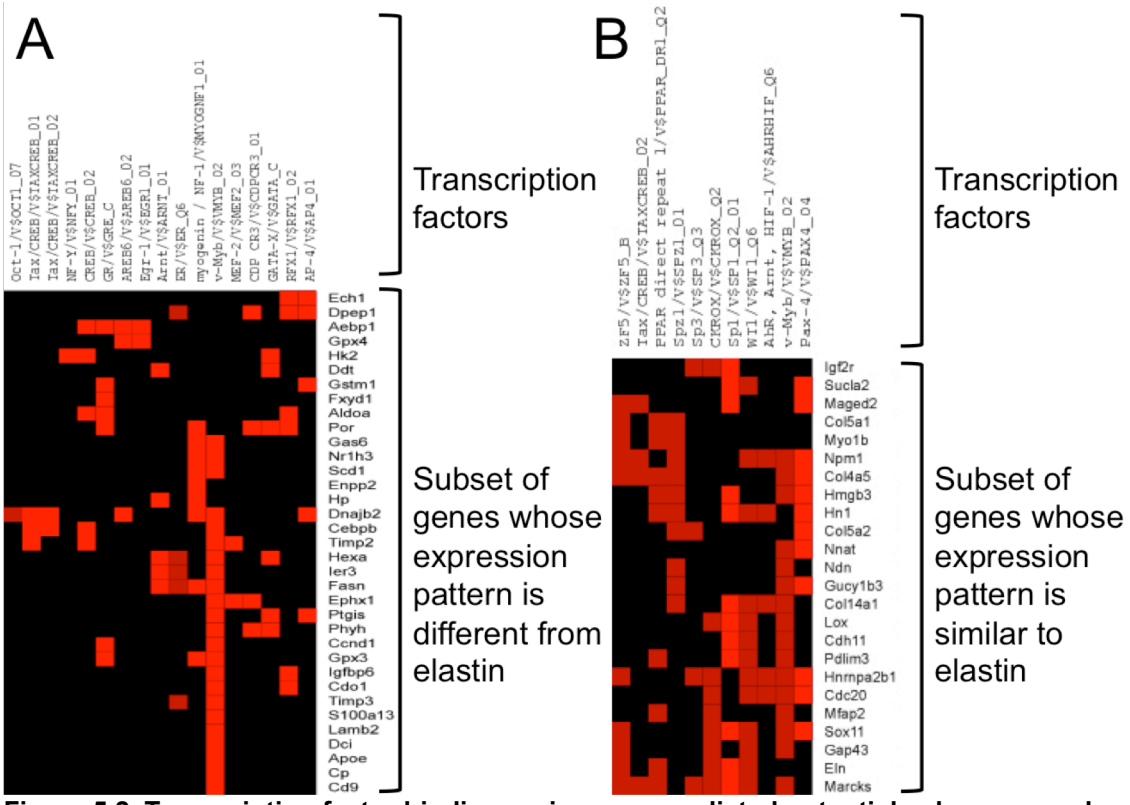

Figure 5.2. Transcription factor binding regions are predicted potential enhancers and potential inhibitors of elastogenesis. The remaining transcription factors have not been associated with regulating elastin or elastogenesis to date. We're interested to determine whether they represent novel regulatory factors in the process of elastogenesis. Several of these have pharmacological antagonists and agonists that can be tested to see if they exert effects on elastogenesis.

determined by dChip heatmap categorization. Among the genes whose expression pattern is similar to elastin, eleven TREs were significantly enriched. Importantly, four of the eleven transcription factors (TFs) binding to the TREs, *B-Myb Sp1, cKrox* and *PPAR,* have been previously implicated in elastogenesis *(146, 237-239)*. For example, studies have shown that B-Myb represses expression of elastin in VSMCs (*237*) and lysyl oxidase (Lox) expression in fibroblasts (*240*). cKrox also repress elastin expression in fibroblasts (36), while Sp1 stimulates elastin expression in fibroblasts (*147*). PPAR has dual effects on elastin transcription: both increasing (*241*) and repressing elastin expression in fibroblasts (*238, 242*). To date, these regulators have not been targeted in tissue engineering approaches.

5.3.2 TREs identified within the Elastin Promoter

PAINT analysis determined five DNA sequences corresponding to TREs to be significantly overrepresented within the elastin promoter region analyzed (Figure 5.3). Two

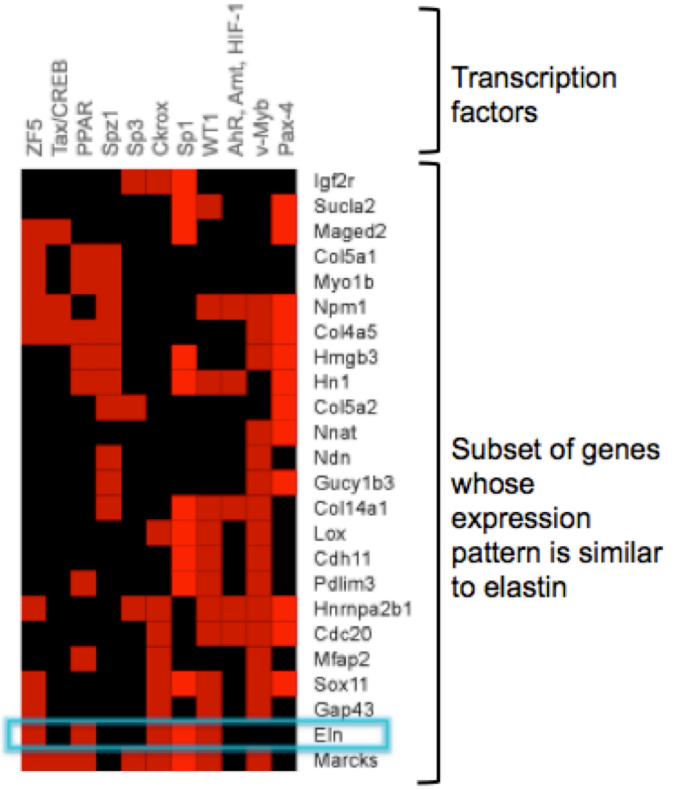

Figure 5.3. PAINT analysis determined five DNA sequences corresponding to TREs to be significantly overrepresented within the elastin promoter region analyzed. Two of the five TREs are known to regulate elastin: PPAR and Sp1. The other three TREs have not be associated with elastin to date: WT1, ZF5, and Ckrox.

of the five TREs are known to regulate elastin: PPAR and Sp1 while the remaining three TREs have not be associated with elastin to date: WT1, ZF5, and Ckrox. Given that 2 of the 5 TREs identified on the elastin promoter through the PAINT analysis have already been demonstrated to regulate elastin transcription, the use of promoter analysis technology is validated to predict candidate regulatory interactions. It would follow that the WT1, ZF5, and Ckrox in the elastin promoter are worth investigating, along with other TREs regulating the genes which are regulated similar to elastin during development.

5.3.3 UCSC Genome Browser Mapping of Transcription Factor Binding Sites

Previous chromatin immunoprecipitation (ChIP) studies using PPARα chip were uploaded to the USCS Genome Browser in the form of broadPeak tracks. Using the UCSC Genome Browser and the ENCODE search function to align

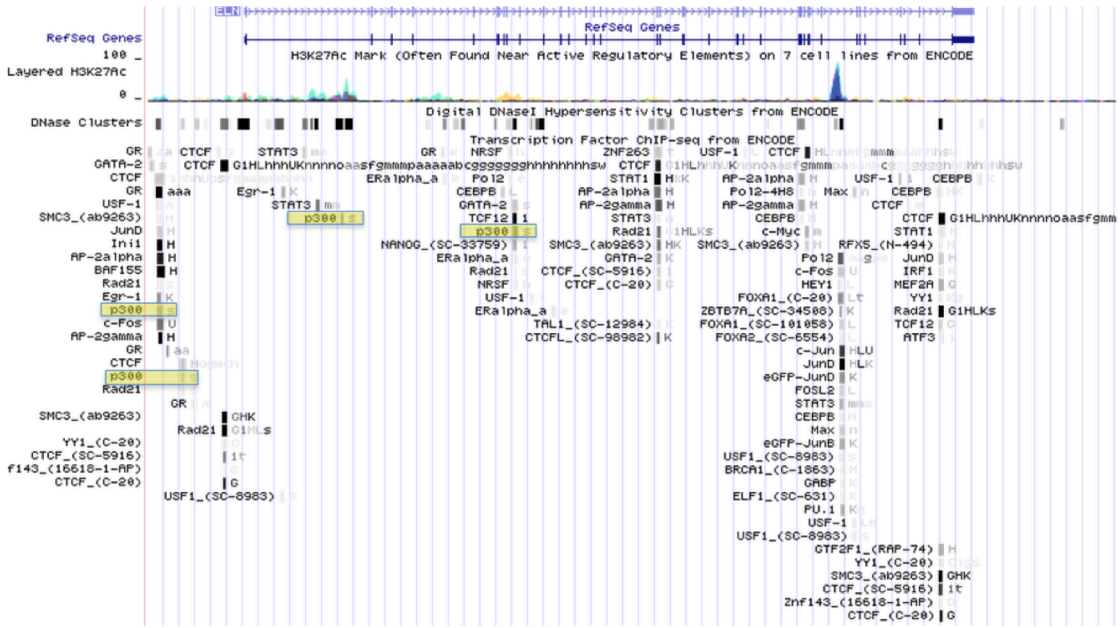

Figure 5.4. Transcription factor binding sites for p300, a PPAR coactivator, are located close to the transcription start site of the human elastin gene. The UCSC Genome Browser allowed visualization of transcription factor binding sites along the elastin gene as compiled from multiple chromatin immunoprecipitation (ChIP) studies.

tracks from PPAR ChIP studies, we located a PPARα transcription factor binding site closest to the start site of elastin transcription approximately 50 kilobasepairs (kbp) upstream. Expansion of the elastin gene in the UCSC Genome Browser also demonstrates multiple binding sites for the PPAR coactivator p300 (*243*) (Figure 5.4).

Previous chromatin immunoprecipitation (ChIP) studies indicate transcription factor binding sites close to the transcription start site of the elastin gene as seen in Figure 5.5. Two binding sites interchangeable for transcription factors WT1 and EGR-1 are located upstream of the transcription start site within the elastin promoter (< 5 kbp) and downstream of the transcription start site (< 2.5 kbp).

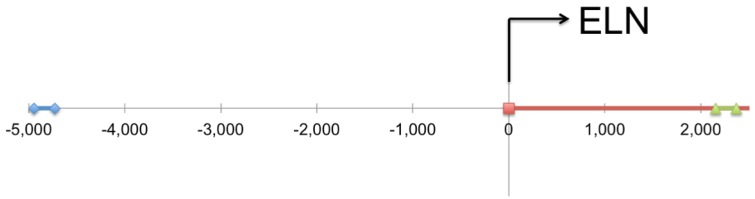

Figure 5.5. Previous chromatin immunoprecipitation (ChIP) studies indicate 2 EGR-1/WT1 Binding Sites within 5kb from the human elastin gene transcription start site.

5.3 4 MicroRNAs Common to Elastogenic Gene Set

MicroRNA analysis of candidate elastogenic gene set identified 177 different miRNAs known to regulate the 63 genes commonly regulated in all five elastogenic processes, of which 112 miRNAs have at least 5 binding sites within the set, and 31 miRNAs bind at least 10 sites. Table 5.2 is organized horizontally by miRNAs in decreasing number of total miRNA binding sites and organized vertically in ascending order from genes with the most number of miRNA binding

sites down to the least regulated genes. The most represented miRNA is miR-200 with 31 binding sites in 16 different genes, followed by miR-181 with 28 binding sites in 7 different genes, and miR-29 with 27 binding sites in 9 different genes. The gene regulated by the most binding sites for miRNA is Hnrnpa2b1 with 53 miRNA binding sites for 43 different miRNAs, followed by Marcks with 43 miRNA binding sites for 34 different RNAs, and lysyl oxidase (Lox) with 42 miRNA binding sites for 32 different miRNAs. The largely regulated Lox, an important crosslinker of elastin fibers and significant presence of miR-29, a known regulator of elastogenesis, within the 63-gene elastogenic gene set indicate miRNAs play a likely role in the regulation of elastogenesis.

Table 5.2. MicroRNAs Common to Elastogenic Gene Set

# of miRNAs/ Gene	# of miRNA types/ Gene	Gene Symbol	miRNA																														
			200	181	29*	23	27	30	125	590	190	302	543	15	19	92	101	186	429	20	34	106	216	449	495	1192	128	129	374	410	26	208	491
53	43	Hnrnpa2b1	1			2				1	2	3	1	2	2			1		2		2	1		1	1			1				
43	34	Marcks	2			2	2			1			1					1	1		3		2	3	1	1	1	1						1
42	32	Lox	1			3	2	2	5		1			1			2		1									1	1	1	2			
42	31	Col5a2			4	3	2	2			1	2		1					1						1	1		1	1	1		2		
40	35	Cdh11	2					2						1	2			2	1	1											1	2		
38	30	Sox11			4		2	2			1					2	2	1					1		1	1								
34	22	Scd1	2		4										2		2		1		3		2	3									
31	23	Timp2			4						1			1		2				2		2			1	1			1	1		2		
31	23	Aldoa													2	2			1		2	3	2	1	3	1	1		1					
29	26	Myo1b								2	1					2								1		1	1			1				
28	22	Gap43					2			1	1			1		2	2												1					1
27	22	Cebpa										2				2	2	2	1										1	1				1
24	20	Igf2r	2						1						2	2			1	1									1					
24	18	Hmgb3	2							2	1	2		1						1	2		2					1						
24	21	Gucy1b3										2	3	1												1	1	1	1					
23	21	Sucla2	2							1				1	2				1	1										1	1			
23	18	Col4a5	3			3	2				1								1	1										1	1			1
23	17	Cdo1			4	3								1																	2		
22	14	Timp3			4				5	1	2			1													1						1
21	17	Hn1											3							2		2			1	1							
20	18	Hk2												1	2																		
19	10	Mfap5				3			5			2							1		2		2										
19	18	Fasn													2									1			1						1
17	11	Npm1	2	4		2							1				2		1								1						
17	15	Cebpb											1			2									1	1			1	1		2	
16	15	Cp							2	1													1					1	1	1			1
16	12	Enpp2	2			3													1								1			1			
16	15	Ndn	2															1	1														1
15	13	Cebpd	2																1													2	
15	13	Col5a1	2																1												2		
14	11	Nnat										3																					
13	9	Ccnd1	2				2			1		3																					
12	9	Eln				3			1								2											1					1
12	11	Gpx3						2																			1						
11	9	Phyh							1	1							2															2	
11	10	Cd9														2			1									1	1	1			
10	9	Col14a1								1													1							1			
10	10	Dnajb2																1							1	1							
10	9	Gbp2						2		1																	1						1
10	4	Hexa				3															3			3									
8	8	Pdlim3																															
8	6	Ier3							2																								
8	6	Mfap2				3																	1				1						
5	3	Ech1					2																				1						
5	4	Igfbp6	2																1														
5	4	Gstm1																													2		
4	4	Nr1h3																		1													
4	3	Dpep1							2																								
2	1	Gas6									2																						
2	2	Por																															
2	2	Ephx1																							1	1							
2	2	Gpx4																															
1	1	Lamb2																															
1	1	Maged2																															
1	1	S100a13																															
1	1	Dci																															
1	1	Ddt																															
1	1	Ptgis							1																								
Total # of miRNA binding sites			31	28	27	18	16	16	16	16	15	15	15	14	14	14	14	14	14	13	12	12	12	12	12	12	11	11	11	11	10	10	10
Total # of genes/ miRNA			16	7	9	9	8	4	11	15	8	5	15	7	7	7	7	14	14	7	4	6	10	4	12	12	11	11	11	11	5	5	10

Only four genes of the 63 were not known to be regulated by any miRNAs including AE binding protein 1 (Aebp1), apolipoprotein E (Apoe), and cell division cycle 20 homolog (Cdc20), and FXYD domain-containing ion transport regulator 1 (Fxyd1).

5.4 Discussion

Transcriptional regulatory network analysis tool PAINT utilized databases containing sequences of gene regulatory regions and transcription factors to detect transcription factors overrepresented in the 63 candidate elastogenic genes. Promoter analysis was performed on the two subsets of genes as determined by dChip heatmap categorization and a total of 28 transcription factors were identified as potential regulators of elastogenesis. In the subset of genes whose expression pattern is regulated similar to elastin and categorized as potential “enhancers” of elastogenesis, eleven transcription factors were overrepresented compared to a reference set of genes. Four of the eleven transcription factors have been previously implicated with elastogenesis (B-Myb Sp1, cKrox and PPAR while the remaining seven have yet to be associated with elastogenesis. The finding of transcription factors known to regulate elastin transcription validated this approach for finding transcriptional regulators of elastogenesis. This finding also increases the likelihood that the 63-gene “elastogenic gene set” group represents a true core of elastogenesis related genes. By extension, the 11 TFs identified by this analysis may represent an elastogenesis regulatory network.

PAINT analysis of the genes whose expression pattern is different from elastin distinguished 17 transcription factors to be enriched, including, v-Myb, which binds TREs in 23 of the 35 gene subset. Of importance to this set is the transcription factor early growth response 1 (EGR-1) that binds to the same consensus sequence as another transcription factor Wilms’ tumor 1 (WT-1) that

was enriched in the alternate subset. Both transcription factors are members of the family and are considered oncogenes and tumor suppressors (*244*).

Wilms tumor regulates the expression of multiple growth factors including colony-stimulating factor (*245*), platelet-derived growth factor (*246*), and known modulator of elastin transcription insulin-like growth factor I (*247*). A mutation resulting in the loss of WT1 expression leads to up-regulation of these growth factors and the formation of Wilms tumor, thus its original classification as a tumor suppressor (*248*). However, subsequent studies have revealed a potential role for WT1 as an oncogene due to its upregulation in a variety of human cancers such as astrocytic tumors (*87, 249*), breast cancer (*250*), leukemia (*251*), and *sporadic* Wilms tumor (*252, 253*), which accounts for ~85% of all Wilms tumors.

Both WT1 and EGR1 are members of the family of zinc finger proteins (*254*) with similar structures and consensus sequences resulting in competition for transcription factor binding sites. WT1/EGR-1 binds 5'-GCG TGG GCG-3' (and similar ones like 5'-GCG GGG GCG-3') (*255, 256*). The effects of binding are most often mutually opposing whereby EGR1 activates the transcription of genes that WT1 represses (*257, 258*). Like WT1, EGR1 expression levels are atypical in multiple neoplastic cell types such as prostate cancer (*259*), glioblastoma (*260*), and Wilms tumor (*253*). Furthermore, EGR1 can also act as either an oncogene (*259*) or a tumor suppressor (*248-253, 257-261*) in different cell types. EGR-1 targets genes including immune effector genes, such as the cytokine IL-2 (*262, 263*), the pro-inflammatory immune mediator TNFα (*264*), a

known suppressor of elastin transcription (*113*) and promoter of elastin degradation (*177*).

Similar structures and consensus sequences results in competition of binding for transcriptions factors WT1 and EGR-1. Binding often results in opposing regulation of the same gene (*257, 258*). The enrichment of both transcription factors in opposing subsets of the 63-gene elastogenic gene set validates the approach of transcriptional regulatory network analysis using PAINT to identify regulators of elastogenesis. It is likely that WT1 and EGR-1 coordinate the up-and down-regulation of elastogenesis.

Analysis of WT1/EGR-1 consensus sequences using the UCSC Genome Browser and previous chromatin immunoprecipitation (ChIP) studies illustrated two binding sites close to the start site of elastin transcription. Additional ChIP studies indicate the binding sites for PPARα upstream of the elastin transcription start site as well as multiple PPAR coactivator p300 binding sites in closer proximity to the transcription start site. The findings from transcriptional regulatory network analysis indicating enriched transcription factor binding sites within the 63-gene elastogenic set and subsequent binding site mapping proximal to the elastin transcription start site using ChIP studies indicate PPAR and WT1/EGR-1 as potential regulatory transcription factors of elastogenesis.

Other important regulators of transcription include microRNAs. Although elastin expression decreases shortly after the perinatal period and remains low in adult tissues (*265*), interestingly tropoelastin premRNA levels remain elevated in adult rat lungs despite considerably reduced steady-state mRNA levels. This

suggests posttranscriptional regulation of mRNA may be a predominant mechanism to regulate elastin mRNA (*87*).

Recent studies show that expression of the microRNA, miR-29, is reduced by TGFβ1 (*129*) and that the 3′UTR of elastin mRNA is a target of miR-29 (*130, 131*). Furthermore, miR-29 mimics decrease elastin mRNA levels in dermal fibroblasts and vascular smooth muscle cells (*132*). Moreover, in the developing mouse aorta, an up regulation in the expression of miR-29 as well as several other microRNAs that have targets in the elastin mRNA (i.e., the miR-15 family members miR-195 and miR-497) accompanies the down regulation of elastin mRNA in the period between the newborn and adult (*130, 131*).

miR-29 was the third most occurring miRNA with binding sites in the elastin (Eln), lysyl oxidase (Lox), microfibrillar associated protein 5 (Mfap5) , and microfibrillar associated protein 2 (Mfap2) which are all known to be involved in elastogenesis. The predominate occurrence of miR-29 binding sites within the set of 63 candidate elastogenic genes supports the analysis of miRNA binding sites to predict regulation of elastogenesis. miR-29 also binds to collagen type V, alpha 2 (Col5a2), collagen type IV, alpha 5 (Col4a5), cysteine dioxygenase 1, cytosolic (Cdo1), ectonucleotide pyrophosphatase/phosphodiesterase 2 (Enpp2), and hexosaminidase A (Hexa) which have not previously been shown to regulate elastin but may warrant investigation.

5.5 Conclusion

The challenge to analyzing the copious amount of data within DNA microarrays is selecting the appropriate computational tools to integrate genomic and functional databases and interpret coordinately regulatory networks of genes. Promoter Analysis and Interaction Network Generation Tool, PAINT, utilizes a database of gene regulatory sequences located in the promoter region upstream of the transcription start site and cross-references with a database of know transcription factor binding sites or response elements (TREs) to predict the likelihood of transcription factor binding in a given set of genes. Enrichment of TREs in a given set of genes is compared to a random reference set of promoters to ensure statistically significant overrepresentation of TREs. Analysis of the subset of the 63-gene candidate elastogenic set in which expression patterns were similar to elastin characterized 11 overrepresented TREs of which four were previously known to regulate elastogenesis: B-Myb Sp1, cKrox and PPAR. A closer look at the TREs enriched within the elastin promoter revealed five overrepresented TREs, of which two were known form previous studies to regulate elastin: PPAR and Sp1. The finding of elastogenic transcription factors validates the use of PAINT to identify regulators of elastogenesis. Many new candidate elastin regulating transcription factors were identified for which pharmacological agents exist and can ultimately be tested for effects on elastogenesis.

Specific mapping of TREs using chromatin immunoprecipitation (ChIP) studies and the UCSC Genome Browser illustrated binding sites for PPAR, a

PPAR coactivator, and WT1/EGR-1 around the elastin transcription start site. The likelihood of TF/TRE binding in the elastin promoter indicates PPAR and WT1/EGR-1 as potential regulators of elastogenesis.

Additional gene regulation was assessed through target mRNA searches with microRNA.org. MicroRNA (miRNA) binding sites on the 63 genes in the candidate elastogenic gene set were particularly prevalent in Lox, an important crosslinker of elastin fibers. Additionally miR-29, a known regulator of elastogenesis, was significantly predominant within the 63-gene elastogenic gene set. It is likely that other miRNAs highlighted in the miRNA analysis play a likely role in the regulation of elastogenesis.

CHAPTER SIX

MODULATORS OF TROPOELASTIN EXPRESSION IN AN IN VITRO CULTURE MODEL

6.1 Introduction

Prior studies have shown that elastin matrix synthesis is regulated by numerous biochemical factors that may be promote elastin synthesis (Table 5.2) or inhibit or degrade elastin (Table 5.3) as summarized previously in Chapter 3. Convergent microarray analysis identified 63 genes as candidate regulators of elastogenesis which can be tested in vitro through pharmacological agonist or antagonists. Subsequent transcriptional regulatory analysis with PAINT identified potential regulatory transcription factors that if targeted with pharmacological agonists or antagonists may prove to regulate multiple elastogenesis regulating genes within the set of 63 candidate regulators. In the case that agonists or antagonists are unavailable, transfection of a plasmid expression vector containing the genetic sequence for a gene or transcription factor of interest can be used to upregulate expression. Conversely, transfection of small interfering RNA (siRNA) can be used to downregulate expression.

6.2 Materials and methods

6.2.1 Cell Culture

Human foreskin fibroblasts (HFF, ATCC no. SCRC-1041) were obtained as a generous gift from Dr. LaRue. HFFs were expanded in Dulbecco's Modified

Eagles Medium (DMEM) High; with Sodium Pyruvate and without L-glutamine (Fisher Scientific) supplemented with 15% v/v FBS (Atlanta Biologicals), 1% v/v GlutaMAX (Life Technologies, Grand Island, NY), and 1% v/v penicillin/streptomycin (Fisher Scientific). Media was changed every 3 days and cells were passaged at 80-90% confluence with TrypLE Express (Life Technologies, Grand Island, NY). Low passage (6-8) HFFs were used for the following studies.

Neonatal rat aortic smooth muscle cells (nRASMCs) were isolated by a method based on that described by Oakes *et. al.*(*266*). Three litters of neonatal Sprague-Dawley rats (~21 rats aged 3 days postnatal) were sacrificed previously by CO_2 asphyxiation and decapitation as per protocols approved by the Animal Research Committee at the Medical University of South Carolina and at Clemson University. Aortal segments were removed from euthanized rats, from arch to the celiac axis, under sterile conditions, and spliced lengthwise in petri dishes containing cold phosphate-buffered saline (PBS) containing 2 mM Ca^{2+}. These spliced sections were then transferred to a dish containing 1-2 ml of collagenase (2 mg/ml; Worthington) and incubated for 10 minutes at 37 °C. Dulbecco's Modified Eagles Medium (DMEM) supplemented with 15% FBS and 1% v/v penicillin/streptomycin (Fisher Scientific) that had been passed through a 0.22 μm sterile filter was then added to these collagenase treated samples and mixed well with gentle pipetting. Isolated aortal segments were further chopped crosswise into 0.5 mm long pieces and transferred using fine needles onto sterile petri dishes, pre-scratched to facilitate cell attachment. The explants were

incubated in limited volumes of the above medium at 37 °C for a week, to establish primary culture. Cells were periodically observed microscopically in order to monitor attachment and proliferation. At the end of one week, the explants were removed carefully and sufficient media added to the dish to promote cell proliferation. After the 2nd passage, cells were proliferated in DMEM High; with Sodium Pyruvate and without L-glutamine (Fisher Scientific) supplemented with 10% v/v FBS (Atlanta Biologicals), 1% v/v GlutaMAX (Life Technologies, Grand Island, NY), and 1% v/v penicillin/streptomycin (Fisher Scientific). Media was changed every 3 days and cells were passaged at 80-90% confluence with TrypLE Express (Life Technologies, Grand Island, NY). Low passage nRASMCs (P4-8) were used for the following studies.

6.2.2 Immunostaining Elastin Fibers.

HFFs were cultured in DMEM previously described in 6.2.1 at a density of 1.0x10^4 cells/cm^2 in an 8-well chamberslide. After 3, 5, 7, and 14 days of culture cells were rinsed twice with PBS and fixed in cold methanol for 10 minutes. The monolayer was rinsed 3 times in PBS before incubation in blocking solution of 5% goat serum in PBS for 30 minutes at room temperature (RT). Cells were then incubated overnight at 4ºC with 1:1000 primary anti-bovine elastin antibody (a generous gift from Dr. Mecham) in solution containing 1% goat serum in PBS. Cells were washed 3 times with PBS before secondary antibody labeling with Alexa Fluor 546-conjugated anti-rabbit IgG (Invitrogen, Carlsbad, CA) in 1% goat serum in PBS for 45 minutes at RT. All unbound antibody was washed away with

3 washes of PBS before nuclear staining with DAPI in Vectashield mounting medium (Vector Laboratories, Burlingame, CA) and coverslipped. Elastin fibers were detected by immunofluorescent imaging using a Leica sp5 confocal microscope with a 20X objective.

6.2.3 Quantitative RT-PCR

RNA was extracted 24h after treatment using Qiagen's RNeasy RNA extraction kit according to the manufacturer's instructions. RNA integrity was assessed by a Bioanalyzer 2100 (Agilent Technologies, Palo Alto, CA), and cDNA was prepared using the iScript cDNA synthesis kit (Bio-Rad, Hercules, CA) with 1 μg RNA according to the manufacturer's instructions. 10 μL reactions of each sample were prepared using 5 μL SSO Fast EvaGreen supermix (Bio-Rad, Hercules, CA), 0.5 μL each 10 μM forward and reverse primers, 1 μL DEPC-treated water, and 3 μL of the optimized dilution of cDNA. Reactions were amplified for forty cycles at optimized temperatures in an iCycler real-time PCR detection system (Bio-Rad, Hercules, CA). The resulting data were analyzed with the PCR Miner software, which calculates individual threshold cycle values and gene efficiency for a set of primers. All gene expression levels were normalized to a housekeeping gene that is constitutively expressed at a relatively constant level across many or all known conditions. (e.g., βactin, GAPDH, and TATA-box binding protein) expression levels.

6.2.4 Pharmacological Agonist/Antagonist Treatment.

In order to screen candidate genes and transcription factors of interest, an in vitro culture model was designed to test pharmacological agonists and antagonists. Human foreskin fibroblasts (ATCC no. SCRC-1041) (HFFs) were plated in 6-well plates at $1.0x10^4$ cells/cm^2 and allowed to attach overnight. In some experiments cells underwent serum starvation for 18 – 24 h in DMEM High; with Sodium Pyruvate and without L-glutamine (Fisher Scientific) supplemented with 0.1% v/v FBS (Atlanta Biologicals), 1% v/v GlutaMAX (Life Technologies, Grand Island, NY), and 1% v/v penicillin/streptomycin (Fisher Scientific) so as to synchronize cell cycle phase (*267*) and maximize mRNA production after treatment. Pharmacological agonists and antagonists to transcription factors were added in fresh DMEM High; with Sodium Pyruvate and without L-glutamine (Fisher Scientific) supplemented with 10% v/v FBS (Atlanta Biologicals), 1% v/v GlutaMAX (Life Technologies, Grand Island, NY), and 1% v/v penicillin/streptomycin (Fisher Scientific) or fresh low serum (0.1%) media for serum starvation experiments.

It was predicted that hypothesized positive effectors of elastogenesis (e.g., neuraminidase, IGF-1) would increase the total amount of elastin transcription, deposition and/or increase the rate of elastin deposition. Conversely, negative effectors of elastogenesis (e.g., chondroitin sulfate) would decrease the total amount of elastin transcription, deposition and/or decrease the rate of elastin.

Sp1. Sp1 is a known regulator of elastic fiber formation (*146; Sen, 2011 #165*) that was implicated in the PAINT analysis as having a potential binding site

in the elastin promoter. In order to validate the PAINT analysis and the culture model we administered mithramycin (Sigma, St. Louis), a Sp1 antagonist, to inhibit elastin.

PPAR. PPAR was identified through PAINT analysis as a potential regulatory transcription factor of elastogenesis with a potential TRE located in the elastin promoter. PPAR has already been shown to have dual effects on elastin transcription: both increasing (*241*) and repressing elastin expression in fibroblasts (*238, 242*). PPARα has yet to be examined for its role in elastogenesis therefore we tested the effects of PPARα agonist and antagonist on elastin expression.

HFFs were plated at confluence and allowed to attach overnight before treatment with 1 – 100 μM PPARα agonist (C7081, Sigma), 3.33 – 30 μM PPARα antagonist (GW6471, Sigma), and/or 10 – 30 μM PPARγ antagonist (GW9662, Sigma). RNA was extracted at 24 h using Qiagen's RNeasy RNA extraction kit according to the manufacturer's instructions. RNA integrity was tested by Bioanalyzer 2100 (Agilent Technologies, Palo Alto, CA) and cDNA was prepared using the iScript cDNA synthesis kit (Bio-Rad, Hercules, CA) with 1 μg RNA according to the manufacturer's instructions. cDNA preparations were diluted 1:10, and 3 μL was used in 10-μl reactions for qRT-PCR as described previously in 6.2.3.

WT1/EGR-1. WT1 was identified as an enriched transcription factor by PAINT in the analysis of the subset of genes whose expression pattern is similar to elastin. A similar transcription factor that binds the same consensus sequence

on a TRE was identified in the other subset of the candidate elastogenic gene set. EGR-1 was enriched to bind the subset of genes with an expression pattern different from elastin. EGR-1 has a similar conformational structure as WT1 and often regulates the same genes in an opposing direction. The identification of these pair of opposing transcription factors in the different subsets suggest WT1 and EGR-1 act to coordinate regulation of the elastin gene.

The one available pharmacological agent to regulate transcription factors WT1 or EGR-1 was the WT1 antagonist Ganetespib (Sta-9090), an investigational anticancer drug developed by Synta Pharmaceuticals (Lexington, MA). Ganetespib is a small molecule inhibitor of heat shock protein 90 (HSP90), a molecular chaperone required for the proper maturation and activation of numerous client proteins and often overexpressed in cancer (*268-271*). Hsp90

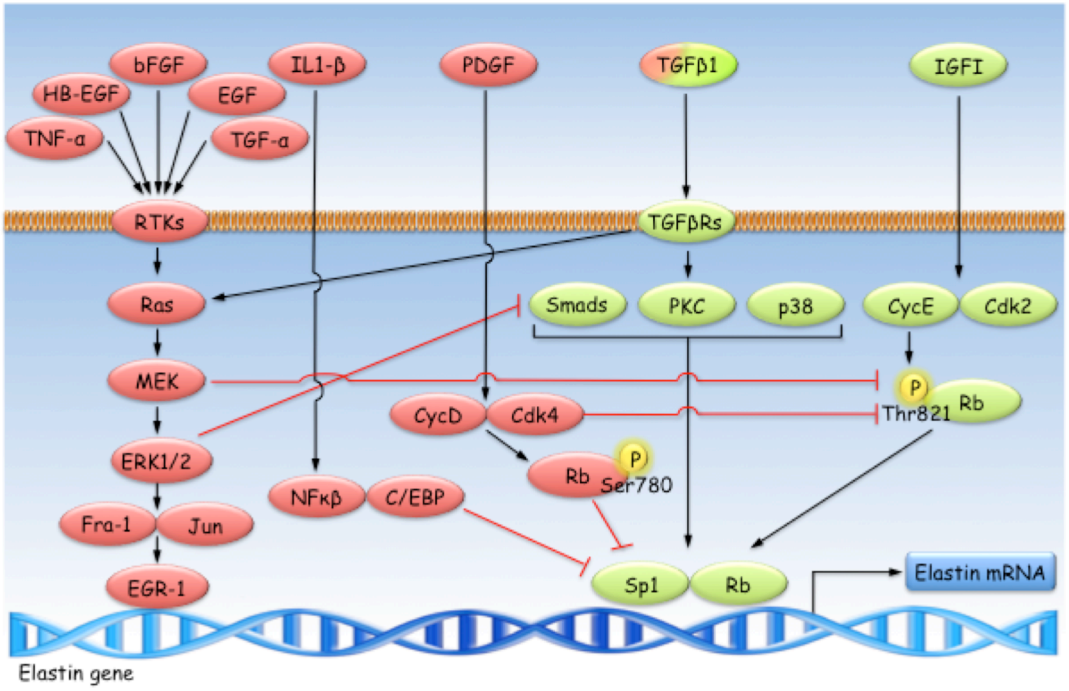

Figure 6.1. Egr-1 is hypothesized to signal through the MAPK pathway and suppress elastin transcription. Conversely, displacement of Egr-1 by transcription factor WT1 will shift the signaling cascade of events toward increase elastin transcription.

also associates with WT1 protein and stabilizes its expression (*272*). Pharmacological inhibition of Hsp90 with Ganetespib resulted in ubiquitination and subsequent proteasome-dependent degradation of WT1 in the human CML cell line K562 and AML cell line KG-1. Downstream targets of WT1, c-Myc and Bcl-2 were also subsequently downregulated (*272*).

EGR-1 was experimentally determined to be a downstream target of extracellular signal-regulated kinase 1 and 2 (ERK1/2) in a mononuclear phagocyte (RAW) cell culture model. Carbon monoxide mediated suppression of ERK activation resulted in Egr-1 inhibition. ERK 1/2-driven Egr-1 expression and regulation of its downstream target genes was cGMP-dependent (*273*). Modification of the signaling cascade of factors regulating elastin transcription by insertion of Egr-1 leads to the hypothesis that Egr-1 is a negative regulator of elastin transcription via the MAPK pathway. Conversely, displacement of Egr-1 by transcription factor WT1 will shift the signaling cascade of events toward increase elastin transcription. Treatment of HFFs with 12 nM – 1 μM Ganetespib is expected to antagonize WT1 and thus decrease elastin transcription compared to MeOH controls. If elastin regulation is mediated via the MAPK pathway, co-culture of 37 nM Ganetespib with 50 nM Mek inhibitor PD98059 may reverse the effects by decreasing downstream Egr-1 and upregulating elastin transcription.

6.2.5 Transfection of Plasmid Expression Vectors

6.2.5.1 Plasmid Stock Culture Preparation

In the absences of pharmacological agents to augment expression of WT1 and EGR-1, transfection of plasmid expression vectors containing the sequence for WT1 and EGR-1 were performed on HFFs. Sequence-Verified human WT1 and EGR1 were generated from the Mammalian Gen Collection (MGC), a trans-NIH initiative, that provides sequence-validated full-length protein-coding (FL-CDS) cDNA clones (Thermo Fisher Scientific, Pittsburgh, PA). Plasmids were obtained as live bacterial cultures containing the plasmid of interest. Stock cultures for each plasmid were prepared by isolation of a single colony from a streak plate on LB agar containing 100 μg/mL ampicillin. Bacterial cultures of stock cultures for WT1 and EGR-1, in addition to empty vector control were proliferated in 100 mL Luria Broth (LB) medium containing 100 μg/mL Ampicillin overnight and plasmid purification performed with a Plasmid Midi Kit (Qiagen, Valencia, CA) according to manufacturer's instructions. Plasmids were extracted and concentration determined by spectrophotometry. Concentrations were adjusted to be equal for each type of plasmid.

6.2.5.2 Transfection with Amaxa Nucleofector Kit

Transfection of human foreskin fibroblasts (HFFs) with plasmid vectors with performed with a Lonza Amaxa Nucleofector Kit (Lonza) according to manufacturer's protocol. For each transfection reaction 82 μL of Nucleofector Solution plus 18 μL of supplement was combined to make 100 μL of total

reaction volume. Passage 7 HFFs were detached from the plate with TrypLE. 3 x 106 cells/transfection were centrifuged at 10,000 rpm x 5 min and the cell pellet resuspended in 100 μL Nucleofector Solution. 2.5 μg plasmid DNA was added to each reaction. Cell/DNA suspension was transferred to a certified cuvette and placed in the Nucleofector device for administration of the program U-023 for normal adult human dermal fibroblasts. Media is immediately added to the cell/DNA suspension and aliquotted into 4 replicate wells of a 6-well plate. 3 individual transfections were performed for each of 3 plasmid expression vectors. RNA was extracted at 24 h post transfection and converted to cDNA for qRT-PCR quantification of elastin expression.

6.2.5.3 Transfection with Lipofectamine

Human foreskin fibroblasts (ATCC no. SCRC-1041) (HFFs) were plated in 6-well plates at $1.0x10^4$ cells/cm^2 overnight prior to transfection. For each well, 2.5 μg DNA (expression vector, and 2.5μL of PLUS reagent was incubated with 100 μL OptiMEM medium for 15 minutes at room temperature. 2.75 μL Lipofectamine was added to the transfection medium and incubated 30 minutes at room temperature. One mixture was prepared with 0.5 μg GFP plasmid following the same procedure; this mixture was used to transfect a separate well of cells. The plated cells were washed twice with sterile PBS before 2 mL OptiMEM medium before the DNA containing transfection mixture was added. Transfection efficiency was assessed at 18 hours by immunofluorescence, specifically determining the percentage of cells producing GFP in the GFP-

transfected population. RNA was extracted, cDNA synthesized, and mRNA expression levels quantified with qRT-PCR as described above.

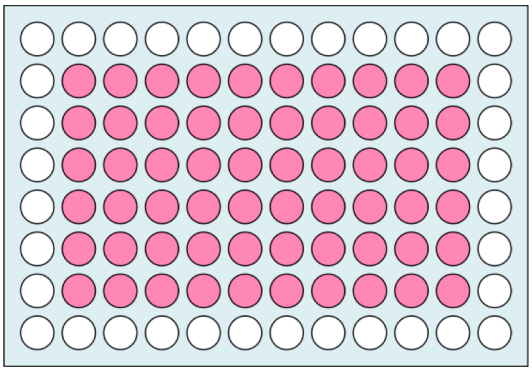

Figure 6.2. 96-well plate setup for development of a quantitative elastin assay. The pink circles represent the 60 wells that contained cells while the outer ring of white circles represent the wells incubated with PBS in order to prevent evaporation from cell-containing wells within the incubator.

6.2.6 Design of a quantitative Elastin ELISA

We have taken steps toward development of a novel in vitro assay that quantifies incorporation of elastin into the ECM of fibroblast monolayers. Human foreskin fibroblasts (ATCC no. SCRC-1041) were seeded into wells of 96 well culture plates at $1x10^4$ cells/cm^2 in media. In order to prevent a ring effect whereby evaporation occurs from wells on the plate perimeter, the outer wells are filled with PBS and the inner 60 wells are utilized for the assay as illustrated in Figure #. Duplicate plates were designed for parallel culture in order to measure elastin in one plate and normalize to cell viability in a replicate plate.

Pharmacological agents were added in varying concentrations. Control wells received delivery vehicles. As a control, we administered bacterial neuraminidase (Neu1) to cultured cells since Neu1 is required for assembly of elastic fibers (*94*) and studies have shown administration of Neu1 augments elastin deposition by VSMCs (*50*).

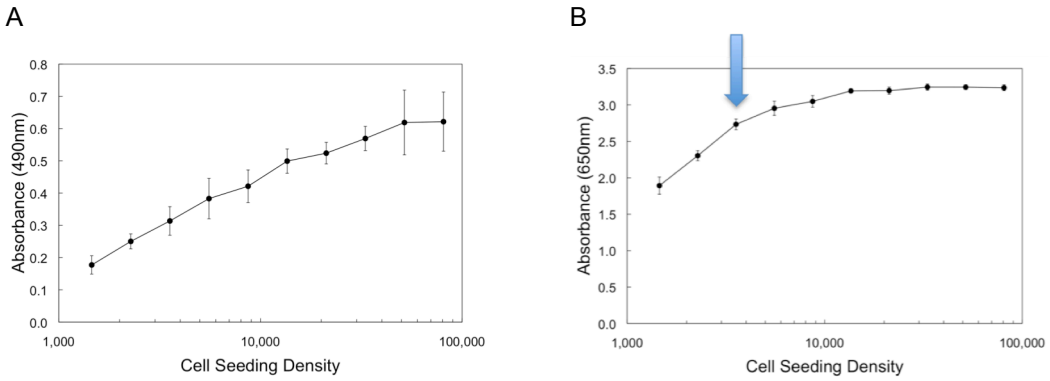

Figure 6.4. Elastin ELISA quantification is optimal for seeding density after 3 days in culture. A. Proliferation of human foreskin fibroblasts (HFFS) as measured by MTS assay reaches a steady state around 3-5 days in culture. **B.** Elastin deposition by HFFs reaches a steady state by approximately 4 days in culture. Immunofluorescence of anti-elastin labeling was detected by elastin ELISA (n=3/timepoint).

Day 3 was chosen as a fixed timepoint because it demonstrates the transition period between human foreskin fibroblast (HFF) proliferation to steady state and the point at which the amount of elastin deposition can be assessed prior to steady state in HFFs (Figure 6.3).

Seeding densities ranging from 10^2 – 10^{11} cells/cm^2 were assayed by MTS assay and anti-elastin ELISA. A seeding density of 1 x 10^4 cells/cm^2 was chosen based on Figure 6.3 where elastogenesis is still occurring in the exponential

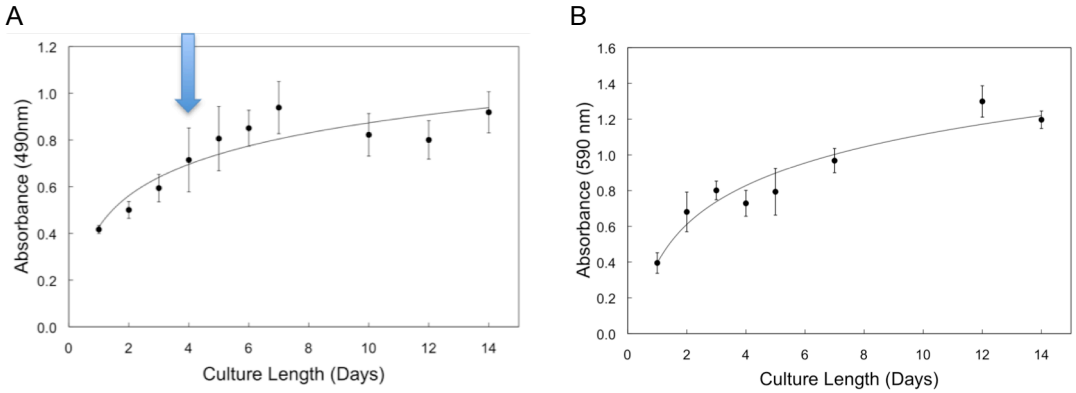

Figure 6.3. Elastin ELISA quantification is optimal for elastin deposition after 3 days in culture. A. Proliferation of human foreskin fibroblasts (HFFS) as measured by MTS assay reaches a steady state around 3-5 days in culture. **B.** Elastin deposition by HFFs reaches a steady state by approximately 4 days in culture. Immunofluorescence of anti-elastin labeling was detected by elastin ELISA (n=3/timepoint).

growth phase but in a large enough quantity to be assayed.

6.2.6.1 Immunostaining Elastin

At 72 hours post treatment, cells were rinsed with PBS and fixed with ice cold methanol. The monolayer was rinsed 3 times in PBS before incubation in blocking solution of 5% goat serum in PBS for 30 minutes at room temperature (RT). Cells were then incubated overnight at 4ºC with 1:1000 primary anti-bovine elastin antibody (a generous gift from Dr. Mecham) in solution containing 1% goat serum in PBS. Cells were washed 3 times with PBS before secondary antibody labeling with 1:10000 horseradish peroxidase (HRP) labeled anti-rabbit IgG in 1% goat serum in PBS for 45 minutes at RT. All unbound antibody was washed away with 3 washes of PBS. The cell layer was then incubated with ECL plus detection reagents containing peroxide to generate chemifluorescence. The assay was incubated in the dark at RT and chemifluorescence was detected at 15 minute time intervals by spectrophotometry at 430nm. Raw absorbance values were normalized to cell viability as assessed by MTS assay described next.

6.2.6.2 MTS Assay for Normalization

Normalization of elastin immunofluorescence was performed using a colorimetric MTS assay using One Solution Reagent (Promega) to measure cell viability as a function of metabolic activity. Replicate 96-well plates of HFFs or

nRASMCs were seeded and cultured identically to conditions set for immunolabeling.

The One Solution Reagent is comprised of a tetrazolium compound MTS (3-(4,5-dimethylthiazol-2-yl)-5-(3-carboxymethoxyphenyl)-2-(4-sulfophenyl)-2H-tetrazolium, inner salt) and an electron coupling reagent PES (phenazine ethosulfate). PES has enhanced chemical stability, which allows it to be combined with MTS to form a stable solution. The MTS tetrazolium compound is reduced by the mitochondria of live cells to yield a formazan product that is soluble in tissue culture medium. This conversion is presumably accomplished by NADPH or NADH produced by dehydrogenase enzymes in metabolically active cells.

At the time of fixation of 96-well plates used in elastin immunolabeling, One Solution Reagent was added to the parallel plates in order to compare total viability. 20 μL One Solution Reagent was added via multichannel pipette to each well of the 96-well plate containing live cells in 100 μL cell culture media and incubated at 37 ºC in a humidified CO_2 incubator. Absorbance was quantified by spectroscopy at 490 nm at the same 15 minute intervals as parallel plates for elastin immunolabeling. Background absorbance from control wells containing no cells was subtracted from the sample absorbance measurements. The MTS assay has a sensitivity of 800 cells per 96-well plate.

6.2.7 Fabrication of 3D Gelatin Constructs

6.2.7.1 Cell Culture of Microcarrier Beads

Macroporous gelatin-coated microcarrier beads, CultiSpher-G, (Percell Biolytica AB, Astorp, Sweden), with an average particle diameter of 130-380 μm, pore size of 20 μm, and density 1.02-1.04 g/cm^3 at 25 ºC, were purchased from Sigma Chemical Co. (St. Louis, MO). The microcarrier beads were rehydrated, autoclaved, and preincubated at 37 ºC in cell culture medium according to manufacturer instructions. Microcarrier beads were combined with HDFs (passage 4) or HFFs (passage 8) at a ratio of 10^6 cells per 0.5 mL suspended microcarrier beads. The cell-microcarrier mixture was added to 50 mL cell culture medium in a 125 mL siliconized Techne biological stirrer flask (R&D Systems, Minneapolis, MN). The suspension was subjected to an intermittent stirring regime (30 min rest, 2 min at 50 rpm) on a Techne Biological Stirrer (model MCS-104S) for 48 h at 37 ºC in a humidified 5% CO_2 incubator. Additional media (25 mL) was added after 24 h incubation.

6.2.7.2 Tubular Structure Formation in Agarose Molds

An agarose mold for assembling 4 mm tubular structures was created with 2% molten agarose (Low EEO, J.T. Baker Chemical Co., Phillipsburg, NJ) in Dulbecco's phosphate buffered saline (PBS) and a template manufactured from acrylic and polyetheretherketone (PEEK). The template was designed to fit into a 6-well tissue culture plate (Falcon; Becton-Dickinson, Franklin Lakes, NJ) containing agarose and removed after the agarose had solidified. The agarose

mold was preincubated with PBS for 1 h and then with cell culture media for 2 h at 37 ºC in a humidified 5% CO_2 incubator. The 48h incubated cell-microcarrier beads described previously were seeded into the tubular molds and covered with cell culture media that was replaced every 24h over a culture period of 7 or 14 days at 37 ºC in a in a humidified 5% CO_2 incubator.

6.2.7.3 Histological Staining and Immunohistochemistry

For histochemical staining, tubular constructs were dissected away from the agarose molds and rinsed twice with PBS and fixed in cold methanol for 10 minutes. The structures were rinsed 3 times in PBS before incubation in blocking solution of 5% goat serum in PBS for 30 minutes at room temperature (RT). Cells were then incubated overnight at 4ºC with 1:1000 primary anti-bovine elastin antibody (Dr. Mecham) in solution containing 1% goat serum in PBS. Cells were washed 3 times with PBS before secondary antibody labeling with Alexa Fluor 546-conjugated anti-rabbit IgG (Invitrogen, Carlsbad, CA) in 1% goat serum in PBS for 45 minutes at RT. All unbound antibody was washed away with 3 washes of PBS before mounting in Vectashield mounting medium (Vector Laboratories, Burlingame, CA). Elastin fibers were detected by immunofluorescent imaging using a Leica sp5 confocal microscope with a 20X objective.

6.3 Results

6.3.1 Elastic Fiber Assembly

Table 6.1. Cell associated elastin immunostaining

Cell Type[3]		Days in Culture					
		3	5	7	10	12	14
VSMC (PAC-1 pulmonary artery line; rat)	Control transfection	+[1]		+[1,2]			+[1,2]
	V3 transfection	+[1]		+[1,2]			+[1,2]
ASMC (neonatal aorta; rat)	Control transfection	+[1]		+[1]			-[1]
	V3 transfection	+[1]		+[1]			-[1]
Fibroblast (dermal; human)		-[2]		-[2]		+[1,2]	
Fibroblast (lung; mouse)		-[1,2]		-[1]+[2]			-[1]+[2]
Fibroblast (foreskin; human)		-[2]	+[2]	+[2]	+[2]	+[2]	+[2]

[1]Rabbit anti-tropoelastin of several species (Elastin Products Co.)
[2]Rabbit anti-bovine tropoelastin (Dr. Mecham)
[3]Cells plated at 5.6E+05 cells/cm[2]
Highlighted cells represent extracellular elastin immunostaining

Of all the different cell types cultured and immunolabeled with the combination of anti-elastin antibodies, only one cell type displayed extracellular elastic fiber staining: the human foreskin fibroblast (HFF). Intracellular tropoelastin is seen at day 3 and by day 5 elastic fibers first appeared in the extracellular matrix space. The density of fibers increased up to a certain plateau by day 7 and did not seem to further increase in number or thickness by day 14.

6.3.2 Comparison of Elastic Fiber Assembly by Cell Type

Anti-tropoelastin immunolabeling of certain in vitro cultured cell types (Table 6.1) produced a diffuse intracellular stain of tropoelastin monomers often

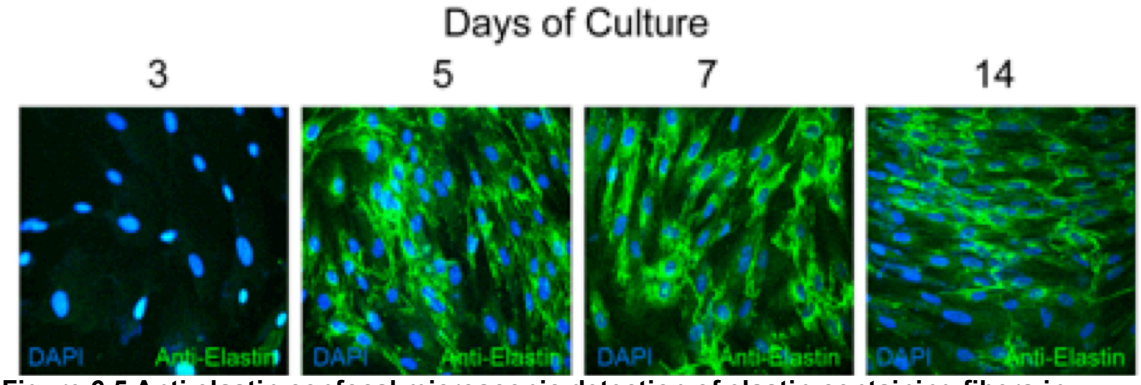

Figure 6.5 Anti-elastin confocal microscopic detection of elastin-containing fibers in human foreskin fibroblast ECM on successive days of culture. Anti-elastin stained fibers are green and DAPI stained nuclei are blue.

appearing punctate. After extended culture length the tropoelastin monomers did not appear to migrate to the extracellular matrix space to form elastic fibers. It is possible that in these cell types under these culture conditions elastic fiber assembly is impaired.

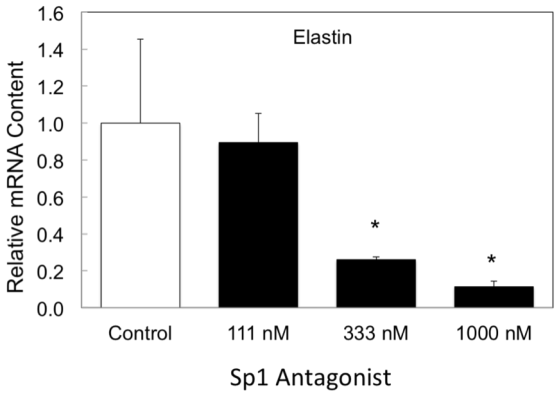

Figure 6.6. Mithramycin, an antagonist of Sp1, inhibits elastin expression in a dose dependent manner in human foreskin fibroblasts (HFFs). It is known from previous studies that transcription factor Sp1 enhances elastogenesis

6.3.3 Screening of Candidate Elastogenic Regulators

The in vitro culture model of HFFs was validated with predicted inhibitor of elastin transcription, mithramycin A. Increasing concentrations of mithramycin decrease elastin expression in a dose dependent manner (Figure 6.6).

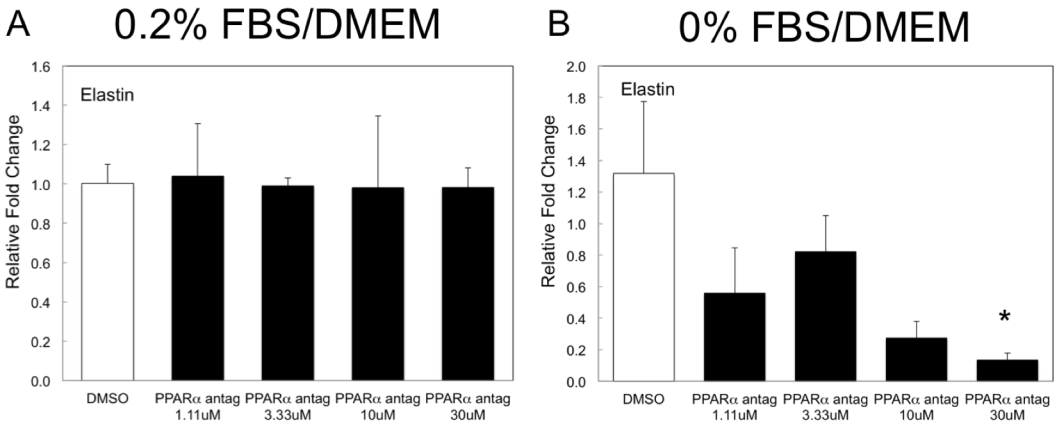

Figure 6.7. Serum starving HFFs treated with PPARα antagonist decreased elastin transcription at high concentrations. Reduction in serum levels 24 hours before and during treatment with PPARα antagonist reversed the previously seen increase in elastin transcription. Statistical analysis was performed with Student's T test ($p<0.05$)

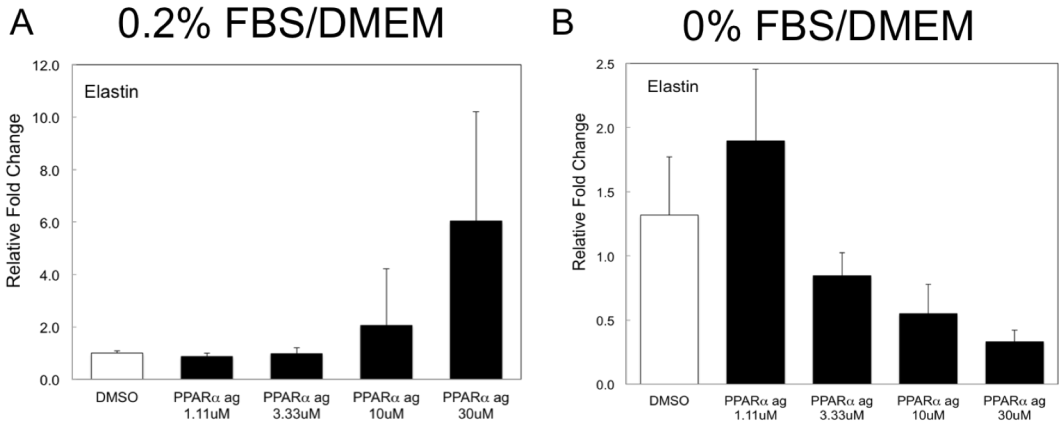

Figure 6.8. Serum starving HFFs treated with PPARα agonist did not augment elastin transcription. Reduction in serum levels 24 hours before and during treatment with PPARα agonist reduced the previously seen increase in elastin transcription. Statistical analysis with Student's T test did not validate any regulation of elastin.

Human foreskin fibroblasts (HFFs) cultured in media containing 10% FBS display seemingly conflicting upregulation of elastin expression in response to both PPARα agonist and antagonist treatment. Experiments employing serum starvation with no or low levels of FBS diminished the statistically significant increase in elastin transcription, however increasing concentrations of PPARα a gonist in 0.2% FBS/DMEM appeared to trend toward an increase (Figure 6.8). Conversely serum starvation prior to treatment with PPARα antagonist displayed a reduction in elastin transcription levels in 0% FBS/DMEM in response to the highest treatment of 30 μM PPARα antagonist (Figure 6.7)

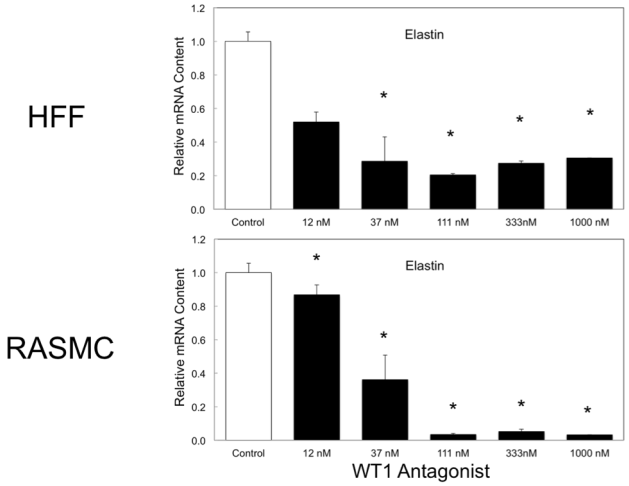

Figure 6.9. WT1 antagonist Ganetespib treatment decreased elastin transcription in a dose dependent manner in both human foreskin fibroblasts (HFFs) and rat aortic smooth muscle cells (RASMCs) as measured by qRT-PCR (n=3 samples/concentration). Statistical analysis calculated with Student's T test ($p<0.05$).

WT1 antagonist Ganetespib treatment decreased elastin transcription in a dose dependent manner in both human foreskin fibroblasts (HFFs) and rat aortic smooth muscle cells (RASMCs) as measured by qRT-PCR (Figure 6.9). Ganetespib is thus a novel regulator of elastogenesis.

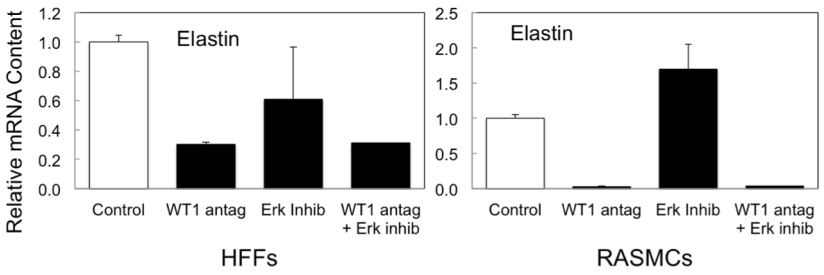

Figure 6.10. Inhibition of Mek1 with PD98059 does not rescue downregulation of elastin in response to WT1 antagonist Ganetespib. Human foreskin fibroblasts (HFFs) and rat aortic smooth muscle cells were co-cultured with 37nM Ganetespib and 50nM Mek1 inhibitor for 24 h. Elastin expression was quantified with qRT-PCR and statistical significance computed with Student's T test ($p<0.05$).

Subsequent experimentation to elucidated the mechanism by which Ganetespib downregulates elastin employed co-culture of a MEK1 inhibitor PD98059. The MEK1 inhibitor was unable to rescue downregulation of elastin transcription in response to WT1 antagonist Ganetespib at the treated concentration and duration (Figure 6.10).

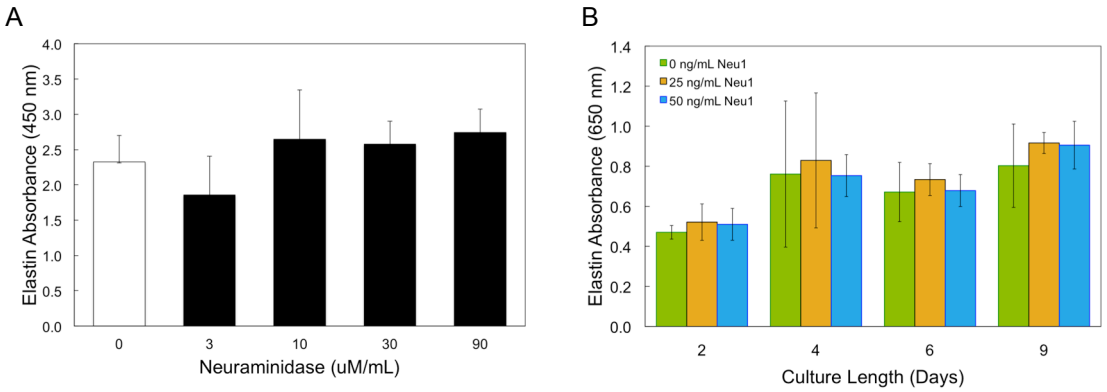

Figure 6.11. Neuraminidase (Neu1) does not affect total elastin deposition (**A)** or rate of deposition (B) by human foreskin fibroblasts (HFFs) in the elastin assay (n=3/timepoint and concentration).

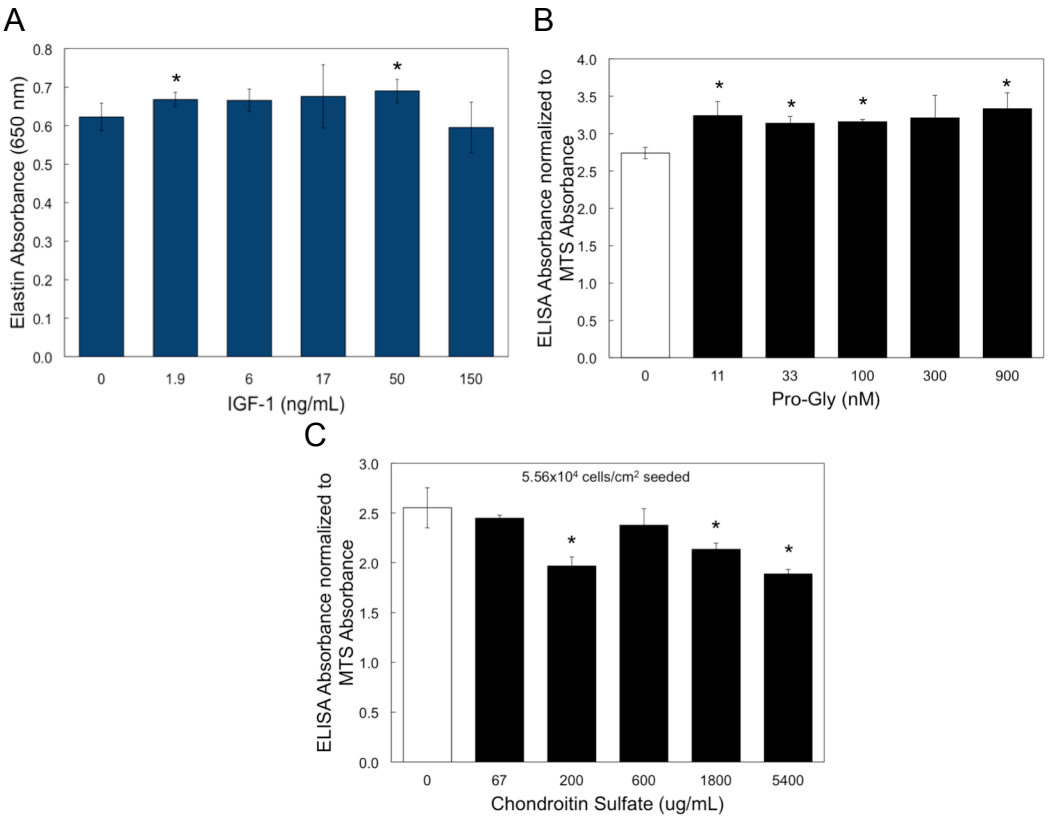

Figure 6.12. Known regulators of elastin were tested in the Elastin ELISA. A, IGF-1 , a known enhancer of elastogenesis, increased elastin deposition, along with **B**, pro-gly, another known enhancer. **C**, Chondroitin Sulfate (CS), a known inhibitor of elastogenesis, reduced elastin deposition by HFFs in an elastin ELISA. (n=3/concentration). Statistical analysis with Student's T test ($p<0.05$).

6.3.4 Development toward an ELISA to quantify elastin deposition

Measurement of elastin deposition in response to the Neuraminidase (Neu1) positive control did not elicit the expected increase in elastin total deposition or rate of deposition (Figure 6.11). Increasing concentrations of Neuraminidase did not have any effect on anti-elastin absorbance, neither did increased culture length. However the proposed negative control Chondroitin Sulfate (CS), a known inhibitor of elastogenesis, reduced elastin deposition by HFFs at day 3.

The elastin assay made use of other positive regulator of elastogenesis, Pro-Gly and IGF-1. Elastin expression was minimally increased with both Pro-Gly

and IGF-1 treatment, however not in a dose dependent manner (Figure 6.12 A and B).

A gene from the 63-gene candidate elastogenic set was screened by exogenous addition of 0.22 – 18 μg/mL Haptoglobin. A significant increase in elastin was quantified at 2 and 18 μg/mL (Figure 6.13).

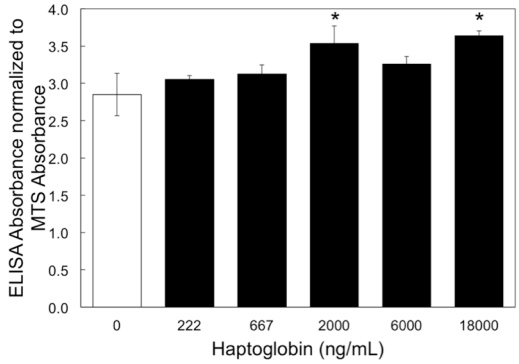

Figure 6.13. Haptoglobin increased elastin deposition by HFFs in an elastin ELISA (n=3/concentration). Statistical analysis with Student's T test ($p<0.04$).

6.3.5 Elastin Expression in Transfectants

Expression vector efficiency was determined with qRT-PCR expression. WT1 transfected HFFs demonstrated an 85 fold increase in WT1 as compared to empty vector transfected HFFs. EGR-1 expression was increased approximately 3 fold (Figure 6.15). Statistical analysis was performed with a Students T-test and determined to be significant for WT1 transfected cells but not for EGR-1.

Figure 6.16 illustrates a dramatic decrease in elastin expression by 89% (p=0.009) in

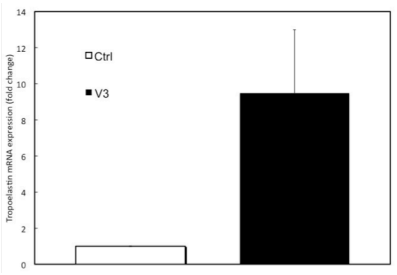

Figure 6.14 . V3 induced tropoelastin expression in smooth muscle cells. PAC-1 cells were transfected with lipofectamine with V3-containing plasmid and empty vector control. RNA was extracted at 24h and expression levels determined by qRT-PCR with TaqMan primers for elastin.

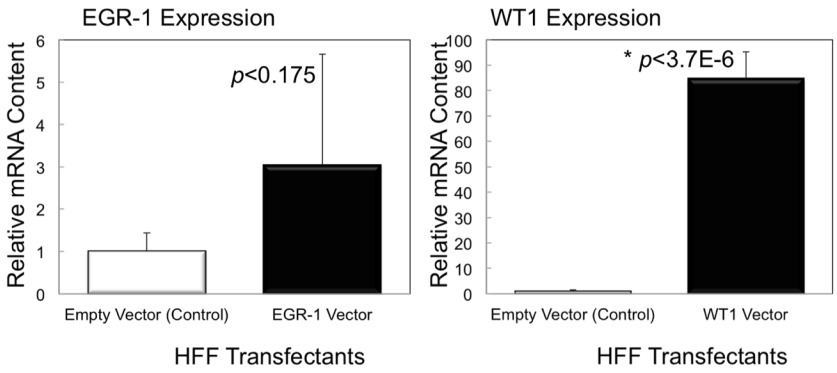

Figure 6.15. Transfection of expression vectors validated with qRT-PCR.

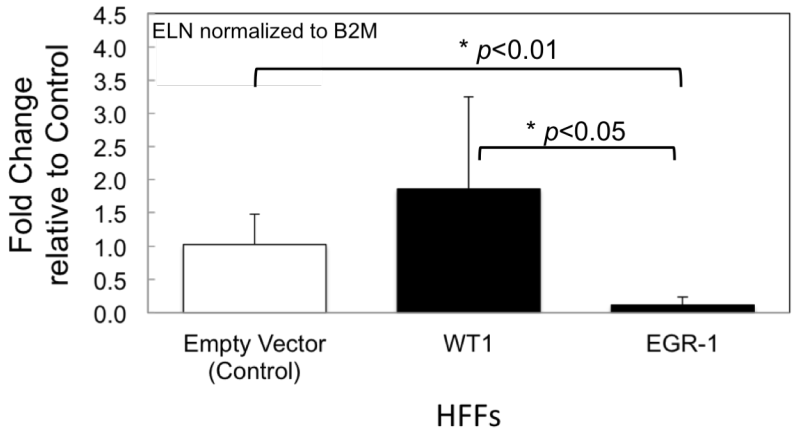

Figure 6.16. Elastin expression is decreased by EGR-1 in HFFs. Transfected HFFs with plasmid expression vectors was performed with Lonza Amaxa Nucleofector Kit and qRT-PCR performed on RNA extracted 24 h post transfection. Elastin expression significantly decreased by EGR-1 expression by 89%. Elastin expression is differentially regulated between the WT1 and EGR-1 transfected

response to a modest, yet not statistically significant, increase in EGR-1 expression. It is possible that expression can be improved with increased number of transfections thus lowering the standard deviation. Surprisingly only a modest increase in EGR-1 expression was required for repeated decreases in elastin expression (n=3). In response to WT1 transfection elastin expression is not significantly regulated however its mean expression level is 82% higher than empty vector control. The standard deviation is too large due to large increases in elastin transcription in only 2 of the 4 transfections. Statistical analysis between the two experimental groups WT1 transfected HFFs and EGR-1 transfected HFFs is significantly different ($p<0.05$).

Comparison of multiple transfections points toward a trend in elastin regulation in response to WT1. As WT1 expression increases with more efficient transfections, the average expression level of elastin increases as measured by qRT-PCR (Figure 6.17).

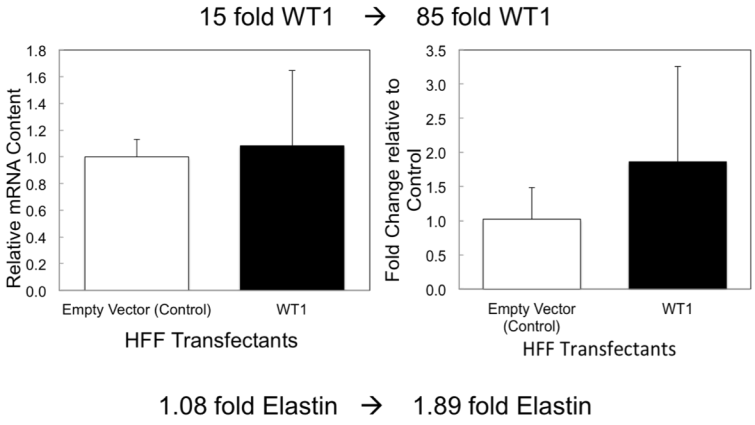

Figure 6.17. Elastin expression is trending toward significance with improved WT1 transfection efficiency. Comparison of elastin expression in two different transfections shows a 75% increase in elastin expression (1.08 vs. 1.89) with a 5.7 fold increase in WT1 (15 vs. 85).

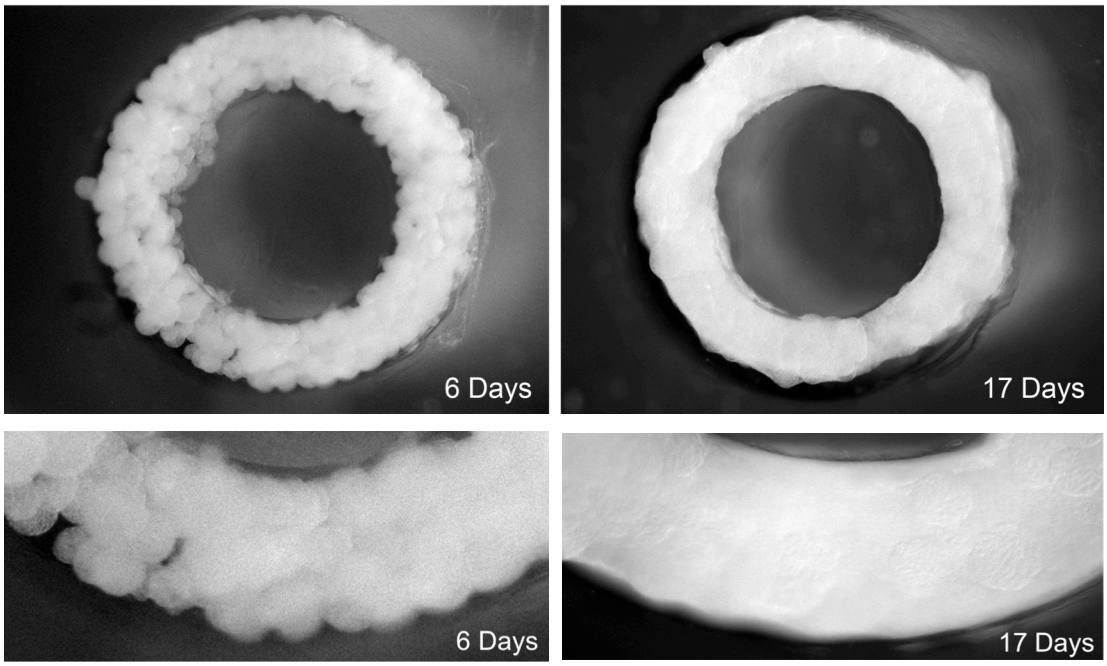

Figure 6.18. Macroporous gelatin microcarrier beads populated with HFFs. Human foreskin fibroblasts (HFFs) adhered to gelatin microcarrier beads over 48 hours in a stirred suspension before seeding into tubular molds. The HFF populated beads fused forming a tubular structure. Brightfield images were taken at 6 days and 17 days in culture. Remodeling and filling of the intrabead space either by cells or extracellular matrix is apparent by 17 days.

6.3.6. Elastin Expression in 3D Gelatin Constructs

The beginnings of construction on the proof of concept model of a 3D gelatin construct from macroporous gelatin-coated microcarrier beads and human foreskin fibroblasts (HFFs) were generated. Fusion of the beads occurred after 7 day of culture in the tubular shaped molds and strengthened in tension as noticed by handling with increasing culture duration. Cellular staining indicated infiltration of some cells into the pores but the majority of HFFs were attached to the bead surface or in the extracellular space between beads. Anti-elastin staining demonstrated the presence of mature elastic fibers at 7 days and 12 days in culture (Figure 6.19).

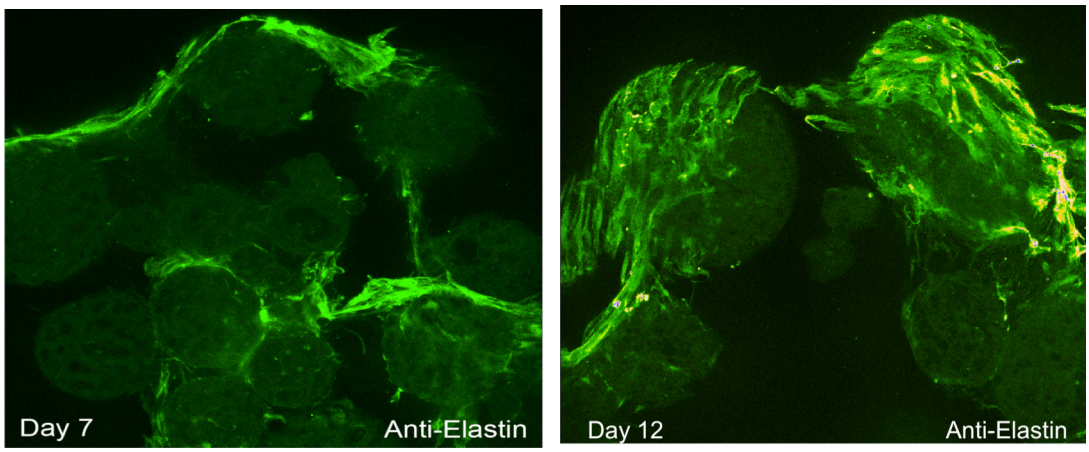

Figure 6.19. Elastin immunostaining of macroporous gelatin microcarrier beads populated with HFFs. Human foreskin fibroblasts (HFFs) adhered to gelatin microcarrier beads over 48 hours in a stirred suspension before seeding into tubular molds. The HFF populated beads fused forming a tubular structure and were fixed at day 7 and day 12 and immunostained for elastin.

6.4 Discussion

Increasing concentrations of mithramycin, an antagonist Sp1, a known augmenter of elastogenesis in HFFs decreased elastin expression, thus validating the tissue culture model as an appropriate assay for regulators of elastin transcription.

WT1 antagonist Ganetespib treatment decreased elastin transcription in a dose dependent manner in both human foreskin fibroblasts (HFFs) and rat aortic smooth muscle cells (RASMCs) as measured by qRT-PCR. This marks the first time a WT1 antagonist has been shown to downregulate elastin transcription.

Subsequent experimentation aimed at elucidating the mechanism by which Ganetespib downregulated elastin targeted the MAPK pathway. Co-culture of a MEK1 inhibitor PD98059 attempted to disrupt downstream signaling of Egr-1, a hypothesized suppressor of elastogenesis. The MEK1 inhibitor was unable to rescue downregulation of elastin transcription in response to WT1 antagonist

Ganetespib at the treated concentration and duration. It is possible that the MEK1 inhibitor did not fully disrupt downstream signaling as it did not block MEK2. Future studies could aim to target MEK1/2 or the downstream target of ERK 1/2 to decrease Egr-1 signaling. It is also possible that the concentration of MEK1 inhibitor at 50 nM was too low to fully suppress all MEK1 signaling. A concentration increase of MEK inhibitor can be performed to possibly generate an increase in elastin transcription.

Contrary to expected results, elastin expression increased in HFFs treated with both PPARα agonist and PPARα antagonist. If only PPARα levels are changing in response to the agonist and antagonist, then it would follow that any effects seen would have opposing expressions. It is likely that the PPARα agonist or PPARα antagonist is inducing transcription via stimulation of another enhancer of elastin transcription. Follow-up qRT-PCR was performed on expression levels of PPAR∂. In smooth muscle cells, PPAR∂ agonist was shown to increase tropoelastin production (*274*). qRT-PCR confirmed that PPARα antagonist increased PPAR∂ expression, possibly as a compensatory response to decreased PPARα activity. Future experimentation should neutralize the increase in PPAR∂ by incorporation of the appropriate concentration of PPAR∂ antagonist.

Steps toward the development of an elastin ELISA based on anti-elastin labeling normalized to MTS assay of cellular proliferation were taken to quantify total elastin deposition and rate of deposition. An optimal timepoint of quantification was established at three days of culture while elastin deposition

and cell proliferation are still in the exponential growth phase prior to steady state. Optimal seeding density of A seeding density of 1 x 10^4 cells/cm^2 was chosen at which point elastin is being deposited in the exponential growth phase at a large enough quantity to be assayed.

Contrary to expected results, Neu1, a positive regulator of elastogenesis did not increase total elastin deposition or rate of deposition as measured by elastin ELISA. Other positive regulators Pro-Gly and IGF-1 did show a marginal increase in elastin deposition with statistical significance assessed by Students T test, however not in a dose dependent manner as expected. Chondroitin Sulfate, a negative regulator of elastogenesis also passed the Student's T test of significant regulation but the decrease in elastin deposition did not occur at intermediate timepoints.

The conflicting or marginal results could be due to the need for increased optimization of the parameters surrounding the elastin ELISA. Subsequent analyses could be performed to alter cellular seeding density, length of culture, and media concentration of FBS. If elastin expression is quantifiable in an in vitro system but elastin deposition is not as easily quantified, It is also possible that oxidative and nitrosative modification of tropoelastin within the in vitro model are preventing elastic fiber assembly (*28*). In a study by Akhtar et al. oxidation reduced crosslinking and interactions with other proteins required for elastic fiber assembly, including fibulin-4, fibulin-5, and fibrillin-2. Measurement of exogenously added oxidized tropoelastin showed less incorporation into the preexisting microfibrils of human retinal pigmented epithelial ARPE-19 cells

compared to unoxidized tropoelastin as detected by immunofluorescence microscopy (*28*). Nitration of TE was confirmed using the rabbit anti-N-Tyr antibody, followed by a FITC-conjugated anti-rabbit secondary antibody (*28*). If the in vitro culture model for the elastin ELISA is undergoing any oxidative stress, it would follow that elastic fiber assembly may be impaired. Gene ontological analysis of the 63 candidate elastogenic genes shows enrichment for the functional group of oxidoreductase which facilitates redox reactions. It is also possible that oxidative and nitrosative modification of tropoelastin within the in vitro model are preventing elastic fiber assembly (*28*). In a study by Akhtar et al. oxidation reduced crosslinking and interactions with other proteins required for elastic fiber assembly, including fibulin-4, fibulin-5, and fibrillin-2. Measurement of exogenously added oxidized tropoelastin showed less incorporation into the preexisting microfibrils of human retinal pigmented epithelial ARPE-19 cells compared to unoxidized tropoelastin as detected by immunofluorescence microscopy (*28*). Nitration of TE was confirmed using the rabbit anti-N-Tyr antibody, followed by a FITC-conjugated anti-rabbit secondary antibody (*28*). If the in vitro culture model for the elastin ELISA is undergoing any oxidative stress, it would follow that elastic fiber assembly may be impaired.

An optional culture model to pursue for screening of elastogenic regulators is the 3D culture of macroporous gelatin microcarrier beads seeding with human foreskin fibroblasts (HFFs). Deposition of elastic fibers is seen at 12 days in culture but not at 7 with an increase in culture duration also correlating with an increased ease in handling. The rings remained solid after 12 days and did not

dissociate into fragments. The 3D model offers advantages to 2D culture models by mimicking the increase in cell-cell contact and cell-scaffold contact in the native ECM environment, thus more closely evoking native cell responses.

Overall 3D, ECM-based cell scaffolds are superior over 3D synthetic scaffolds or two dimensional (2D) monolayer cell cultures in efforts to simulate the chemical and physical environment of tissues (*86, 88*). This model can serve to screen potential regulatory gene and transcription factors in future studies.

6.5 Conclusion

Increasing concentrations of mithramycin, an antagonist Sp1, a known augmenter of elastogenesis in HFFs decreased elastin expression, thus validating the tissue culture model as an appropriate assay for regulators of elastin transcription. While elastin transcription can be appropriately assessed, steps toward development of an elastin ELISA displayed conflicting or marginal variance of elastin deposition between experimental and control wells. Further optimization of the assay is required in order to clearly distinguish the effects of elastogenic regulators.

Screening of transcription factors identified as potential regulators of elastogenesis by PAINT with pharmacological agents discovered a novel regulator of elastin transcription. Ganetespib, a WT1 antagonist, repeatedly downregulates elastin expression in a dose dependent manner. The mechanism by which Ganetespib mediates elastin downregulation has yet to be determined,

however it wasn't altered with co-culture of 50 nM MEK1 inhibitor aimed at disrupting downstream regulation of EGR-1 via the MAPK pathway.

Egr-1, a member of the same transcription factor family as WT1, binds the same transcriptional regulatory elements (TREs) and is known to regulate the same genes, often in opposing directions whereby EGR1 activates the transcription of genes that WT1 represses (*257, 258*). Expression of Egr-1 by transfection of plasmid expression vectors results in decreased elastin transcription. This result fits the story of opposing roles of WT1 and Egr-1 for regulation of elastin transcription. Experimentation to augment elastin expression by expression of WT1 plasmid expression vector is trending toward an increase in elastin expression, however it has not approached statistical significance. Incorporation of additional transfections to increase statistical power may overcome standard deviation to yield an increase in elastin.

Future studies can also employ the use of an elastin producing 3D culture model incorporating human foreskin fibroblasts (HFFs) with gelatin microcarrier beads. Tubular constructs were created and after 12 days of culture were manageable and populated with mature elastic fibers. This proof of concept culture system provides the advantages of more closely mimicking the native cell environment in a 3D environment as compared to a 2D monolayer culture.

CHAPTER SEVEN

CONCLUSIONS, STUDY LIMITATIONS, AND FUTURE DIRECTIONS

7.1 Conclusions

Particularly important to the mechanical performance of tissues is elastin, an extracellular matrix (ECM) protein deposited by vascular smooth muscle cells (VSMCs) in the form of elastic fibers. In addition to serving as major structural elements of tissues, providing extensibility and elastic recoil, elastic fibers also influence vascular cell behaviors such as biochemical signaling pathways. Disruption of elastic fibers can initiate and progressively lead to the pathology of life threatening complications such as atherosclerosis, aneurysm and vasospasms (*4, 5*). Failure to regenerate a healthy elastin matrix in response to damage during disease (e.g., inflammation-mediated elastin degradation in atherosclerosis) can severely compromise elastic tissue homeostasis (*13, 14*). A major concern in the construction of tissue engineered elastin-rich tissue is the ability to regulate cell behavior and encourage the regeneration of elastin fibers.

The overarching goal of this application was to advance an approach to regenerative medicine involving accelerated production of elastic fibers. Severe quantitative and qualitative deficiencies in the process of elastogenesis exhibited by cultured cells (*28, 29*) create an impediment to the engineering of tissues requiring functional elastin architecture.

Through convergent DNA microarray analysis of gene expression profiles associated with normal elastogenesis occurring during 1) mouse lung and aorta development, 2) elastogenesis in lung and skin in response to injury, and 3) in

vascular smooth muscle cells (VSMCs) stimulated to produce elastin fibers, 63 commonly regulated genes were identified genes with known regulators of elastin formation (Eln, Lox, Mfap2, Mfap5) and genes that appear to represent new players in the process of elastogenesis.

Gene ontological analysis highlighted functional categories of extracellular matrix (ECM) and secretion, which follow the elastin gene beginning with secretion of a tropoelastin monomer and subsequent assimilation into mature elastic fibers comprising the ECM. The enrichment for the ontological group of oxidoreductase enzymes may prove to be a hindrance to elastogenesis as oxidation of tropoelastin prevents proper elastic fiber assembly. This may pertain primarily to the elastogenic processes of wound healing that are undergoing oxidative stress and ultimate assembly of inferior elastic fibers compared to developmental elastic fibers. Hierarchical organization of gene regulation within the 5 different elastogenic processes yielded a table of genes ranging from most similarly expressed as elastin to down to most differentially regulated compared to elastin (Appendix A). Group V highlights genes regulated similar to elastin during injury and different from elastin during development. These genes may provide insight into inferior elastic fiber quality in injury models.

Promoter Analysis and Interaction Network Generation Tool, PAINT, predicted the likelihood of transcription factor binding subset of the 63-gene candidate elastogenic set in which expression patterns were similar to elastin characterized 11 overrepresented TREs of which four were previously known to regulate elastogenesis: B-Myb Sp1, cKrox and PPAR. A closer look at the TREs

enriched within the elastin promoter revealed five overrepresented TREs, of which two were known form previous studies to regulate elastin: PPAR and Sp1. The finding of elastogenic transcription factors validates the use of PAINT to identify regulators of elastogenesis. Many new candidate elastin regulating transcription factors were identified for which pharmacological agents exist and can ultimately be tested for effects on elastogenesis.

Specific mapping of TREs using chromatin immunoprecipitation (ChIP) studies and the UCSC Genome Browser illustrated binding sites for PPAR, a PPAR coactivator, and WT1/EGR-1 around the elastin transcription start site. The likelihood of TF/TRE binding in the elastin promoter indicates PPAR and WT1/EGR-1 as potential regulators of elastogenesis.

Additional gene regulation was assessed through target mRNA searches with microRNA.org. MicroRNA (miRNA) binding sites on the 63 genes in the candidate elastogenic gene set were particularly prevalent in Lox, an important crosslinker of elastin fibers. Additionally miR-29, a known regulator of elastogenesis, was significantly predominant within the 63-gene elastogenic gene set. It is likely that other miRNAs highlighted in the miRNA analysis play a likely role in the regulation of elastogenesis.

Increasing concentrations of mithramycin, an antagonist Sp1, a known augmenter of elastogenesis in HFFs decreased elastin expression, thus validating the tissue culture model as an appropriate assay for regulators of elastin transcription. While elastin transcription can be appropriately assessed, steps toward development of an elastin ELISA displayed conflicting or marginal

variance of elastin deposition between experimental and control wells. Further optimization of the assay is required in order to clearly distinguish the effects of elastogenic regulators.

Screening of transcription factors identified as potential regulators of elastogenesis by PAINT with pharmacological agents discovered a novel regulator of elastin transcription. Ganetespib, a WT1 antagonist, repeatedly downregulates elastin expression in a dose dependent manner. The mechanism by which Ganetespib mediates elastin downregulation has yet to be determined, however it wasn't altered with co-culture of 50 nM MEK1 inhibitor aimed at disrupting downstream regulation of EGR-1 via the MAPK pathway.

Egr-1, a member of the same transcription factor family as WT1, binds the same transcriptional regulatory elements (TREs) and is known to regulate the same genes, often in opposing directions whereby EGR1 activates the transcription of genes that WT1 represses (*257, 258*). Expression of Egr-1 by transfection of plasmid expression vectors results in decreased elastin transcription. This result fits the story of opposing roles of WT1 and Egr-1 for regulation of elastin transcription. Experimentation to augment elastin expression by expression of WT1 plasmid expression vector is trending toward an increase in elastin expression, however it has not approached statistical significance. Incorporation of additional transfections to increase statistical power may overcome standard deviation to yield an increase in elastin.

Future studies can also employ the use of an elastin producing 3D culture model incorporating human foreskin fibroblasts (HFFs) with gelatin microcarrier

beads. Tubular constructs were created and after 12 days of culture were manageable and populated with mature elastic fibers. This proof of concept culture system provides the advantages of more closely mimicking the native cell environment in a 3D environment as compared to a 2D monolayer culture.

7.2 Study Limitations

7.2.1 Microarray Limitations

Elastin is highly expressed in utero and then strongly downregulated after birth (*275, 276*). Only low maintenance levels of tropoelastin mRNA are found in most elastic tissues in adults (*276, 277*). Repair of severe injuries, such as third-degree burns, produces tissue that is often heavily scarred and severely limited in flexibility, range of motion, and tissue function (*278*). Similar scarring is seen after prolonged cancer radiation therapy, in sun-damaged skin (*279*), and in systemic sclerosis (*280, 281*), In the vasculature, Eln haploinsufficient phenotypes include narrowing (stenosis) of the ascending aorta in the perinatal period and hypertension later in life. Production of a collagen-rich extracellular matrix (ECM) that is deficient in elastic fibers occurs following these injury induced conditions. A major cause of the deficiency in elastic fiber production is the failure to upregulate tropoelastin gene expression in postnatal tissues. It is a recognized risk that in models of elastogenesis not occurring during development in which lower quality or defective elastic fibers are produced, comparison of commonly regulated genes may exclude certain critical genes. It is however necessary to include processes in which elastogenesis occurs outside of

development so as to preen the convergent list of regulated genes from commonly regulated genes specific to development. Comparison of the genes common to developmental processes of elastogenesis to injury models or in vitro models could shed light on key genes responsible for elastic fiber defects in wound repair and in vitro.

7.2.2 Epigenetic Regulation

In addition to studying gene expression, transcription factor induction of gene expression and microRNA inhibition of gene expression, newer findings suggest the importance of regulation at the epigenetic level. Epigenetic regulation refers to heritable changes in gene regulation that occur without a change in the DNA sequence and are therefore not encoded at the genomic level and can therefore not be assessed by microarray technology. Epigenetic regulation primarily concerns the chromatin structure and the possible chemical modification of some DNA bases.

DNA molecules are tightly wound around proteins known as histones to form a complex known as chromatin. Post-translational modification of histones alters their interaction with DNA and with proteins in the cell's nucleus. Combinations of such modifications are thought to constitute a code, the so-called “histone code” that plays a role in genome function, including gene regulation and DNA repair. Additionally DNA can be modified mainly by DNA methylation, typically occurring at CpG sites, that is, at sites where a cytosine (C) is directly followed by a guanine (G) in the DNA sequence. Such sites are often

found at higher density near gene promoter sequences where they are collectively referred to as CpG islands. Both chromatin structure and CpG islands have become an increasing concern of computational biologists although good models and data are often missing to be able to conduct large-scale exploratory computer studies.

7.2.3. 2D culture model

In summary I have shown HFFs are very efficient producing elastin fibers after 3 days in culture as compared to other cell types which did not produce any extracellular fibers (PAC-1, HDF, HASMC, RASMC, MLF). Also relative amounts of elastin mRNA are higher in HFFs compared to other cells (PAC-1, HDF, HASMC). These findings indicate that HFFs are efficient at in vitro elastin formation. Because of the known opposing regulatory roles of transcription factors WT1 and Egr-1 along with experimental findings of a decrease in elastin transcription in both HFFs treated with a WT1 antagonist and also HFFs transfected to express EGR-1, it would follow that elastin transcription would be upregulated in response to WT1 expression. Because repeated experiments have yet to yield significantly upregulated elastin transcription it may not be possible in this 2D culture system of HFFs to see a substantial increase in elastin transcription. It is possible that HFFs are assembling elastic fibers at maximum capacity with no possible cellular resources for augmentation of transcription.

It has been shown that 3D, ECM-based cellular scaffolds offer overall superiority over 3D synthetic scaffolds and 2D monolayer cell cultures in in efforts to simulate the chemical and physical environment of tissues (*86, 88*). 3D

culture models most closely mimic native cell environment whereby cells within 3D scaffolds come into contact with other cells and ECM in three dimensions and are therefore expected to more closely evoke native cell responses than 2D substrates.

7.3 Future Directions

7.3.1 Modulation of Differentially Expressed Genes in Development vs. Injury

Hierarchical organization of gene regulation within the 5 different elastogenic processes yielded a table of genes ranging from most similarly expressed as elastin to down to most differentially regulated compared to elastin (Appendix A). Group V highlights genes regulated similar to elastin during injury and different from elastin during development. These genes may provide insight into inferior elastic fiber quality in injury models. Inhibition of this set of genes may suppress inherent inhibitors or adult elastin expression, inflammation associated genes, or oxidative stress resulting in an upregulation of elastogenesis quantity and quality.

Wound healing models incorporating an injury such as naphthalene injection or skin punch biopsy and subsequent elastin regeneration as described in the convergent microarray analysis would provide an excellent model for testing this group of genes. In vitro culture models of wound healing can also be evaluated such as a scratch test assay. A confluent monolayer of elastin producing cells (e.g., HFFs, nRASMCs) is first cultured with sufficient time to deposit a rich extracellular matrix (~7 days). The monolayer is then disrupted and

a group of cells destroyed or displaced by scratching a line through the layer. The open gap is then slowly closed during “healing” by migrating cells to cover the damaged area. Addition of pharmacological antagonists to Aebp1, Cebpa, Cebpb, Hk2, Por, or Ptgis can be added in experimental groups. Some antagonists may need to be added under serum starved conditions to increase effectiveness. Cell layers can be fixed at 2, 3, 4, and 5 days post injury for immunostaining of elastin to assess elastic fiber quality. Cell monolayers can be rinsed twice with PBS and fixed in cold methanol for 10 minutes. The monolayers can be rinsed 3 times in PBS before incubation in blocking solution of 5% goat serum in PBS for 30 minutes at room temperature (RT). Cells can then incubate overnight at 4ºC with 1:1000 primary anti-bovine elastin antibody (Dr. Mecham) in solution containing 1% goat serum in PBS. Cells can then be washed 3 times with PBS before secondary antibody labeling with Alexa Fluor 546-conjugated anti-rabbit IgG (Invitrogen, Carlsbad, CA) in 1% goat serum in PBS for 45 minutes at RT. All unbound antibody will be washed away with 3 washes of PBS before mounting in Vectashield mounting medium (Vector Laboratories, Burlingame, CA). Elastin fibers can be detected by immunofluorescent imaging using a Leica sp5 confocal microscope.

An alternate in vitro wound healing model could incorporate Electronic Cell-substrate Impedance Sensing (ECIS) plates. A monolayer of cells could be cultured as before and injured via high voltage shocks. This model has the advantage of reducing injury variability. Immunostaining can be performed as described previously.

RNA can be extracted and qRT-PCR performed as described previously. This model also offers the increased data collection capabilities of impedance as cells migrate to cover the gap during the wound healing process. Antagonism to the genes identified as upregulated in wound healing of elastogenesis and downregulated during developmental elastogenesis may lead to increased elastic fiber quality, larger diameter or length of continuous fibers, or increased rate to elastic fiber deposition.

7.3.2 MicroRNA Studies

miRNAs inhibition may prove to enhance elastin transcription. miR-23 is known to restrict cardiac valve formation by inhibiting hyaluronic acid synthase 2 (Has2) and production of extracellular hyaluronic acid (HA) (*282*). HA facilitates the synthesis and organization of microfibrils (fibrillin), a microfibrillar scaffold component for elastic fiber deposition (*283*). HA has been suggested to play an indirect role in elastogenesis through its intimate binding of versican (*65*) which in turn interacts with microfibrillar proteins (fibulin-1, 2) and elastin-associated proteins to form higher-order macromolecular structures important for elastic fiber assembly (*65, 284-286*). The highly anionic nature of HA causes soluble tropoelastin to assemble and facilitates LOX-mediated crosslinking into an insoluble matrix (*287, 288*), and stabilize elastin fibers against degradation by elastase (*286, 289, 290*). Inhibition of miR-23 may increases HAS2 and HA and subsequent elastin may be upregulated.

Alternate miRNAs to target in future studies are miR-133 and miR-590. In a study by Shan et al. nicotine produced significant upregulation of expression of TGF-β1 and TGF-βRII at the protein level, and a 60–70% decrease in the levels of miRNAs miR-133 and miR-590 (*291*). TGF-β1 and TGF-βRII are targets for miR-133 and miR-590 repression so the downregulation of miR-133 and miR-590 partly accounts for the upregulation of TGF-β1 and TGF-βRII. Additionally, transfection of miR-133 or miR-590 into cultured atrial fibroblasts decreased TGF-β1 and TGF-βRII levels and collagen content (*291*). Canonical TGFβ signaling has been shown to upregulate elastin in fibroblasts (*118, 122*) and aortic cells (*120*). Inhibition of miR-133 and miR-590 with anti-sense miRNAs may increase levels of TGF-β1 and TGF-βRII and stimulate tropoelastin expression.

Experimentation to assess the effects of miR-23, miR-133, or miR-590 on elastogenesis can incorporate antisense oligonucleotides (ASOs) or anti-miRNA oligonucleotides (AMOs) to selectively bind target miRNAs or their mRNA targets. AMOs are synthetic nucleotides that can be transfected into the cell to inhibit miRNA activity. Human foreskin fibroblasts can be plated in 6-well plates at $1.0x10^4$ cells/cm^2 overnight prior to transfection. For each well, 2.5 μg DNA (expression vector, and 2.5μL of PLUS reagent can be incubated with 100 μL OptiMEM medium for 15 minutes at room temperature. 2.75 μL Lipofectamine can be added to the transfection medium and incubated 30 minutes at room temperature. One mixture can be prepared with 0.5 μg GFP plasmid following the same procedure; this mixture can be used to transfect a separate well of cells.

The plated cells will need to be washed twice with sterile PBS before 2 mL OptiMEM medium before the DNA containing transfection mixture was added. Transfection efficiency can be assessed at 18 hours by immunofluorescence, specifically determining the percentage of cells producing GFP in the GFP-transfected population.

RNA can then be extracted at 12 h, 24 h, 48 h, and 72 h post injury and converted to cDNA. Elastin transcription can be assessed by qRT-PCR of elastin normalized to a reference gene (B2M) as described in Chapter 4.2.

7.3.3 PPAR delta Regulation

QRT-PCR confirmed that PPARα antagonist increased PPAR∂ expression in HFFs, possibly as a compensatory response to decreased PPARα activity. The next experimentation should attempt to neutralize PPARα-mediated upregulation of PPAR∂ and subsequent upregulation on elastin expression. PPAR∂ can be eliminated from the PPARα experimentation as an independent variable by determining the appropriate concentration of PPAR∂ antagonist to add to all experimental samples and control.

Preliminary studies assessed the effects of varying concentrations of PPAR∂ antagonist on HFFS (1.11, 3.33, 10 and 30 μM) with no significant effects on elastin expression (Figure 7.1). The next step in experimentation should be to coculture PPARα antagonist with varying concentrations of PPAR∂.

HFFs can be plated at confluence and allowed to attach overnight before treatment with 1.11 – 10 μM PPARα antagonist (GW6471, Sigma), and/or 1.11 - 10 μM PPAR∂ antagonist.

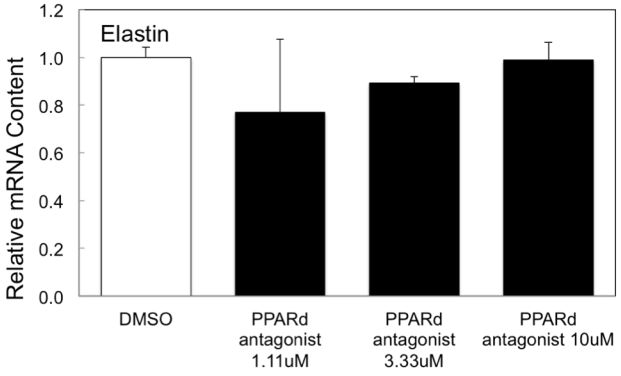

Figure 7.1. HFFs treated with PPAR∂ did not effect elastin expression. HFFs were cultured with 1.11, 3.33, 10, and 30 μM PPAR∂ antagonist (4 samples/concentration).

Different PPAR∂ antagonists can be tested as well. GSK0660 is a potent PPARβ/δ antagonist with a pIC50 of 6.8 (160 nM). GSK0660 is nearly inactive on PPARα and PPARγ with IC50s greater than 10 μM. Another PPAR∂ antagonist, PT-S58, is a PPAR β/δ full antagonist, and a derivative of GSK0660. PT-S58 has a three-fold higher affinity for the receptor than GSK0660 and is a potent inhibitor of agonist-induced target gene expression. Unlike GSK0660, PT-S58 blocks the recruitment co-repressor molecules such as SMRT.

Because the antagonists inhibit PPAR∂ activity, QRT-PCR cannot be used to validate inhibition by PPAR∂ expression. PPAR∂ activity can be measured by immunoblotting. Cell lysates can be fractionated into cytosolic and nuclear fractions, and proteins separated by SDS-PAGE, transferred to polyvinylidene difluoride membranes and immunoblotted with specific antibodies as described by . Protein levels can then be determined by densitometry and PPAR∂ antagonist concentration can be optimized to reduce PPAR∂ levels to the same as control treated samples.

Experimentation can then be performed with coculture of PPARα antagonist and PPAR∂ antagonist for 24 h, 48 h, and 72 h prior to RNA extraction using Qiagen's RNeasy RNA extraction kit according to the manufacturer's instructions. RNA integrity can be tested by Bioanalyzer 2100 (Agilent Technologies, Palo Alto, CA) and cDNA can be prepared using the iScript cDNA synthesis kit (Bio-Rad, Hercules, CA) with 1 μg RNA according to the manufacturer's instructions. cDNA preparations can be diluted 1:10, and 3 μL used in 10-μl reactions for qRT-PCR as described previously in 6.2.3 to assess elastin expression levels. It is expected that PPAR∂ antagonist treatment will reduce PPAR∂ levels back to baseline levels when cocultured with PPARα antagonist and elastin expression levels will be decreased.

7.3.4 Elucidation of the Mechanism by which Ganetespib Decreases Elastin Expression

Future studies could aim to target MEK1/2 or the downstream target of ERK 1/2 to decrease Egr-1 signaling. It is also possible that the concentration of MEK 1 inhibitor at 50 nM was too low to fully suppress all MEK 1 signaling. A concentration increase of MEK inhibitor PD98059 can be performed in a 3-fold dose dependent manner at 50 nM, 150 nM, 450 nM, and 1.35 μM PD98059. Increased concentration is expected to fully inhibit Mek1 and generate an increase in elastin transcription. An alternate inhibitor, U0126, displayed a higher affinity for MEK 1 and also inhibits MEK 2. Treatment of HFFs with variable concentrations of U0126 may be a more potent inhibitor of the MAPK pathway

and potential downstream EGR-1 signaling. Experiments can aim to reverse the downregulatory effects of Ganetespib on elastin expression through coculture of Ganetespib and U0126. RNA can be extracted at 12 h, 24 h, and 36 h post treatment and elastin expression can be quantified by qRT-PCR for elastin.

Alternately these experiments can be conducted under serum-free conditions along with serum starvation pre-treatment with antagonists in order to increase potency of antagonists.

7.3.5 Candidate Regulator Screening in 3D HFF-Gelatin Microcarriers Culture Model

The proof of concept of construction of a 3D tubular structure offers advantages to 2D culture models by mimicking the increase in cell-cell contact and cell-scaffold contact in the native ECM environment, thus more closely evoking native cell responses. An optional culture model to pursue for screening of elastogenic regulators is the 3D culture of macroporous gelatin microcarrier beads seeding with human foreskin fibroblasts (HFFs). Deposition of elastic fibers is seen at 12 days in culture but not at 7 with an increase in culture duration also correlating with an increased ease in handling. The rings remained solid after 12 days and did not dissociate into fragments.

Experimentation aimed to test candidate regulatory genes, transcription factors, and miRNAs can utilize the 3D culture model to hopefully obtain more substantial effects on elastin deposition and/or rate to elastin deposition.

Following the same protocol for HFF seeding of gelatin microcarrier beads as described in 6.2.7. Experimental agonists, antagonists, or antisense-miRNAs can be added exogenously in the media after plating the HFF-bead complexes into a tubular structure. After 5 d, 7 d, and 9 d of treatment, the tubular structures can be fixed in ice cold methanol and labeled with anti-elastin antibodies as described in 6.2.7.

It is expected that potential enhancers of elastogenesis may increase the rate of elastin deposition, therefore those tubular structures can be fixed for anti-elastin immunohistochemistry earlier than control rings are expected to display intact elastic fibers. Potential inhibitors can be fixed at later timepoints to address whether an inhibitor may act to decrease overall elastin deposition or decrease rate to elastic fiber formation. Total elastin deposition can be semi-quantitated with densitometry of immunoflurorescent images. Additional measurements of elastic fiber diameter and length can be used to address overall elastic fiber quality. A truly quantitative measurement of total elastin deposition can be determined with immunoblotting. Elastin protein can be isolated and purified as described by Dr. Mecham (*265*)wt1.

APPENDICES

Appendix A

A. Hierarchical Table of 63 Regulated Genes in Convergent Microarray Analysis of Processes in which Elastogenesis is a Key Component

			Expression Pattern Similar to Elastin			Expression Pattern Different from Elastin		
Group	Gene Symbol	Gene Name	Develop-ment	Injury	V3-Trans-duced VSMCs	Develop-ment	Injury	V3-Trans-duced VSMCs
	Eln	**elastin**	**X**	**X**	**X**			
I	Cdc20	cell division cycle 20 homolog (S. cerevisiae)	X	X	X			
	Gap43	growth associated protein 43	X	X	X			
	Maged2	melanoma antigen, family D, 2	X	X	X			
	Mfap2	microfibrillar-associated protein 2	X	X	X			
	Ndn	necdin	X	X	X			
	Col5a1	procollagen, type V, alpha 1	X	X	X			
II	Igf2r	insulin-like growth factor 2 receptor	X	X				X
	Lox	lysyl oxidase	X	X				X
	Col5a2	procollagen, type V, alpha 2	X	X				X
	Col14a1	procollagen, type XIV, alpha 1	X	X				X
	Sox11	SRY-box containing gene 11	X	X				X
III	Cdh11	cadherin 11	X		X			
	Hn1	hematological and neurological expressed sequence 1	X		X			
	Hnrnpa2b1	heterogeneous nuclear ribonucleoprotein A2/B1	X		X			
	Hmgb3	high mobility group box 3	X		X			
	Marcks	myristoylated alanine rich protein kinase C substrate	X		X			
	Myo1b	myosin Ib	X					X
	Nnat	neuronatin	X					X
	Npm1	nucleophosmin 1	X					X
IV	Hexa	hexosaminidase A		X	X	X		
	S100a13	S100 calcium binding protein A13		X	X	X		
V	Aebp1	AE binding protein 1		X		X		X
	Cebpa	CCAAT/enhancer binding protein (C/EBP), alpha		X		X		X
	Cebpb	CCAAT/enhancer binding protein (C/EBP), beta		X		X		X
	Hk2	hexokinase 2		X		X		X
	Por	P450 (cytochrome) oxidoreductase		X		X		X
	Ptgis	prostaglandin I2 (prostacyclin) synthase		X		X		X
VI	Lamb2	laminin, beta 2		X	X			
	Pdlim3	PDZ and LIM domain 3		X	X			
VII	Ccnd1	cyclin D1		X				X
	Mfap5	microfibrillar associated protein 5		X				X
VIII	Gucy1b3	guanylate cyclase 1, soluble, beta 3			X			
	Col4a5	procollagen, type IV, alpha 5			X			
	Sucla2	succinate-Coenzyme A ligase, ADP-forming, beta subunit			X		X	
IX	Dci	dodecenoyl-Coenzyme A delta isomerase (3,2 trans-enoyl-Coenzyme A isomerase)						X
	Gbp2	guanylate nucleotide binding protein 2						X
	Scd1	stearoyl-Coenzyme A desaturase 1						X
X	Ephx1	epoxide hydrolase 1, microsomal			X	X		
	Fasn	fatty acid synthase			X	X		
	Fxyd1	FXYD domain-containing ion transport regulator 1			X	X		
	Gas6	growth arrest specific 6			X	X		
	Timp3	tissue inhibitor of metalloproteinase 3			X	X		
XI	Enpp2	ectonucleotide pyrophosphatase/phosphodiesterase 2					X	X
XII	Aldoa	aldolase 1, A isoform				X		X
	Apoe	apolipoprotein E				X		X
	Cebpd	CCAAT/enhancer binding protein (C/EBP), delta				X		X
	Cd9	CD9 antigen				X		X
	Cdo1	cysteine dioxygenase 1, cytosolic				X		X
	Ddt	D-dopachrome tautomerase				X		X
	Dpep1	dipeptidase 1 (renal)				X		X
	Dnajb2	DnaJ (Hsp40) homolog, subfamily B, member 10				X		X
	Ech1	enoyl coenzyme A hydratase 1, peroxisomal				X		X
	Gpx3	glutathione peroxidase 3				X		X
	Gpx4	glutathione peroxidase 4				X		X
	Gstm1	glutathione S-transferase, mu 1				X		X
	Hp	haptoglobin				X		X
	Ier3	immediate early response 3				X		X
	Igfbp6	insulin-like growth factor binding protein 6				X		X
	Nr1h3	nuclear receptor subfamily 1, group H, member 3				X		X
	Phyh	phytanoyl-CoA hydroxylase				X		X
	Timp2	tissue inhibitor of metalloproteinase 2				X		X
XIII	**Cp**	**ceruloplasmin**				**X**	**X**	**X**

Table A: Convergent microarray analysis of processes in which elastogenesis is a key component identified 63 genes as potential regulators of elastogenesis which are depicted in a hierarchal Table A-2 from genes whose expression pattern is most similar to elastin descending to genes whose expression pattern is most different from elastin across all 5 processes. An “X” in the table is representative of having met the criteria in Table A-1.

Appendix B

Figure B: Heatmaps of Significantly Regulated Genes in Response to Versican V3 Expression in Vascular Smooth Muscle Cells (VSMCs)

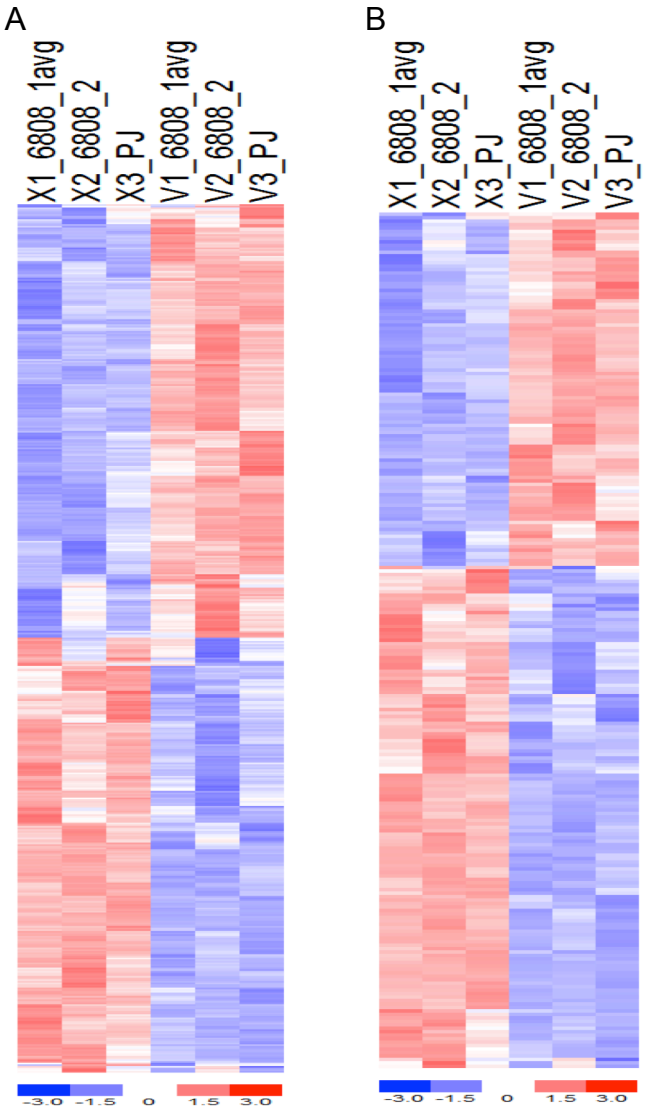

Figure B-1: The 3 sample pair analysis of yielded 521 genes significantly regulated in response to V3 with a fold change > 1.5 and a paired Student's T-test $p<0.05$. The false discovery rate (FDR) is 1.7%. Increasing the fold change to 2.0 decreases the number of significant genes to 247 with an FDR of 0.0%.

Appendix C

Figure C: Versican effects on TGFβ Signaling

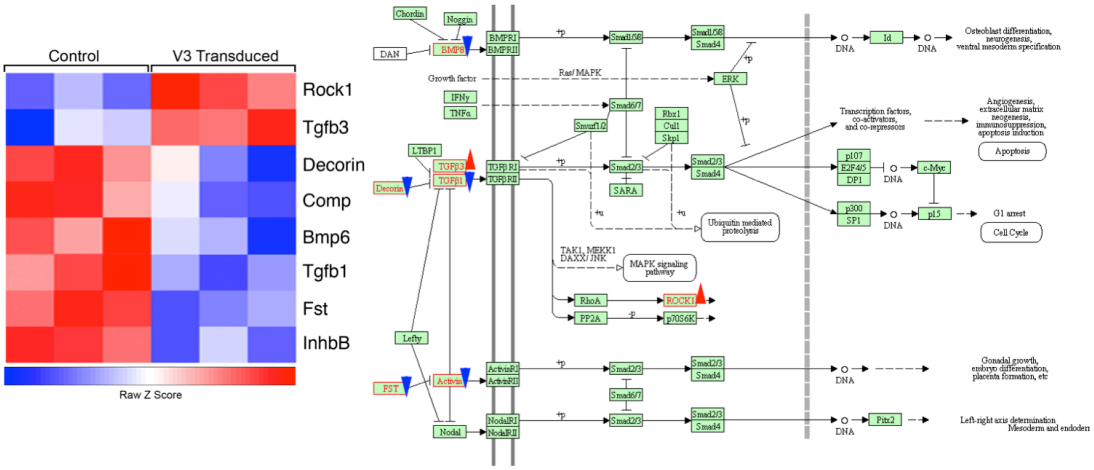

Figure C: The 3 sample pair analysis yielded 8 significantly regulated genes in the TGFβ pathway. Increases of expression are seen in ROCK1 and TGFβ3 while decreases in the expression of Decorin, Comp, Bmp6, TGFβ1, Fst, and InhbB.

Appendix D

Figure D. Human Elastin Splice Variants

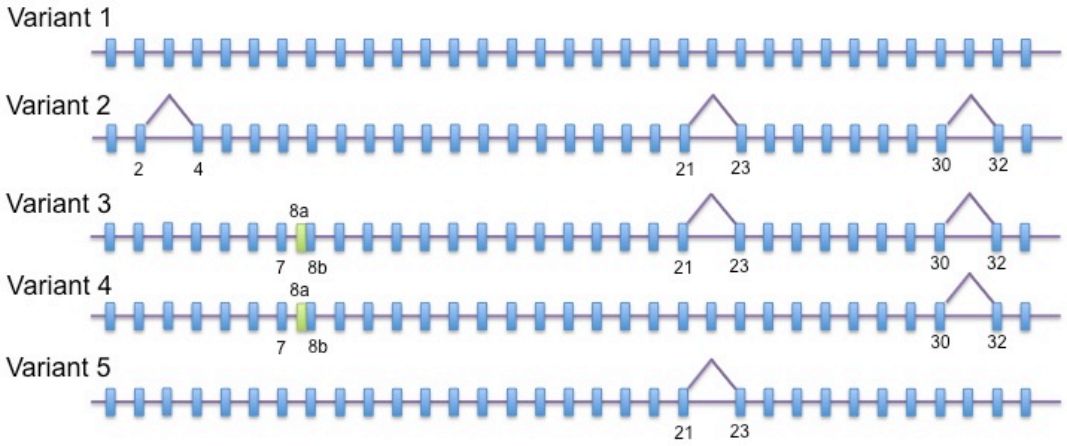

Figure D. The human elastin gene mRNA is alternately spliced into 5 different variants. Elastogenic cells produce multiple forms of tropoelastin mRNA within the same tissue, suggesting there may not be a functional or architectural difference between isoforms (*292*). The isoforms vary in size from 692 – 724 translated amino acid residues. The exons code for either hydrophobic (Variable) segments or lysine-rich crosslinkable (conserved) segments of elastin.

References

1. B. Chailley-Heu, O. Boucherat, A. M. Barlier-Mur, J. R. Bourbon, FGF-18 is upregulated in the postnatal rat lung and enhances elastogenesis in myofibroblasts. *American journal of physiology. Lung cellular and molecular physiology* **288**, L43 (Jan, 2005).

2. A. a. L. R. Robert, Ed., *Biology and Pathology of Elastic Tissues*, (1980).

3. E. D. Hay, *The cell biology of the extracellular matrix*. (Platinum Press, Ney York, 1991).

4. S. S. Ahanchi, N. D. Tsihlis, M. R. Kibbe, The role of nitric oxide in the pathophysiology of intimal hyperplasia. *Journal of vascular surgery* **45 Suppl A**, A64 (Jun, 2007).

5. W. H. Pearce, V. P. Shively, Abdominal aortic aneurysm as a complex multifactorial disease: interactions of polymorphisms of inflammatory genes, features of autoimmunity, and current status of MMPs. *Ann N Y Acad Sci* **1085**, 117 (Nov, 2006).

6. F. Sato *et al.*, Distinct steps of cross-linking, self-association, and maturation of tropoelastin are necessary for elastic fiber formation. *Journal of molecular biology* **369**, 841 (Jun 8, 2007).

7. M. J. Rock *et al.*, Molecular basis of elastic fiber formation. Critical interactions and a tropoelastin-fibrillin-1 cross-link. *The Journal of biological chemistry* **279**, 23748 (May 28, 2004).

8. T. Nakamura *et al.*, Fibulin-5/DANCE is essential for elastogenesis in vivo. *Nature* **415**, 171 (Jan 10, 2002).

9. H. Yanagisawa *et al.*, Fibulin-5 is an elastin-binding protein essential for elastic fibre development in vivo. *Nature* **415**, 168 (Jan 10, 2002).

10. P. R. Parks WC, Lee KA, Mecham R. Elastin, Elastin. *Advances in Cell Molecular Biology* **6**, (1993).

11. A. J. Bank *et al.*, Contribution of collagen, elastin, and smooth muscle to in vivo human brachial artery wall stress and elastic modulus. *Circulation* **94**, 3263 (Dec 15, 1996).

12. E. W. Raines, The extracellular matrix can regulate vascular cell migration, proliferation, and survival: relationships to vascular disease. *International journal of experimental pathology* **81**, 173 (Jun, 2000).

13. Y. Kimura, H. Okuda, Inhibitory effects of soluble elastin on intraplatelet free calcium concentration. *Thrombosis research* **52**, 61 (Oct 1, 1988).

14. Z. Urban *et al.*, Connection between elastin haploinsufficiency and increased cell proliferation in patients with supravalvular aortic stenosis and Williams-Beuren syndrome. *Am J Hum Genet* **71**, 30 (Jul, 2002).

15. Z. Urban *et al.*, Isolated supravalvular aortic stenosis: functional haploinsufficiency of the elastin gene as a result of nonsense-mediated decay. *Hum Genet* **106**, 577 (Jun, 2000).

16. C. A. Morris, C. B. Mervis, Williams syndrome and related disorders. *Annual review of genomics and human genetics* **1**, 461 (2000).

17. F. Ringpfeil, Selected disorders of connective tissue: pseudoxanthoma elasticum, cutis laxa, and lipoid proteinosis. *Clin Dermatol* **23**, 41 (Jan-Feb, 2005).

18. B. Loeys *et al.*, Homozygosity for a missense mutation in fibulin-5 (FBLN5) results in a severe form of cutis laxa. *Human molecular genetics* **11**, 2113 (Sep 1, 2002).

19. P. N. Robinson *et al.*, The molecular genetics of Marfan syndrome and related disorders. *J Med Genet* **43**, 769 (Oct, 2006).

20. H. C. Dietz, B. Loeys, L. Carta, F. Ramirez, Recent progress towards a molecular understanding of Marfan syndrome. *Am J Med Genet C Semin Med Genet* **139C**, 4 (Nov 15, 2005).

21. R. Mecham, E. Davis, *Elastic fiber structure and assembly.* P. D. Yurchenco, Birk, D.E. and Mecham, R.P., eds., Ed., In Extracellular Matrix Assembly and Structure (Academic Press, New York, USA, 1994).

22. C. M. Kielty, M. J. Sherratt, A. Marson, C. Baldock, Fibrillin microfibrils. *Adv Protein Chem* **70**, 405 (2005).

23. S. M. Mithieux, A. S. Weiss, Elastin. *Adv Protein Chem* **70**, 437 (2005).

24. C. M. Kielty, M. J. Sherratt, C. A. Shuttleworth, Elastic fibres. *Journal of cell science* **115**, 2817 (Jul 15, 2002).

25. J. Rosenbloom, W. R. Abrams, R. Mecham, Extracellular matrix 4: the elastic fiber. *FASEB J* **7**, 1208 (Oct, 1993).

26. L. Debelle, A. J. Alix, The structures of elastins and their function. *Biochimie* **81**, 981 (Oct, 1999).

27. E. H. Sonnenblick, The structural basis and importance of restoring forces and elastic recoil for the filling of the heart. *European heart journal* **Suppl A**, 107 (1980).

28. K. Akhtar *et al.*, Oxidative and nitrosative modifications of tropoelastin prevent elastic fiber assembly in vitro. *The Journal of biological chemistry* **285**, 37396 (Nov 26, 2010).

29. F. Opitz *et al.*, Tissue engineering of ovine aortic blood vessel substitutes using applied shear stress and enzymatically derived vascular smooth muscle cells. *Ann Biomed Eng* **32**, 212 (Feb, 2004).

30. L. Chen *et al.*, Positional differences in the wound transcriptome of skin and oral mucosa. *BMC genomics* **11**, 471.

31. J. C. Snyder, A. C. Zemke, B. R. Stripp, Reparative capacity of airway epithelium impacts deposition and remodeling of extracellular matrix. *Am J Respir Cell Mol Biol* **40**, 633 (Jun, 2009).

32. C. Kuhn, S. Y. Yu, M. Chraplyvy, H. E. Linder, R. M. Senior, The induction of emphysema with elastase. II. Changes in connective tissue. *Lab Invest* **34**, 372 (Apr, 1976).

33. Y. Fukuda, Y. Masuda, M. Ishizaki, Y. Masugi, V. J. Ferrans, Morphogenesis of abnormal elastic fibers in lungs of patients with panacinar and centriacinar emphysema. *Human pathology* **20**, 652 (Jul, 1989).

34. C. R. Hoff, D. R. Perkins, J. M. Davidson, Elastin gene expression is upregulated during pulmonary fibrosis. *Connect Tissue Res* **40**, 145 (1999).

35. J. M. Maki *et al.*, Lysyl oxidase is essential for normal development and function of the respiratory system and for the integrity of elastic and collagen fibers in various tissues. *The American journal of pathology* **167**, 927 (Oct, 2005).

36. I. K. Hornstra *et al.*, Lysyl oxidase is required for vascular and diaphragmatic development in mice. *The Journal of biological chemistry* **278**, 14387 (Apr 18, 2003).

37. P. J. McLaughlin *et al.*, Targeted disruption of fibulin-4 abolishes elastogenesis and causes perinatal lethality in mice. *Molecular and cellular biology* **26**, 1700 (Mar, 2006).

38. M. J. Fazio *et al.*, Human elastin gene: new evidence for localization to the long arm of chromosome 7. *Am J Hum Genet* **48**, 696 (Apr, 1991).

39. J. M. Davidson, Smad about elastin regulation. *Am J Respir Cell Mol Biol* **26**, 164 (Feb, 2002).

40. Z. Indik *et al.*, Alternative splicing of human elastin mRNA indicated by sequence analysis of cloned genomic and complementary DNA. *Proceedings of the National Academy of Sciences of the United States of America* **84**, 5680 (Aug, 1987).

41. L. Debelle, A. M. Tamburro, Elastin: molecular description and function. *Int J Biochem Cell Biol* **31**, 261 (Feb, 1999).

42. B. Vrhovski, A. S. Weiss, Biochemistry of tropoelastin. *Eur J Biochem* **258**, 1 (Nov 15, 1998).

43. J. Rosenbloom, Elastin: relation of protein and gene structure to disease. *Lab Invest* **51**, 605 (Dec, 1984).

44. D. D. Carson, Extracellular matrix: forum introduction. *Reproductive biology and endocrinology : RB&E* **2**, 1 (Jan 7, 2004).

45. J. D. Hood, D. A. Cheresh, Role of integrins in cell invasion and migration. *Nature reviews. Cancer* **2**, 91 (Feb, 2002).

46. C. C. Lynch, L. M. Matrisian, Matrix metalloproteinases in tumor-host cell communication. *Differentiation; research in biological diversity* **70**, 561 (Dec, 2002).

47. M. Larsen, V. V. Artym, J. A. Green, K. M. Yamada, The matrix reorganized: extracellular matrix remodeling and integrin signaling. *Current opinion in cell biology* **18**, 463 (Oct, 2006).

48. L. Alberts J, Raff, Roberts, Walter, *Molecular Biology of The Cell. 4th ed*. (Garland Science, 2002).

49. R. L. Robert AM, in *Frontiers of Matrix Biology,* S. Karger, Ed. (1980), vol. 9.

50. A. Hinek, A. V. Pshezhetsky, M. von Itzstein, B. Starcher, Lysosomal sialidase (neuraminidase-1) is targeted to the cell surface in a multiprotein complex that facilitates elastic fiber assembly. *The Journal of biological chemistry* **281**, 3698 (Feb 10, 2006).

51. F. Antonicelli, G. Bellon, S. Lorimier, W. Hornebeck, Role of the elastin receptor complex (S-Gal/Cath-A/Neu-1) in skin repair and regeneration. *Wound repair and regeneration : official publication of the Wound Healing Society [and] the European Tissue Repair Society* **17**, 631 (Sep-Oct, 2009).

52. Y. Tatano *et al.*, Elastogenesis in cultured dermal fibroblasts from patients with lysosomal beta-galactosidase, protective protein/cathepsin A and neuraminidase-1 deficiencies. *J Med Invest* **53**, 103 (Feb, 2006).

53. A. Hinek, R. P. Mecham, F. Keeley, M. Rabinovitch, Impaired elastin fiber assembly related to reduced 67-kD elastin-binding protein in fetal lamb ductus arteriosus and in cultured aortic smooth muscle cells treated with chondroitin sulfate. *J Clin Invest* **88**, 2083 (Dec, 1991).

54. R. P. Mecham, Overview of extracellular matrix. *Current protocols in cell biology / editorial board, Juan S. Bonifacino ... [et al.]* **Chapter 10**, Unit 10 1 (May, 2001).

55. L. Robert, Aging of connective tissue. *Mechanisms of ageing and development* **14**, 273 (Nov-Dec, 1980).

56. A. Tsamis, J. T. Krawiec, D. A. Vorp, Elastin and collagen fibre microstructure of the human aorta in ageing and disease: a review. *Journal of the Royal Society, Interface / the Royal Society* **10**, 20121004 (Jun 6, 2013).

57. N. Gundiah, B. R. M, A. P. L, Determination of strain energy function for arterial elastin: Experiments using histology and mechanical tests. *Journal of biomechanics* **40**, 586 (2007).

58. C. G. Cho *et al.*, A study of the solar effect on actinic keratoses by quantification of elastic fibres using an image analysis system. *Acta dermato-venereologica* **79**, 278 (Jul, 1999).

59. S. L. Chapman *et al.*, Fibulin-2 and fibulin-5 cooperatively function to form the internal elastic lamina and protect from vascular injury. *Arteriosclerosis, thrombosis, and vascular biology* **30**, 68 (Jan, 2010).

60. R. Huang *et al.*, Inhibition of versican synthesis by antisense alters smooth muscle cell phenotype and induces elastic fiber formation in vitro and in neointima after vessel injury. *Circulation research* **98**, 370 (Feb 17, 2006).

61. J. Y. Hwang *et al.*, Retrovirally mediated overexpression of glycosaminoglycan-deficient biglycan in arterial smooth muscle cells induces tropoelastin synthesis and elastic fiber formation in vitro and in neointimae after vascular injury. *Am J Pathol* **173**, 1919 (Dec, 2008).

62. M. J. Merrilees *et al.*, Changes in elastin, elastin binding protein and versican in alveoli in chronic obstructive pulmonary disease. *Respir Res* **9**, 41 (2008).

63. S. Privitera, C. A. Prody, J. W. Callahan, A. Hinek, The 67-kDa enzymatically inactive alternatively spliced variant of beta-galactosidase is

identical to the elastin/laminin-binding protein. *J Biol Chem* **273**, 6319 (Mar 13, 1998).

64. A. Hinek, S. E. Wilson, Impaired elastogenesis in Hurler disease: dermatan sulfate accumulation linked to deficiency in elastin-binding protein and elastic fiber assembly. *Am J Pathol* **156**, 925 (Mar, 2000).

65. T. N. Wight, Versican: a versatile extracellular matrix proteoglycan in cell biology. *Current opinion in cell biology* **14**, 617 (Oct, 2002).

66. M. Ikeda *et al.*, Elastic fiber assembly is disrupted by excessive accumulation of chondroitin sulfate in the human dermal fibrotic disease, keloid. *Biochem Biophys Res Commun* **390**, 1221 (Dec 25, 2009).

67. A. Hinek, K. R. Braun, K. Liu, Y. Wang, T. N. Wight, Retrovirally mediated overexpression of versican v3 reverses impaired elastogenesis and heightened proliferation exhibited by fibroblasts from Costello syndrome and Hurler disease patients. *The American journal of pathology* **164**, 119 (Jan, 2004).

68. M. J. Merrilees *et al.*, Retrovirally mediated overexpression of versican v3 by arterial smooth muscle cells induces tropoelastin synthesis and elastic fiber formation in vitro and in neointima after vascular injury. *Circulation research* **90**, 481 (Mar 8, 2002).

69. P. A. Keire *et al.*, Expression of versican isoform V3 in the absence of ascorbate improves elastogenesis in engineered vascular constructs. *Tissue Eng Part A* **16**, 501 (Feb, 2010).

70. R. L. Robert AM*,* S. Karger, Ed. (1980).

71. W. B. Keeling, P. A. Armstrong, P. A. Stone, D. F. Bandyk, M. L. Shames, An overview of matrix metalloproteinases in the pathogenesis and treatment of abdominal aortic aneurysms. *Vascular and endovascular surgery* **39**, 457 (Nov-Dec, 2005).

72. B. S. Brooke, A. Bayes-Genis, D. Y. Li, New insights into elastin and vascular disease. *Trends in cardiovascular medicine* **13**, 176 (Jul, 2003).

73. U. R. Rodgers, A. S. Weiss, Cellular interactions with elastin. *Pathol Biol (Paris)* **53**, 390 (Sep, 2005).

74. T. M. Seasholtz, M. Majumdar, J. H. Brown, Rho as a mediator of G protein-coupled receptor signaling. *Mol Pharmacol* **55**, 949 (Jun, 1999).

75. S. K. Karnik *et al.*, Elastin induces myofibrillogenesis via a specific domain, VGVAPG. *Matrix Biol* **22**, 409 (Sep, 2003).

76. E. A. Thomas, J. R. Matli, J. L. Hu, M. J. Carson, J. G. Sutcliffe, Pertussis toxin treatment prevents 5-HT(5a) receptor-mediated inhibition of cyclic AMP accumulation in rat C6 glioma cells. *Journal of neuroscience research* **61**, 75 (Jul 1, 2000).

77. R. Amar, [Breast morphology, or the breast as part of the general morphology of the trunk. Method for the localization of the nipples]. *Annales de chirurgie plastique* **25**, 249 (1980).

78. P. R. Parks WC, Lee KA, Mecham R., Elastin. *Advances in Cell Molecular Biology* **6**, 133 (1993).

79. A. Krettek, G. K. Sukhova, P. Libby, Elastogenesis in human arterial disease: a role for macrophages in disordered elastin synthesis. *Arteriosclerosis, thrombosis, and vascular biology* **23**, 582 (Apr 1, 2003).

80. H. Wolinsky, S. Glagov, A lamellar unit of aortic medial structure and function in mammals. *Circulation research* **20**, 99 (Jan, 1967).

81. U. Hedin, J. Roy, P. K. Tran, K. Lundmark, A. Rahman, Control of smooth muscle cell proliferation--the role of the basement membrane. *Thrombosis and haemostasis* **82 Suppl 1**, 23 (Sep, 1999).

82. C. M. Spofford, W. M. Chilian, The elastin-laminin receptor functions as a mechanotransducer in vascular smooth muscle. *American journal of physiology. Heart and circulatory physiology* **280**, H1354 (Mar, 2001).

83. C. M. Spofford, W. M. Chilian, Mechanotransduction via the elastin-laminin receptor (ELR) in resistance arteries. *Journal of biomechanics* **36**, 645 (May, 2003).

84. A. Patel, B. Fine, M. Sandig, K. Mequanint, Elastin biosynthesis: The missing link in tissue-engineered blood vessels. *Cardiovasc Res* **71**, 40 (Jul 1, 2006).

85. U. A. Stock *et al.*, Dynamics of extracellular matrix production and turnover in tissue engineered cardiovascular structures. *Journal of cellular biochemistry* **81**, 220 (Mar 26, 2001).

86. J. L. Long, R. T. Tranquillo, Elastic fiber production in cardiovascular tissue-equivalents. *Matrix Biol* **22**, 339 (Jun, 2003).

87. M. H. Swee, W. C. Parks, R. A. Pierce, Developmental regulation of elastin production. Expression of tropoelastin pre-mRNA persists after down-regulation of steady-state mRNA levels. *The Journal of biological chemistry* **270**, 14899 (Jun 23, 1995).

88. J. Stitzel *et al.*, Controlled fabrication of a biological vascular substitute. *Biomaterials* **27**, 1088 (Mar, 2006).

89. S. H. Lee *et al.*, Elastic biodegradable poly(glycolide-co-caprolactone) scaffold for tissue engineering. *Journal of biomedical materials research. Part A* **66**, 29 (Jul 1, 2003).

90. P. Chen, E. Marsilio, R. H. Goldstein, I. V. Yannas, M. Spector, Formation of lung alveolar-like structures in collagen-glycosaminoglycan scaffolds in vitro. *Tissue Eng* **11**, 1436 (Sep-Oct, 2005).

91. R. A. Pierce, T. J. Mariani, R. M. Senior, Elastin in lung development and disease. *Ciba Found Symp* **192**, 199 (1995).

92. M. C. Bruce, C. E. Honaker, Transcriptional regulation of tropoelastin expression in rat lung fibroblasts: changes with age and hyperoxia. *The American journal of physiology* **274**, L940 (Jun, 1998).

93. B. A. Kozel *et al.*, Genetic modifiers of cardiovascular phenotype caused by elastin haploinsufficiency act by extrinsic noncomplementation. *The Journal of biological chemistry* **286**, 44926 (Dec 30, 2011).

94. B. Starcher *et al.*, Neuraminidase-1 is required for the normal assembly of elastic fibers. *American journal of physiology. Lung cellular and molecular physiology* **295**, L637 (Oct, 2008).

95. W. C. Parks, H. Secrist, L. C. Wu, R. P. Mecham, Developmental regulation of tropoelastin isoforms. *The Journal of biological chemistry* **263**, 4416 (Mar 25, 1988).

96. K. A. Holbrook, P. H. Byers, Structural abnormalities in the dermal collagen and elastic matrix from the skin of patients with inherited connective tissue disorders. *The Journal of investigative dermatology* **79 Suppl 1**, 7s (Jul, 1982).

97. G. C. Sephel, A. Sturrock, M. G. Giro, J. M. Davidson, Increased elastin production by progeria skin fibroblasts is controlled by the steady-state levels of elastin mRNA. *The Journal of investigative dermatology* **90**, 643 (May, 1988).

98. M. D. Botney *et al.*, Extracellular matrix protein gene expression in atherosclerotic hypertensive pulmonary arteries. *The American journal of pathology* **140**, 357 (Feb, 1992).

99. E. F. Bernstein *et al.*, Enhanced elastin and fibrillin gene expression in chronically photodamaged skin. *The Journal of investigative dermatology* **103**, 182 (Aug, 1994).

100. K. R. Stenmark, A. G. Durmowicz, J. D. Roby, R. P. Mecham, W. C. Parks, Persistence of the fetal pattern of tropoelastin gene expression in severe neonatal bovine pulmonary hypertension. *J Clin Invest* **93**, 1234 (Mar, 1994).

101. M. Yamamoto *et al.*, Increase in elastin gene expression and protein synthesis in arterial smooth muscle cells derived from patients with Moyamoya disease. *Stroke; a journal of cerebral circulation* **28**, 1733 (Sep, 1997).

102. G. Deslee *et al.*, Elastin expression in very severe human COPD. *The European respiratory journal* **34**, 324 (Aug, 2009).

103. T. Rangasamy *et al.*, Cigarette smoke-induced emphysema in A/J mice is associated with pulmonary oxidative stress, apoptosis of lung cells, and global alterations in gene expression. *American journal of physiology. Lung cellular and molecular physiology* **296**, L888 (Jun, 2009).

104. J. Vila Torres, M. Pineda Marfa, M. A. Gonzalez Ensenat, J. Lloreta Trull, Pathology of the elastic tissue of the skin in Costello syndrome. An image analysis study using mathematical morphology. *Analytical and quantitative cytology and histology / the International Academy of Cytology [and] American Society of Cytology* **16**, 421 (Dec, 1994).

105. E. Morava, M. Guillard, D. J. Lefeber, R. A. Wevers, Autosomal recessive cutis laxa syndrome revisited. *Eur J Hum Genet* **17**, 1099 (Sep, 2009).

106. M. C. Zweers *et al.*, Deficiency of tenascin-X causes abnormalities in dermal elastic fiber morphology. *The Journal of investigative dermatology* **122**, 885 (Apr, 2004).

107. H. C. Dietz, R. P. Mecham, Mouse models of genetic diseases resulting from mutations in elastic fiber proteins. *Matrix Biol* **19**, 481 (Nov, 2000).

108. J. E. Wagenseil, R. P. Mecham, New insights into elastic fiber assembly. *Birth Defects Res C Embryo Today* **81**, 229 (Dec, 2007).

109. H. Yanagisawa, E. C. Davis, Unraveling the mechanism of elastic fiber assembly: The roles of short fibulins. *Int J Biochem Cell Biol* **42**, 1084 (Jul, 2010).

110. J. P. Annes, J. S. Munger, D. B. Rifkin, Making sense of latent TGFbeta activation. *Journal of cell science* **116**, 217 (Jan 15, 2003).

111. P. J. Sime, Z. Xing, F. L. Graham, K. G. Csaky, J. Gauldie, Adenovector-mediated gene transfer of active transforming growth factor-beta1 induces prolonged severe fibrosis in rat lung. *J Clin Invest* **100**, 768 (Aug 15, 1997).

112. J. Dai *et al.*, Overexpression of transforming growth factor-beta1 stabilizes already-formed aortic aneurysms: a first approach to induction of functional healing by endovascular gene therapy. *Circulation* **112**, 1008 (Aug 16, 2005).

113. V. M. Kahari, Y. Q. Chen, M. M. Bashir, J. Rosenbloom, J. Uitto, Tumor necrosis factor-alpha down-regulates human elastin gene expression. Evidence for the role of AP-1 in the suppression of promoter activity. *The Journal of biological chemistry* **267**, 26134 (Dec 25, 1992).

114. J. M. Liu, J. M. Davidson, The elastogenic effect of recombinant transforming growth factor-beta on porcine aortic smooth muscle cells. *Biochem Biophys Res Commun* **154**, 895 (Aug 15, 1988).

115. S. E. McGowan, R. McNamer, Transforming growth factor-beta increases elastin production by neonatal rat lung fibroblasts. *Am J Respir Cell Mol Biol* **3**, 369 (Oct, 1990).

116. M. C. Zhang, M. Giro, D. Quaglino, Jr., J. M. Davidson, Transforming growth factor-beta reverses a posttranscriptional defect in elastin synthesis in a cutis laxa skin fibroblast strain. *J Clin Invest* **95**, 986 (Mar, 1995).

117. Y. Katsuta *et al.*, Fibulin-5 accelerates elastic fibre assembly in human skin fibroblasts. *Exp Dermatol* **17**, 837 (Oct, 2008).

118. P. P. Kuang *et al.*, Activation of elastin transcription by transforming growth factor-beta in human lung fibroblasts. *American journal of physiology. Lung cellular and molecular physiology* **292**, L944 (Apr, 2007).

119. S. D. Katchman, S. Hsu-Wong, I. Ledo, M. Wu, J. Uitto, Transforming growth factor-beta up-regulates human elastin promoter activity in transgenic mice. *Biochem Biophys Res Commun* **203**, 485 (Aug 30, 1994).

120. V. Marigo, D. Volpin, G. M. Bressan, Regulation of the human elastin promoter in chick embryo cells. Tissue-specific effect of TGF-beta. *Biochimica et biophysica acta* **1172**, 31 (Feb 20, 1993).

121. V. M. Kahari *et al.*, Transforming growth factor-beta up-regulates elastin gene expression in human skin fibroblasts. Evidence for post-transcriptional modulation. *Lab Invest* **66**, 580 (May, 1992).

122. S. E. McGowan, Influences of endogenous and exogenous TGF-beta on elastin in rat lung fibroblasts and aortic smooth muscle cells. *The American journal of physiology* **263**, L257 (Aug, 1992).

123. V. Marigo, D. Volpin, G. Vitale, G. M. Bressan, Identification of a TGF-beta responsive element in the human elastin promoter. *Biochem Biophys Res Commun* **199**, 1049 (Mar 15, 1994).

124. U. Kucich, J. C. Rosenbloom, W. R. Abrams, M. M. Bashir, J. Rosenbloom, Stabilization of elastin mRNA by TGF-beta: initial characterization of signaling pathway. *Am J Respir Cell Mol Biol* **17**, 10 (Jul, 1997).

125. M. Zhang, R. A. Pierce, H. Wachi, R. P. Mecham, W. C. Parks, An open reading frame element mediates posttranscriptional regulation of tropoelastin and responsiveness to transforming growth factor beta1. *Molecular and cellular biology* **19**, 7314 (Nov, 1999).

126. Y. Hew, C. Lau, Z. Grzelczak, F. W. Keeley, Identification of a GA-rich sequence as a protein-binding site in the 3'-untranslated region of chicken elastin mRNA with a potential role in the developmental regulation of elastin mRNA stability. *The Journal of biological chemistry* **275**, 24857 (Aug 11, 2000).

127. J. E. Lee, J. Y. Lee, J. Wilusz, B. Tian, C. J. Wilusz, Systematic analysis of cis-elements in unstable mRNAs demonstrates that CUGBP1 is a key regulator of mRNA decay in muscle cells. *PLoS One* **5**, e11201 (2010).

128. U. Kucich, J. C. Rosenbloom, W. R. Abrams, J. Rosenbloom, Transforming growth factor-beta stabilizes elastin mRNA by a pathway requiring active Smads, protein kinase C-delta, and p38. *Am J Respir Cell Mol Biol* **26**, 183 (Feb, 2002).

129. E. van Rooij *et al.*, Dysregulation of microRNAs after myocardial infarction reveals a role of miR-29 in cardiac fibrosis. *Proceedings of the National Academy of Sciences of the United States of America* **105**, 13027 (Sep 2, 2008).

130. R. A. Boon *et al.*, MicroRNA-29 in aortic dilation: implications for aneurysm formation. *Circulation research* **109**, 1115 (Oct 28, 2011).

131. C. E. Ott *et al.*, MicroRNAs differentially expressed in postnatal aortic development downregulate elastin via 3' UTR and coding-sequence binding sites. *PLoS One* **6**, e16250 (2011).

132. P. Zhang *et al.*, Inhibition of microRNA-29 enhances elastin levels in cells haploinsufficient for elastin and in bioengineered vessels--brief report. *Arteriosclerosis, thrombosis, and vascular biology* **32**, 756 (Mar, 2012).

133. B. Joddar, A. Ramamurthi, Elastogenic effects of exogenous hyaluronan oligosaccharides on vascular smooth muscle cells. *Biomaterials* **27**, 5698 (Nov, 2006).

134. C. R. Kothapalli, C. E. Gacchina, A. Ramamurthi, Utility of hyaluronan oligomers and transforming growth factor-beta1 factors for elastic matrix regeneration by aneurysmal rat aortic smooth muscle cells. *Tissue Eng Part A* **15**, 3247 (Nov, 2009).

135. B. P. Toole, Hyaluronan-CD44 Interactions in Cancer: Paradoxes and Possibilities. *Clinical cancer research : an official journal of the American Association for Cancer Research* **15**, 7462 (Dec 15, 2009).

136. S. J. DiCamillo *et al.*, Neutrophil elastase-initiated EGFR/MEK/ERK signaling counteracts stabilizing effect of autocrine TGF-beta on tropoelastin mRNA in lung fibroblasts. *American journal of physiology. Lung cellular and molecular physiology* **291**, L232 (Aug, 2006).

137. C. M. Alvira *et al.*, Inhibition of transforming growth factor beta worsens elastin degradation in a murine model of Kawasaki disease. *The American journal of pathology* **178**, 1210 (Mar, 2011).

138. S. Akool el *et al.*, Nitric oxide induces TIMP-1 expression by activating the transforming growth factor beta-Smad signaling pathway. *The Journal of biological chemistry* **280**, 39403 (Nov 25, 2005).

139. S. M. Kutz *et al.*, TGF-beta 1-induced PAI-1 expression is E box/USF-dependent and requires EGFR signaling. *Experimental cell research* **312**, 1093 (Apr 15, 2006).

140. J. A. Foster, M. L. Miller, M. R. Benedict, R. A. Richmann, C. B. Rich, Evidence for insulin-like growth factor-I regulation of chick aortic elastogenesis. *Matrix* **9**, 328 (Aug, 1989).

141. C. B. Rich, H. D. Goud, M. Bashir, J. Rosenbloom, J. A. Foster, Developmental regulation of aortic elastin gene expression involves disruption of an IGF-I sensitive repressor complex. *Biochem Biophys Res Commun* **196**, 1316 (Nov 15, 1993).

142. K. J. Conn *et al.*, Insulin-like growth factor-I regulates transcription of the elastin gene through a putative retinoblastoma control element. A role for Sp3 acting as a repressor of elastin gene transcription. *The Journal of biological chemistry* **271**, 28853 (Nov 15, 1996).

143. D. B. Badesch, P. D. Lee, W. C. Parks, K. R. Stenmark, Insulin-like growth factor I stimulates elastin synthesis by bovine pulmonary arterial smooth muscle cells. *Biochem Biophys Res Commun* **160**, 382 (Apr 14, 1989).

144. C. B. Rich *et al.*, IGF-I regulation of elastogenesis: comparison of aortic and lung cells. *The American journal of physiology* **263**, L276 (Aug, 1992).

145. B. L. Wolfe *et al.*, Insulin-like growth factor-I regulates transcription of the elastin gene. *The Journal of biological chemistry* **268**, 12418 (Jun 15, 1993).

146. D. E. Jensen, C. B. Rich, A. J. Terpstra, S. R. Farmer, J. A. Foster, Transcriptional regulation of the elastin gene by insulin-like growth factor-I involves disruption of Sp1 binding. Evidence for the role of Rb in mediating Sp1 binding in aortic smooth muscle cells. *The Journal of biological chemistry* **270**, 6555 (Mar 24, 1995).

147. S. Sen *et al.*, Retinoblastoma protein modulates the inverse relationship between cellular proliferation and elastogenesis. *The Journal of biological chemistry* **286**, 36580 (Oct 21, 2011).

148. I. Carreras, C. B. Rich, M. P. Panchenko, J. A. Foster, Basic fibroblast growth factor decreases elastin gene transcription in aortic smooth muscle cells. *Journal of cellular biochemistry* **85**, 592 (2002).

149. C. B. Rich, M. A. Nugent, P. Stone, J. A. Foster, Elastase release of basic fibroblast growth factor in pulmonary fibroblast cultures results in down-regulation of elastin gene transcription. A role for basic fibroblast growth factor in regulating lung repair. *The Journal of biological chemistry* **271**, 23043 (Sep 20, 1996).

150. M. Weinstein, X. Xu, K. Ohyama, C. X. Deng, FGFR-3 and FGFR-4 function cooperatively to direct alveogenesis in the murine lung. *Development* **125**, 3615 (Sep, 1998).

151. J. Gao, T. W. Jordan, T. W. Cutress, Immunolocalization of basic fibroblast growth factor (bFGF) in human periodontal ligament (PDL) tissue. *J Periodontal Res* **31**, 260 (May, 1996).

152. A. Palmon *et al.*, Basic fibroblast growth factor suppresses tropoelastin gene expression in cultured human periodontal fibroblasts. *J Periodontal Res* **36**, 65 (Apr, 2001).

153. C. B. Rich, M. R. Fontanilla, M. Nugent, J. A. Foster, Basic fibroblast growth factor decreases elastin gene transcription through an AP1/cAMP-response element hybrid site in the distal promoter. *The Journal of biological chemistry* **274**, 33433 (Nov 19, 1999).

154. I. Carreras *et al.*, Functional components of basic fibroblast growth factor signaling that inhibit lung elastin gene expression. *American journal of physiology. Lung cellular and molecular physiology* **281**, L766 (Oct, 2001).

155. M. Takamiya, K. Saigusa, N. Nakayashiki, Y. Aoki, Studies on mRNA expression of basic fibroblast growth factor in wound healing for wound

age determination. *International journal of legal medicine* **117**, 46 (Feb, 2003).

156. J. M. Davidson, O. Zoia, J. M. Liu, Modulation of transforming growth factor-beta 1 stimulated elastin and collagen production and proliferation in porcine vascular smooth muscle cells and skin fibroblasts by basic fibroblast growth factor, transforming growth factor-alpha, and insulin-like growth factor-I. *J Cell Physiol* **155**, 149 (Apr, 1993).

157. H. H. Hong, P. C. Trackman, Cytokine regulation of gingival fibroblast lysyl oxidase, collagen, and elastin. *Journal of periodontology* **73**, 145 (Feb, 2002).

158. W. Li *et al.*, Lysyl oxidase oxidizes basic fibroblast growth factor and inactivates its mitogenic potential. *Journal of cellular biochemistry* **88**, 152 (Jan 1, 2003).

159. K. Thompson, M. Rabinovitch, Exogenous leukocyte and endogenous elastases can mediate mitogenic activity in pulmonary artery smooth muscle cells by release of extracellular-matrix bound basic fibroblast growth factor. *J Cell Physiol* **166**, 495 (Mar, 1996).

160. N. S. Gibran, F. F. Isik, D. M. Heimbach, D. Gordon, Basic fibroblast growth factor in the early human burn wound. *The Journal of surgical research* **56**, 226 (Mar, 1994).

161. C. Bertram, R. Hass, Cellular senescence of human mammary epithelial cells (HMEC) is associated with an altered MMP-7/HB-EGF signaling and increased formation of elastin-like structures. *Mechanisms of ageing and development* **130**, 657 (Oct, 2009).

162. J. Liu *et al.*, Heparin-binding EGF-like growth factor regulates elastin and FGF-2 expression in pulmonary fibroblasts. *American journal of physiology. Lung cellular and molecular physiology* **285**, L1106 (Nov, 2003).

163. V. Moulin, Growth factors in skin wound healing. *European journal of cell biology* **68**, 1 (Sep, 1995).

164. L. S. Van Winkle, J. M. Isaac, C. G. Plopper, Distribution of epidermal growth factor receptor and ligands during bronchiolar epithelial repair from naphthalene-induced Clara cell injury in the mouse. *The American journal of pathology* **151**, 443 (Aug, 1997).

165. S. J. DiCamillo *et al.*, Elastase-released epidermal growth factor recruits epidermal growth factor receptor and extracellular signal-regulated kinases to down-regulate tropoelastin mRNA in lung fibroblasts. *The Journal of biological chemistry* **277**, 18938 (May 24, 2002).

166. T. Ichiro, S. Tajima, T. Nishikawa, Preferential inhibition of elastin synthesis by epidermal growth factor in chick aortic smooth muscle cells. *Biochem Biophys Res Commun* **168**, 850 (Apr 30, 1990).

167. D. K. Madtes, H. K. Busby, T. P. Strandjord, J. G. Clark, Expression of transforming growth factor-alpha and epidermal growth factor receptor is increased following bleomycin-induced lung injury in rats. *Am J Respir Cell Mol Biol* **11**, 540 (Nov, 1994).

168. T. P. Strandjord, J. G. Clark, D. E. Guralnick, D. K. Madtes, Immunolocalization of transforming growth factor-alpha, epidermal growth factor (EGF), and EGF-receptor in normal and injured developing human lung. *Pediatr Res* **38**, 851 (Dec, 1995).

169. W. D. Hardie *et al.*, Immunolocalization of transforming growth factor alpha and epidermal growth factor receptor in lungs of patients with cystic fibrosis. *Pediatric and developmental pathology : the official journal of the Society for Pediatric Pathology and the Paediatric Pathology Society* **2**, 415 (Sep-Oct, 1999).

170. T. D. Le Cras *et al.*, Transient induction of TGF-alpha disrupts lung morphogenesis, causing pulmonary disease in adulthood. *American journal of physiology. Lung cellular and molecular physiology* **287**, L718 (Oct, 2004).

171. K. Kohri, I. F. Ueki, J. A. Nadel, Neutrophil elastase induces mucin production by ligand-dependent epidermal growth factor receptor activation. *American journal of physiology. Lung cellular and molecular physiology* **283**, L531 (Sep, 2002).

172. F. S. Carneiro *et al.*, TNF-alpha knockout mice have increased corpora cavernosa relaxation. *The journal of sexual medicine* **6**, 115 (Jan, 2009).

173. W. Xiong *et al.*, Blocking TNF-alpha attenuates aneurysm formation in a murine model. *J Immunol* **183**, 2741 (Aug 15, 2009).

174. M. Fujita *et al.*, Overexpression of tumor necrosis factor-alpha produces an increase in lung volumes and pulmonary hypertension. *American journal of physiology. Lung cellular and molecular physiology* **280**, L39 (Jan, 2001).

175. A. C. Lau, T. T. Duong, S. Ito, R. S. Yeung, Matrix metalloproteinase 9 activity leads to elastin breakdown in an animal model of Kawasaki disease. *Arthritis and rheumatism* **58**, 854 (Mar, 2008).

176. Z. W. She, M. D. Wewers, D. J. Herzyk, W. B. Davis, Tumor necrosis factor increases the elastolytic potential of adherent neutrophils: a role for hypochlorous acid. *Am J Respir Cell Mol Biol* **9**, 386 (Oct, 1993).

177. C. R. Kothapalli, A. Ramamurthi, Induced elastin regeneration by chronically activated smooth muscle cells for targeted aneurysm repair. *Acta biomaterialia* **6**, 170 (Jan, 2010).

178. A. Churg, J. Dai, H. Tai, C. Xie, J. L. Wright, Tumor necrosis factor-alpha is central to acute cigarette smoke-induced inflammation and connective tissue breakdown. *American journal of respiratory and critical care medicine* **166**, 849 (Sep 15, 2002).

179. J. S. Hui-Yuen, T. T. Duong, R. S. Yeung, TNF-alpha is necessary for induction of coronary artery inflammation and aneurysm formation in an animal model of Kawasaki disease. *J Immunol* **176**, 6294 (May 15, 2006).

180. A. C. Lau, T. T. Duong, S. Ito, G. J. Wilson, R. S. Yeung, Inhibition of matrix metalloproteinase-9 activity improves coronary outcome in an animal model of Kawasaki disease. *Clinical and experimental immunology* **157**, 300 (Aug, 2009).

181. K. F. Chung, Cytokines as targets in chronic obstructive pulmonary disease. *Current drug targets* **7**, 675 (Jun, 2006).

182. F. Croute *et al.*, Interleukin-1 beta stimulates fibroblast elastase activity. *Br J Dermatol* **124**, 538 (Jun, 1991).

183. A. Ito, P. C. Leppert, Y. Mori, Human recombinant interleukin-1 alpha increases elastase-like enzyme in human uterine cervical fibroblasts. *Gynecologic and obstetric investigation* **30**, 239 (1990).

184. K. Bry, J. A. Whitsett, U. Lappalainen, IL-1beta disrupts postnatal lung morphogenesis in the mouse. *Am J Respir Cell Mol Biol* **36**, 32 (Jan, 2007).

185. U. Lappalainen, J. A. Whitsett, S. E. Wert, J. W. Tichelaar, K. Bry, Interleukin-1beta causes pulmonary inflammation, emphysema, and airway remodeling in the adult murine lung. *Am J Respir Cell Mol Biol* **32**, 311 (Apr, 2005).

186. K. Isoda *et al.*, Deficiency of interleukin-1 receptor antagonist promotes spontaneous femoral artery aneurysm formation in mice. *The American journal of pathology* **180**, 1254 (Mar, 2012).

187. J. L. Berk, C. Franzblau, R. H. Goldstein, Recombinant interleukin-1 beta inhibits elastin formation by a neonatal rat lung fibroblast subtype. *The Journal of biological chemistry* **266**, 3192 (Feb 15, 1991).

188. P. P. Kuang *et al.*, NF-kappaB induced by IL-1beta inhibits elastin transcription and myofibroblast phenotype. *American journal of physiology. Cell physiology* **283**, C58 (Jul, 2002).

189. P. P. Kuang, R. H. Goldstein, Regulation of elastin gene transcription by interleukin-1 beta-induced C/EBP beta isoforms. *American journal of physiology. Cell physiology* **285**, C1349 (Dec, 2003).

190. R. A. Rippe, L. W. Schrum, B. Stefanovic, J. A. Solis-Herruzo, D. A. Brenner, NF-kappaB inhibits expression of the alpha1(I) collagen gene. *DNA and cell biology* **18**, 751 (Oct, 1999).

191. N. Miglino *et al.*, Cigarette smoke inhibits lung fibroblast proliferation by translational mechanisms. *The European respiratory journal* **39**, 705 (Mar, 2012).

192. P. P. Kuang, R. H. Goldstein, Regulation of elastin gene transcription by proteasome dysfunction. *American journal of physiology. Cell physiology* **289**, C766 (Sep, 2005).

193. A. Charles, X. Tang, E. Crouch, J. S. Brody, Z. X. Xiao, Retinoblastoma protein complexes with C/EBP proteins and activates C/EBP-mediated transcription. *Journal of cellular biochemistry* **83**, 414 (Aug 21-Sep 5, 2001).

194. A. Mauviel *et al.*, Human recombinant interleukin-1 beta up-regulates elastin gene expression in dermal fibroblasts. Evidence for transcriptional regulation in vitro and in vivo. *The Journal of biological chemistry* **268**, 6520 (Mar 25, 1993).

195. J. Song, Lee, K., Kong, S., Choi, D., The effects of interleukin-1B and interleukin-10 in the expression of elastin gene in cultured human fibrolasts. *Korean J. Dermatol.* **37**, 846 (1999).

196. J. Uitto, S. Hsu-Wong, S. D. Katchman, M. M. Bashir, J. Rosenbloom, Skin elastic fibres: regulation of human elastin promoter activity in transgenic mice. *Ciba Found Symp* **192**, 237 (1995).

197. E. R. Neptune *et al.*, Dysregulation of TGF-beta activation contributes to pathogenesis in Marfan syndrome. *Nature genetics* **33**, 407 (Mar, 2003).

198. Z. Yao *et al.*, A Marfan syndrome gene expression phenotype in cultured skin fibroblasts. *BMC genomics* **8**, 319 (2007).

199. T. M. Holm *et al.*, Noncanonical TGFbeta signaling contributes to aortic aneurysm progression in Marfan syndrome mice. *Science* **332**, 358 (Apr 15, 2011).

200. M. Kretzschmar, J. Doody, I. Timokhina, J. Massague, A mechanism of repression of TGFbeta/ Smad signaling by oncogenic Ras. *Genes & development* **13**, 804 (Apr 1, 1999).

201. R. B. Rucker, M. A. Dubick, Elastin metabolism and chemistry: potential roles in lung development and structure. *Environ Health Perspect* **55**, 179 (Apr, 1984).

202. S. D. Shapiro, S. K. Endicott, M. A. Province, J. A. Pierce, E. J. Campbell, Marked longevity of human lung parenchymal elastic fibers deduced from prevalence of D-aspartate and nuclear weapons-related radiocarbon. *J Clin Invest* **87**, 1828 (May, 1991).

203. G. L. Argraves, S. Jani, J. L. Barth, W. S. Argraves, ArrayQuest: a web resource for the analysis of DNA microarray data. *BMC bioinformatics* **6**, 287 (2005).

204. C. Li, W. Hung Wong, Model-based analysis of oligonucleotide arrays: model validation, design issues and standard error application. *Genome biology* **2**, RESEARCH0032 (2001).

205. C. M. Kelleher, S. E. McLean, R. P. Mecham, Vascular extracellular matrix and aortic development. *Curr Top Dev Biol* **62**, 153 (2004).

206. S. McLean, B. Mecham, C. Kelleher, T. Mariani, R. Mecham, *Extracellular matrix gene expression in the developing mouse aorta*. Miner, Ed., Advances in Developmental Biology (Elsevier, 2005), vol. 15.

207. E. L. Rawlins, B. L. Hogan, Epithelial stem cells of the lung: privileged few or opportunities for many? *Development* **133**, 2455 (Jul, 2006).

208. A. Alibes, P. Yankilevich, A. Canada, R. Diaz-Uriarte, IDconverter and IDClight: conversion and annotation of gene and protein IDs. *BMC bioinformatics* **8**, 9 (2007).

209. L. Chen *et al.*, Positional differences in the wound transcriptome of skin and oral mucosa. *BMC genomics* **11**, 471 (2010).

210. J. M. Lemire, M. J. Merrilees, K. R. Braun, T. N. Wight, Overexpression of the V3 variant of versican alters arterial smooth muscle cell adhesion, migration, and proliferation in vitro. *J Cell Physiol* **190**, 38 (Jan, 2002).

211. M. Lin *et al.*, dChipSNP: significance curve and clustering of SNP-array-based loss-of-heterozygosity data. *Bioinformatics* **20**, 1233 (May 22, 2004).

212. C. Li, W. H. Wong, Model-based analysis of oligonucleotide arrays: expression index computation and outlier detection. *Proceedings of the National Academy of Sciences of the United States of America* **98**, 31 (Jan 2, 2001).

213. S. D. Jani, G. L. Argraves, J. L. Barth, W. S. Argraves, GeneMesh: a web-based microarray analysis tool for relating differentially expressed genes to MeSH terms. *BMC bioinformatics* **11**, 166 (2010).

214. R. C. Gentleman *et al.*, Bioconductor: open software development for computational biology and bioinformatics. *Genome biology* **5**, R80 (2004).

215. M. B. Eisen, P. T. Spellman, P. O. Brown, D. Botstein, Cluster analysis and display of genome-wide expression patterns. *Proceedings of the National Academy of Sciences of the United States of America* **95**, 14863 (Dec 8, 1998).

216. C. M. RR Sokal, *Univ Kans Sci Bull*, 1409 (1958).

217. R. K. Curtis, M. Oresic, A. Vidal-Puig, Pathways to the analysis of microarray data. *Trends in biotechnology* **23**, 429 (Aug, 2005).

218. G. E. Gonye, P. Chakravarthula, J. S. Schwaber, R. Vadigepalli, From promoter analysis to transcriptional regulatory network prediction using PAINT. *Methods Mol Biol* **408**, 49 (2007).

219. R. Sharan. (Scribe: Shaul Karni and Yifat Felder, Tel-Aviv University, 2007).

220. R. Vadigepalli, P. Chakravarthula, D. E. Zak, J. S. Schwaber, G. E. Gonye, PAINT: a promoter analysis and interaction network generation tool for gene regulatory network identification. *Omics : a journal of integrative biology* **7**, 235 (Fall, 2003).

221. M. Madan Babu, S. A. Teichmann, Evolution of transcription factors and the gene regulatory network in Escherichia coli. *Nucleic acids research* **31**, 1234 (Feb 15, 2003).

222. P. J. Farnham, In vivo assays to examine transcription factor localization and target gene specificity. *Methods* **26**, 1 (Jan, 2002).

223. S. H. Kang, K. Vieira, J. Bungert, Combining chromatin immunoprecipitation and DNA footprinting: a novel method to analyze protein-DNA interactions in vivo. *Nucleic acids research* **30**, e44 (May 15, 2002).

224. M. S. Ricci, W. S. El-Deiry, DNA footprinting. *Methods Mol Biol* **223**, 117 (2003).

225. J. D. Hughes, P. W. Estep, S. Tavazoie, G. M. Church, Computational identification of cis-regulatory elements associated with groups of functionally related genes in Saccharomyces cerevisiae. *Journal of molecular biology* **296**, 1205 (Mar 10, 2000).

226. A. J. Hartemink, D. K. Gifford, T. S. Jaakkola, R. A. Young, Combining location and expression data for principled discovery of genetic regulatory network models. *Pacific Symposium on Biocomputing. Pacific Symposium on Biocomputing*, 437 (2002).

227. T. Ideker, O. Ozier, B. Schwikowski, A. F. Siegel, Discovering regulatory and signalling circuits in molecular interaction networks. *Bioinformatics* **18 Suppl 1**, S233 (2002).

228. B. P. Berman *et al.*, Exploiting transcription factor binding site clustering to identify cis-regulatory modules involved in pattern formation in the Drosophila genome. *Proceedings of the National Academy of Sciences of the United States of America* **99**, 757 (Jan 22, 2002).

229. E. H. Davidson *et al.*, A genomic regulatory network for development. *Science* **295**, 1669 (Mar 1, 2002).

230. R. Elkon, C. Linhart, R. Sharan, R. Shamir, Y. Shiloh, Genome-wide in silico identification of transcriptional regulators controlling the cell cycle in human cells. *Genome research* **13**, 773 (May, 2003).

231. K. Bury. (Cambridge University Press, Cambridge, UK, 1999).

232. L. M. Jakt, L. Cao, K. S. Cheah, D. K. Smith, Assessing clusters and motifs from gene expression data. *Genome research* **11**, 112 (Jan, 2001).

233. C. Xu *et al.*, The muscle-specific microRNAs miR-1 and miR-133 produce opposing effects on apoptosis by targeting HSP60, HSP70 and caspase-9 in cardiomyocytes. *Journal of cell science* **120**, 3045 (Sep 1, 2007).

234. J. Kim *et al.*, A MicroRNA feedback circuit in midbrain dopamine neurons. *Science* **317**, 1220 (Aug 31, 2007).

235. B. John *et al.*, Human MicroRNA targets. *PLoS biology* **2**, e363 (Nov, 2004).

236. P. Landgraf *et al.*, A mammalian microRNA expression atlas based on small RNA library sequencing. *Cell* **129**, 1401 (Jun 29, 2007).

237. C. S. Hofmann *et al.*, B-Myb represses elastin gene expression in aortic smooth muscle cells. *The Journal of biological chemistry* **280**, 7694 (Mar 4, 2005).

238. R. L. Widom, J. Y. Lee, C. Joseph, I. Gordon-Froome, J. H. Korn, The hcKrox gene family regulates multiple extracellular matrix genes. *Matrix Biol* **20**, 451 (Nov, 2001).

239. P. Takacs, Y. Zhang, K. Candiotti, S. Jaramillo, C. A. Medina, Effects of PPAR-delta agonist and zinc on vaginal smooth muscle cells collagen and tropoelastin production. *Int Urogynecol J*, (May 11).

240. C. Reynaud, C. Gleyzal, C. Jourdan-Le Saux, P. Sommer, Comparative functional study of the lysyl oxidase promoter in fibroblasts, Ras-transformed fibroblasts, myofibroblasts and smooth muscle cells. *Cell Mol Biol (Noisy-le-grand)* **45**, 1237 (Dec, 1999).

241. H. J. Kim *et al.*, Peroxisome proliferator-activated receptor {delta} regulates extracellular matrix and apoptosis of vascular smooth muscle cells through the activation of transforming growth factor-{beta}1/Smad3. *Circulation research* **105**, 16 (Jul 2, 2009).

242. S. E. McGowan, S. K. Jackson, M. M. Doro, P. J. Olson, Peroxisome proliferators alter lipid acquisition and elastin gene expression in neonatal rat lung fibroblasts. *Am J Physiol* **273**, L1249 (Dec, 1997).

243. P. Dowell *et al.*, p300 functions as a coactivator for the peroxisome proliferator-activated receptor alpha. *The Journal of biological chemistry* **272**, 33435 (Dec 26, 1997).

244. M. F. Ritchie, C. Yue, Y. Zhou, P. J. Houghton, J. Soboloff, Wilms tumor suppressor 1 (WT1) and early growth response 1 (EGR1) are regulators of STIM1 expression. *The Journal of biological chemistry* **285**, 10591 (Apr 2, 2010).

245. M. A. Harrington *et al.*, Inhibition of colony-stimulating factor-1 promoter activity by the product of the Wilms' tumor locus. *The Journal of biological chemistry* **268**, 21271 (Oct 5, 1993).

246. Z. Y. Wang, S. L. Madden, T. F. Deuel, F. J. Rauscher, 3rd, The Wilms' tumor gene product, WT1, represses transcription of the platelet-derived growth factor A-chain gene. *The Journal of biological chemistry* **267**, 21999 (Nov 5, 1992).

247. R. Sarfstein, H. Werner, The WT1 Wilms' tumor suppressor gene is a downstream target for insulin-like growth factor-I (IGF-I) action in PC12 cells. *Journal of neurochemistry* **99**, 818 (Nov, 2006).

248. M. Little, C. Wells, A clinical overview of WT1 gene mutations. *Human mutation* **9**, 209 (1997).

249. Y. Oji *et al.*, Overexpression of the Wilms' tumor gene W T1 in primary astrocytic tumors. *Cancer science* **95**, 822 (Oct, 2004).

250. D. M. Loeb *et al.*, Wilms' tumor suppressor gene (WT1) is expressed in primary breast tumors despite tumor-specific promoter methylation. *Cancer Res* **61**, 921 (Feb 1, 2001).

251. H. Miwa, M. Beran, G. F. Saunders, Expression of the Wilms' tumor gene (WT1) in human leukemias. *Leukemia* **6**, 405 (May, 1992).

252. G. R. Grubb, K. Yun, B. R. Williams, M. R. Eccles, A. E. Reeve, Expression of WT1 protein in fetal kidneys and Wilms tumors. *Lab Invest* **71**, 472 (Oct, 1994).

253. M. A. Ghanem *et al.*, Expression and prognostic value of Wilms' tumor 1 and early growth response 1 proteins in nephroblastoma. *Clinical cancer research : an official journal of the American Association for Cancer Research* **6**, 4265 (Nov, 2000).

254. N. P. Pavletich, C. O. Pabo, Zinc finger-DNA recognition: crystal structure of a Zif268-DNA complex at 2.1 A. *Science* **252**, 809 (May 10, 1991).

255. B. Christy, D. Nathans, DNA binding site of the growth factor-inducible protein Zif268. *Proceedings of the National Academy of Sciences of the United States of America* **86**, 8737 (Nov, 1989).

256. A. H. Swirnoff, J. Milbrandt, DNA-binding specificity of NGFI-A and related zinc finger transcription factors. *Molecular and cellular biology* **15**, 2275 (Apr, 1995).

257. V. P. Sukhatme *et al.*, A zinc finger-encoding gene coregulated with c-fos during growth and differentiation, and after cellular depolarization. *Cell* **53**, 37 (Apr 8, 1988).

258. B. R. Dey *et al.*, Repression of the transforming growth factor-beta 1 gene by the Wilms' tumor suppressor WT1 gene product. *Mol Endocrinol* **8**, 595 (May, 1994).

259. V. Baron *et al.*, Inhibition of Egr-1 expression reverses transformation of prostate cancer cells in vitro and in vivo. *Oncogene* **22**, 4194 (Jul 3, 2003).

260. B. H. Ahn, M. H. Park, Y. H. Lee, S. Min do, Phorbol myristate acetate-induced Egr-1 expression is suppressed by phospholipase D isozymes in human glioma cells. *FEBS letters* **581**, 5940 (Dec 22, 2007).

261. A. Krones-Herzig *et al.*, Early growth response 1 acts as a tumor suppressor in vivo and in vitro via regulation of p53. *Cancer Res* **65**, 5133 (Jun 15, 2005).

262. S. Kuhn, C. Skerka, P. F. Zipfel, Mapping of the complement regulatory domains in the human factor H-like protein 1 and in factor H1. *J Immunol* **155**, 5663 (Dec 15, 1995).

263. C. Skerka, E. L. Decker, P. F. Zipfel, A regulatory element in the human interleukin 2 gene promoter is a binding site for the zinc finger proteins Sp1 and EGR-1. *The Journal of biological chemistry* **270**, 22500 (Sep 22, 1995).

264. B. Kramer, A. Meichle, G. Hensel, P. Charnay, M. Kronke, Characterization of an Krox-24/Egr-1-responsive element in the human tumor necrosis factor promoter. *Biochimica et biophysica acta* **1219**, 413 (Oct 18, 1994).

265. R. P. Mecham, Methods in elastic tissue biology: elastin isolation and purification. *Methods* **45**, 32 (May, 2008).

266. P. C. Dartsch, H. Hammerle, E. Betz, Orientation of cultured arterial smooth muscle cells growing on cyclically stretched substrates. *Acta anatomica* **125**, 108 (1986).

267. T. J. Langan, R. C. Chou, Synchronization of mammalian cell cultures by serum deprivation. *Methods Mol Biol* **761**, 75 (2011).

268. H. Kubota *et al.*, Increased expression of co-chaperone HOP with HSP90 and HSC70 and complex formation in human colonic carcinoma. *Cell stress & chaperones* **15**, 1003 (Nov, 2010).

269. L. Neckers, Hsp90 inhibitors as novel cancer chemotherapeutic agents. *Trends in molecular medicine* **8**, S55 (2002).

270. E. Pick *et al.*, High HSP90 expression is associated with decreased survival in breast cancer. *Cancer Res* **67**, 2932 (Apr 1, 2007).

271. L. Whitesell, S. L. Lindquist, HSP90 and the chaperoning of cancer. *Nature reviews. Cancer* **5**, 761 (Oct, 2005).

272. H. Bansal *et al.*, Heat shock protein 90 regulates the expression of Wilms tumor 1 protein in myeloid leukemias. *Blood* **116**, 4591 (Nov 25, 2010).

273. S. Mishra *et al.*, Carbon monoxide rescues ischemic lungs by interrupting MAPK-driven expression of early growth response 1 gene and its downstream target genes. *Proceedings of the National Academy of Sciences of the United States of America* **103**, 5191 (Mar 28, 2006).

274. P. Takacs, Y. Zhang, K. Candiotti, S. Jaramillo, C. A. Medina, Effects of PPAR-delta agonist and zinc on vaginal smooth muscle cells collagen and tropoelastin production. *Int Urogynecol J* **23**, 1775 (Dec, 2012).

275. M. M. Bashir *et al.*, Characterization of the complete human elastin gene. Delineation of unusual features in the 5'-flanking region. *The Journal of biological chemistry* **264**, 8887 (May 25, 1989).

276. E. C. Davis, Stability of elastin in the developing mouse aorta: a quantitative radioautographic study. *Histochemistry* **100**, 17 (Jul, 1993).

277. M. J. Sherratt, Tissue elasticity and the ageing elastic fibre. *Age (Dordr)* **31**, 305 (Dec, 2009).

278. J. Rnjak, S. G. Wise, S. M. Mithieux, A. S. Weiss, Severe burn injuries and the role of elastin in the design of dermal substitutes. *Tissue engineering. Part B, Reviews* **17**, 81 (Apr, 2011).

279. H. Suwabe, A. Serizawa, H. Kajiwara, M. Ohkido, Y. Tsutsumi, Degenerative processes of elastic fibers in sun-protected and sun-exposed skin: immunoelectron microscopic observation of elastin, fibrillin-1, amyloid P component, lysozyme and alpha1-antitrypsin. *Pathology international* **49**, 391 (May, 1999).

280. E. C. Davis, S. A. Blattel, R. P. Mecham, Remodeling of elastic fiber components in scleroderma skin. *Connect Tissue Res* **40**, 113 (1999).

281. B. L. Loeys *et al.*, Mutations in fibrillin-1 cause congenital scleroderma: stiff skin syndrome. *Science translational medicine* **2**, 23ra20 (Mar 17, 2010).

282. A. K. Lagendijk, M. J. Goumans, S. B. Burkhard, J. Bakkers, MicroRNA-23 restricts cardiac valve formation by inhibiting Has2 and extracellular hyaluronic acid production. *Circulation research* **109**, 649 (Sep 2, 2011).

283. B. J. Reinboth, M. L. Finnis, M. A. Gibson, L. B. Sandberg, E. G. Cleary, Developmental expression of dermatan sulfate proteoglycans in the elastic bovine nuchal ligament. *Matrix Biol* **19**, 149 (May, 2000).

284. A. I. Olin *et al.*, The proteoglycans aggrecan and Versican form networks with fibulin-2 through their lectin domain binding. *The Journal of biological chemistry* **276**, 1253 (Jan 12, 2001).

285. Z. Isogai *et al.*, Versican interacts with fibrillin-1 and links extracellular microfibrils to other connective tissue networks. *The Journal of biological chemistry* **277**, 4565 (Feb 8, 2002).

286. D. R. Zimmermann, M. T. Dours-Zimmermann, M. Schubert, L. Bruckner-Tuderman, Versican is expressed in the proliferating zone in the epidermis and in association with the elastic network of the dermis. *The Journal of cell biology* **124**, 817 (Mar, 1994).

287. W. Volker *et al.*, Mapping of proteoglycans in atherosclerotic lesions. *European heart journal* **11 Suppl E**, 29 (Aug, 1990).

288. C. Fornieri, M. Baccarani-Contri, D. Quaglino, Jr., I. Pasquali-Ronchetti, Lysyl oxidase activity and elastin/glycosaminoglycan interactions in growing chick and rat aortas. *The Journal of cell biology* **105**, 1463 (Sep, 1987).

289. J. O. Cantor *et al.*, The effect of hyaluronan on elastic fiber injury in vitro and elastase-induced airspace enlargement in vivo. *Proc Soc Exp Biol Med* **225**, 65 (Oct, 2000).

290. J. O. Cantor, G. M. Turino, Can exogenously administered hyaluronan improve respiratory function in patients with pulmonary emphysema? *Chest* **125**, 288 (Jan, 2004).

291. H. Shan *et al.*, Downregulation of miR-133 and miR-590 contributes to nicotine-induced atrial remodelling in canines. *Cardiovasc Res* **83**, 465 (Aug 1, 2009).

292. W. C. Parks, M. E. Kolodziej, R. A. Pierce, Phorbol ester-mediated downregulation of tropoelastin expression is controlled by a posttranscriptional mechanism. *Biochemistry* **31**, 6639 (Jul 28, 1992).